ASIAN JOURNAL OF MEDICAL TECHNOLOGY

Contents

Volume 4 **Number 1** **2024**

No. *Title* *Page*

Original Article

VIGNA RADIATA (MUNG BEANS) AS AN ALTERNATIVE CULTURE MEDIUM FOR TRYPTICASE SOY AGAR

C. Condrillon[1,*], L. Masong[1,*], C.E. Sandoval[1,*], and C. Siojo[1]

[1]University of Cebu-Banilad.

[*]Corresponding Author's Email: lovelynmasong@gmail.com, choren2002@gmail.com, elyssasandoval07@gmail.com

Article History: Received 20 Dec 2023; Revised 6 Mar 2024; Accepted 25 Mar 2024

ABSTRACT: High costs of commercial culture media poses challenge in microbiology research, driving a quest for cost-effective culture mediums. The study investigates the potential of Mung beans (Vigna radiata) as a potential alternative culture medium for Trypticase Soy Agar (TSA). This study utilized a quantitative experimental research design with the use of Absolute Growth Index (AGI) Scale and Centers for Disease Control and Prevention (CDC) categorized characteristics of colony morphologies. Mung beans are ground into powder, mixed with 1.5% agar, and processed similarly to TSA. Four-quadrant streaking is performed, followed by incubation at 37°C for 24 hours. Test microorganisms include Escherichia coli, Staphylococcus aureus, Pseudomonas aeruginosa, and Candida albicans. Colony growth from both the formulated Mung Bean Agar (MBA) and TSA were scored according to AGI and compared with the use of two-way ANOVA. Colony morphology observations reveal that Mung Bean Agar (MBA) produces pinpoint, smooth, grayish, opaque, punctiform colonies with entire margins, whereas TSA yields small/medium, yellow, mucoid, transparent, circular colonies with entire margins. Statistical analysis shows no significant difference in AGI between MBA and TSA. In conclusion, MBA can serve as a cost-effective alternative to TSA for microbiological culture, offering a similar growth performance while being more economically feasible.

KEYWORDS: *Mung Beans, Alternative Culture Medium, Trypticase Soy Agar*

1.0 INTRODUCTION

The ability to cultivate and maintain microorganisms in the laboratory by supplying the right culture medium that provides a favorable environmental condition is the foundation of microbiological studies [1]. As the ever-increasing demands of culture media continue to grow, the dehydrated culture media was reported to hold the largest market share in 2021 globally [2]. The primary factor that drives this demand is the surge in need for innovative vaccines, antibiotics, and oral insulin. According to trade statistics from 2023, 69% of the culture media products in the Philippines are total imports from largest culture media suppliers in China, the United States, and Thailand [3]. The lack of local companies and supply chain constraints made the ready-to- use and quality-assured culture media either prohibitively expensive or completely unavailable in LMICs [4]. Thus, local researchers seek a cost-effective alternative culture medium for commercially produced culture media. [5] Across the countries, the growth in agricultural production has allowed food to become more abundant and cheaper. Fruits and vegetables served as dietary guidance due to their vitamin, mineral concentration, and phytochemical compositions.

Mung bean, scientifically known as Vigna radiata, has been long recognized as an inexpensive and readily available source of balanced nutrients, including protein, minerals, vitamins, and dietary fiber, as per Hou et al. [6]. In the review study of Tang et al. (2014), mung beans contain about 50-60% carbohydrates and 20-24% protein, where the rest of the constituent percentage accounts for minerals, vitamins, and fat. The main storage proteins of mung beans are globulin and albumin which accounts for 60% and 25% of the total protein, respectively [7]. With its excellent source of protein, mung beans have an ideal essential amino acid profile [8]. It is rich in essential amino acids such as leucine, isoleucine, and valine. Mung beans have more excellent carbohydrate content than soybeans which are present in Trypticase Soy Agar [9]. The predominant carbohydrate found is starch. The other

carbohydrates are made up of oligosaccharides such as raffinose, stachyose, and verbascose The development and evaluation of culture media derived from easily accessible raw materials as an alternative to commercial culture media has been the focus of numerous studies over the past few years [9].

The potential of mung beans was investigated by Fadhilah et al. (2022) [10] as an alternative culture medium for bacterial growth using a pure isolate of *Bacillus subtilis* through the streak quadrant method. The findings revealed that the mung bean medium provides a favorable environmental condition comparable to that of Nutrient Agar, which is used as a control medium, enough to support the growth of *B. subtilis* [10]. In addition, a study reported by Berde and Berde [11] revealed that using vegetables to make an alternative culture media can be beneficial given that they consist of several nutrients necessary for the development of microorganisms. Since many of these media involve food products or portions of food products that are not intended for human consumption, institutions can access them with resources sufficient for commercial culture media. By utilizing food waste, formulating alternative culture media supports sustainability in addition to advancing access to knowledge as per Santos et al. [12].

Most cheap protein sources (soy protein, cowpea, lentil, chickpea, mung beans, and split pea), except for rice-based medium, were influential in promoting the growth of the tested microorganisms, including *Staphylococcus aureus*, *Escherichia coli*, *Bacillus cereus*, *Pseudomonas aeruginosa*, *Penicillium sp*., and *Aspergillus sp*.. Shareef (2019) reported that all tested microorganisms had significantly high growth rates on most protein sources mentioned except rice. *B. cereus* exhibited high growth and large colonies on formulated media. *E. coli* and *P. aeruginosa* showed good growth, while the Pigmentation of *P. aeruginosa* was unaffected. On the other hand, *B. cereus*, *S. aureus*, and *P. aeruginosa* produced beta hemolysis on all formulated agar media. Using protein sources as alternative culture media in laboratories are

feasible and cheaper than commercially manufactured culture media [13]. Arulanantham et al. observed that legume seeds are a rich source of protein for nutritional purposes. Legume seeds (Cowpea, green and black gram, and soya meat) were used in their study as an alternative nutrient source to grow bacteria. Results showed that *Klebsiella sp.* typically grows the least in the protein formulations studied, while *Staphylococcus sp.* grows well in all protein formulations. All the tested bacteria demonstrated more significant growth in nutrient agar across the other media used. In addition, the number of colony growths indicates that Soya meat agar (soya meat + agar) is an effective alternative culture media source to nutritional agar for growing bacteria [14]. *Staphylococcus aureus* and *Escherichia coli* can thrive in corn husk extract, according to a study conducted in the Philippines by Gabunia et al. The results revealed that the corn husk extract was an effective culture medium and produced results similar to nutrient agar sold commercially [15]. The viability of other culture media was evaluated by Uthayasooriyan et al. (2016) using cheap protein sources (rice, chickpea, corn, dhal, thinai, natural soy flour, and processed soy flour) as an alternative medium to Potato Dextrose Agar and Nutrient Agar. *Klebsiella sp*. exhibited more growth for the tested bacteria, while *Bacillus sp.* grew less in all alternative culture media. For tested fungi, *Sclerotium sp.* demonstrated significantly ($p<0.05$) higher growth in rice, while *Penicillium sp.* showed especially ($p<0.05$) low growth in rice and corn. The authors also utilized soy flour as a culture medium, but the results were more satisfying with the fungi than with the bacteria tested [1]. Mohammed et al. [16] utilized mixtures of seven different legumes to formulate an alternative culture media for the growth and stimulation of prodigiosin pigment production of *Serratia marcescens*. To prepare the culture media, white beans, fava beans, mung beans, green peas, chickpeas, black beans, and lentils were powdered and sieved. The color intensity of prodigiosin was used to compare the pigment production. Among the legumes tested, mung beans are one of the legumes that supported the maximum stimulation rate of

pigment production of *S. marcescens*, but the mixture of all legumes shows the highest production. The study proves that legumes are an excellent source of protein and can be used as alternatives for bacterial growth [16]. Gram beans, a member of the legume family, is known to be rich in proteins enough to support the growth of microorganisms in various studies. Black, yellow, green, and horse gram were used as an alternative culture media in the study of Raju [17]. The study did not involve any quantification of the number of colonies present in alternative solid culture and focuses on the comparison of the presence and morphology of *E. coli* and *S. aureus*. Before the microbial inoculation onto the alternative culture media, the researcher prepared a microbial culture of *E. coli* and *S. aureus* from the original stock culture to ensure its purity and freshness. Result shows that there weren't any significant variations in the morphology of the colonies between the alternative gram beans media and NA [17]. Moreover, the use of almond — known to have higher nutritional value compared to other nuts — to replace peptone and meat extract on Nutrient agar was performed by Nurmalasari et al. [18]. The identity of *Escherichia coli* and *Staphylococcus aureus* was confirmed by the researchers through gram staining. Although colony morphology of the alternative media was quite similar to NA, the number of colonies of *E. coli* and *S. aureus* being observed in alternative almond media was less as compared to NA. Subsequently, almond media as being a complex media, the researchers pointed out the several possible causes of the microorganisms' growth. One possible cause includes the boiling process of almonds during media preparation. Boiling the almonds can lead to reduced or loss enzyme activity, solubility changes, and denaturation of proteins causing its decreased level. As a result, decreased nutrient content in alternative almond media leads to impeding growth of bacteria [18]. Among the local plant materials used by Oledibe et al. (2023) [19] is *Glycine max*, or locally known as soybeans. Soybeans are a member of legume family that is present as one of the components in Trypticase Soy Agar. The study focuses on

the evaluation of the *P. expansum* and *A. niger* colony, sporulation, and aerial mycelia growth using the combination of *Zea mays, Dioscorea dumetorum,* and *Glycine max* as alternative culture medium to Sabouraud Dextrose Agar. One of the procedures being carried out in the preparation of alternative culture media is washing thoroughly the *Glycine max* seeds with clean water and dried 3 hours at 60°C in the oven. Dried sample was then blended into powder to enhance solubility and sieved until it reached a flour consistency. The rest of the preparation is just like any commercial culture medium and was autoclaved. Visual evaluation of various media consistency on plates was also done. The alternative culture media showed a strong gelling ability but slowly liquified after a few days. The researchers pointed out that it could be due to a pH decrease while autoclaving that reduces the gel stability. Overall, the colony diameters of test fungi were not significantly different from SDA, remarkable mycelia growth and sporulation were also observed [19].

In this current study, the formulation of alternative culture media out of mung beans will be compared to that of Trypticase Soy Agar (TSA) because mung beans have a similar nutrient composition to the soybean component of TSA. In addition, to address the problem of the high-cost commercial culture media, the cost of the preparation of Mung Bean Agar (MBA) will be recorded and compared to the local price of TSA. As this study seeks an alternative to nonselective culture media, various biochemical tests will also be performed to confirm the identity of test microorganisms utilized in the study. This study is anchored on the theory of microbial growth curve. Louis Pasteur developed the artificial culture medium as a model of the human body, as indicated by Sandle [20]. The microbial growth curve was defined as a nonequilibrium thermodynamic process. The anchored theory is supported by the principle of pure culture technique, which forms the basis of the procedures.

This study aims to determine the potential of Mung bean (Vigna radiata) as an alternative culture medium for Trypticase Soy Agar.

Specifically, it seeks to Formulate an alternative culture medium using mung bean as the main component of the culture medium; Identify the needed concentration of agar powder to be added in Mung bean to obtain a firm gel consistency comparable to that of the Trypticase Soy Agar; Inoculate ATCC cultures of Escherichia coli, Staphylococcus aureus, Pseudomonas aeruginosa and Candida albicans onto the MBA and TSA by four-quadrant streaking method; Describe the colony morphology of test microorganisms in MBA and TSA with the use of modified Centers for Disease Control and Prevention (CDC) categorized description of colony characterization; Compare the standard absolute growth index of the test microorganisms in the Mung Bean Agar to Trypticase Soy Agar, the control medium; Confirm the identity of the test microorganisms by performing gram stain and various biochemical tests; Compare the total cost of the preparation of Trypticase Soy Agar and Mung Bean Agar; and Recommend Mung Bean Agar as a potential alternative culture medium to Trypticase Soy Agar.

2.0 METHODOLOGY

2.1 Research Design

This study employed an experimental design with a quantitative approach in comparing the absolute growth index and noting the morphology of colonies of the test microorganisms in Mung Bean Agar as a potential alternative to the commercial media, Trypticase Soy Agar.

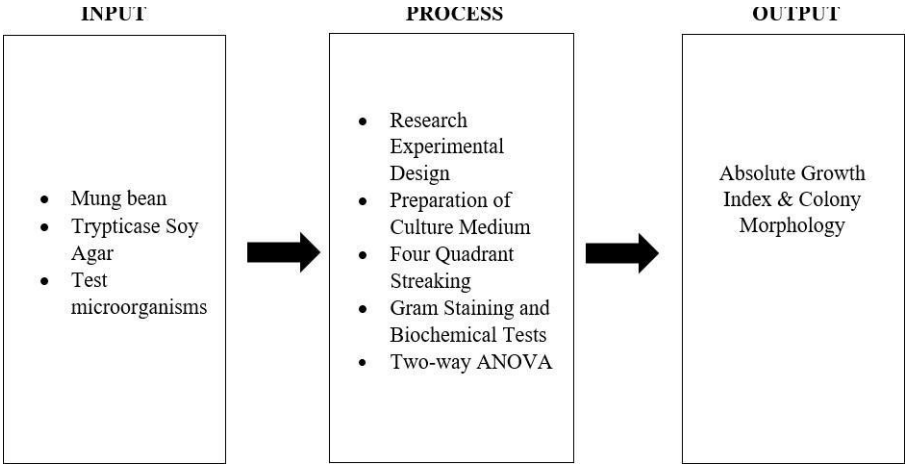

Figure 1: Research Flow Process

2.2 Research Environment

The research was conducted at the University of Cebu-Banilad, 8th floor, Microbiology laboratory, College of Medical Technology. The University of Cebu-Banilad is located along Gov. M. Cuenco Ave, Cebu City, 6000. Moreover, the Mung bean was procured from a farm in Looc Norte, Asturias, Cebu through delivery. The samples were packed in a sterile polyethylene bag and were taken to a taxonomist in the Department of Agriculture (DA), Mandaue City, for authentication.

2.3 Research Subjects

This study utilized purposive convenience as the implemented sampling method. The researchers used Mung beans as they are of the same taxonomic family and similar compositions of soybean in Trypticase Soy Agar. Data were obtained from replicates of the formulated Mung bean culture medium and Trypticase Soy Agar with test microorganisms.

To increase the precision of model parameter estimations, it is a common practice in scientific research to measure each sample unit in triplicates [21] as being the minimum for any inferential statistics [22]. Furthermore, it is valid to compute ANOVA even with just duplicates

in each group in determination of significant difference [23]. As consulted by a statistician, the researchers utilized three replicates of each microorganism in each culture medium, a triplicate of a particular organism in formulated Mung beans culture medium, and another triplicate for the commercial Trypticase soy agar in three trials. A confidence value of 95% with a margin of error of 5% was utilized.

i. **Inclusion Criteria.** The formulation of alternative culture media using a low-cost natural source as a substitute for Trypticase Soy Agar (TSA) was evaluated in this study. Mung beans were bought from a farm in Looc Norte, Asturias, Cebu. Mung beans from Asturias, Cebu, were the only subject for bacteria and fungi culture. The Mung beans that were used are only green seeds. In addition, tested bacteria only include E. coli, S. aureus, and P. aeruginosa. Likewise, the tested fungi include C. albicans. The mentioned tested microorganisms are the only subjects for media culture. The tested bacteria and fungi were provided by the Microbiology laboratory at the University of Cebu-Banilad.

ii. **Exclusion Criteria.** This study does not involve other protein sources for cultivating bacteria and fungi. Mung beans that had sprouted and not green in color were not gathered. The tested microorganisms were not obtained from another laboratory.

2.4 Research Instrument

This section confers the data collection tool that is used in the study. The study utilized the modified Centers for Disease Control and Prevention (CDC)-categorized description of size, surface appearance, color, density, form, and margin in describing the colony morphologies. The Absolute Growth Index (AGI) developed by Mossel et al., was used for quantification. The growth score in each test microorganism in all replicates and trials of Trypticase Soy Agar and Mung Bean Agar was averaged. The microbiology lab provided the necessary tools and supplies for the experiment to be possibly done.

2.5 Data Collection and Treatment

A loopful from ATCC culture of E. coli, S. aureus, P. aeruginosa and C.albicans were inoculated separately to Trypticase Soy Agar using the four-quadrant streaking method. The aseptic method was observed by sterilizing the wire loop over a flame of an alcohol lamp until red hot. The plates were incubated for about 18-24 hours. All glassware and apparatuses were thoroughly cleaned and sterilized using an autoclave. These procedures ensured the creation of sterile media for microbiological experiments.To prepare Mung Bean Agar (MBA) using a mung bean grinder, 1 kg of mung beans was ground into powder and sieved. Researchers mixed 25 g of powdered mung bean and 15 g of agar in 1 L of distilled water, sterilized it in an autoclave, and poured it into petri dishes to solidify. TSA was prepared as per the manufacturer's instructions by suspending 40 g of TSA in 1 L of distilled water, followed by sterilization in an autoclave and pouring into petri dishes. Trypticase Soy Broth (TSB), Pseudomonas Agar Medium (PAM), and Eosin-Methylene Blue Agar (EMB) were also prepared following the respective manufacturer's instructions, sterilized, and dispensed into suitable containers.

The procedures that were performed by the researchers are referred to the set of guidelines made by the Australian Society for Microbiology, whose content is not dissimilar to the standard procedures of Clinical and Laboratory Standards Institute (CLSI) in M22A3 document entitled ‘Quality Assurance for Commercially Prepared Microbiological Culture Media’. The researchers made a Trypticase Soy Broth (TSB) suspension equivalent to 0.5 Mc Farland of E. coli, S. aureus, P. aeruginosa, and C. albicans from the subculture separately. Only one of the researchers performed the streaking using only one wire loop to ensure the uniformity of the technique. With a sterile metal wire loop, one loopful of TSB suspension was streaked on the solid culture media vertically by partially lifting the lid of the petri dish. With utmost caution, the liquid bubble on the loop collapsed in the first streak on

the first quadrant of each plate. The inoculum was then spread horizontally by streaking it back and forth on the first quadrant. The petri dish was turned 90o, and the loop streaked across the first quarter a few times, then over the second quadrant repeatedly. The loop was always meant to initially touch the corner of the preceding quadrant to streak over the following quadrant. There should never be any overlap between the final streaks of any two adjacent quadrants. The same procedure is followed until the fourth quadrant. The researchers then incubated the plates in an inverted position at 37 oC for 24 hours. Such procedure was followed for both Trypticase Soy Agar and Mung Bean Agar. The test microorganisms are described according to its characterization in size, surface appearance, color, density, form, and margin in both Mung Bean Agar and Trypticase Soy Agar. The extent of colonization of each test microorganism along the four quadrants in Mung bean Agar and Trypticase Soy Agar was rated according to the Absolute Growth Index (AGI). Colony morphologies and resulting scores of each growth of certain microorganisms were validated by one microbiologist and one registered medical technologist as recommended by the statistician to ensure accuracy of results. On both ends of the slides, place a drop of normal saline and mix the thin smears of the cultures as mentioned earlier: one for the isolates from Trypticase Soy Agar and one for Mung Bean Agar. Gentian violet solution, a primary stain, should be applied to the prepared smear and left on for one minute before being washed with tap water. Flood the smear with Gram's iodine for a minute, then rinse with tap water. With acetone alcohol, decolorize the smear until the primary stain washes off and color flows off from the slide. Wash with tap water. Safranin as a counterstain, flood for 30 seconds, then wash with tap water. Blot dry and examine under OIO. The tests utilized in the study to confirm the identity of S. aureus in subcultured media, Trypticase Soy Agar and Mung Bean Agar are as follows:

i. Catalase Test

ii. Slide Coagulation Test

iii. Tube Coagulation Test

The tests utilized in the study to confirm the identity of E. coli in subcultured media, Trypticase Soy Agar, and Mung Bean Agar are as follows:

i. Eosin-Methylene Blue

The tests utilized in the study to confirm the identity of P. aeruginosa in subcultured media, Trypticase Soy Agar and Mung Bean Agar are as follows:

i. Pyoverdine Production

The tests utilized in the study to confirm the identity of C. albicans in subcultured media, Trypticase Soy Agar and Mung Bean Agar are as follows:

i. Germ Tube Production

This section presents the statistical tools utilized in the analysis and interpretation of the data to acquire the necessary results in the study. In this study, the following statistical treatments were utilized:

i. Frequency Count and Simple Percentage were used to determine the number of plates that showed a particular colony morphology per the CDC-categorized description of colony characterization.

ii. Summation of the Costs was used to calculate how much it cost overall to prepare Mung Bean Agar and Trypticase Soy Agar. Next, direct comparisons of the prices of each culture media were made.

iii. Two-way ANOVA was utilized to determine the significant difference between the absolute growth index of the formulated Mung Bean Agar and Trypticase Soy Agar. With the use of dependable software like Microsoft Excel, the researchers were able to employ these statistical techniques to provide precise and accurate

data analysis and outcomes. Additionally, a statistical basis of error was used, with an alpha (a) value of 0.05. If the F-critical value is greater than the alpha, then the null hypothesis is rejected, which implies a significant difference between the absolute growth index of Mung beans culture medium and commercial Trypticase soy agar. Otherwise, the researchers were required to accept the null hypothesis.

3.0 RESULTS AND DISCUSSION

3.1 Colony Morphology

Table 1: Colony Morphology of Escherichia coli in Trypticase Soy Agar and Mung Bean Agar

	Mung Bean Agar			Trypticase Soy Agar		
	Morphology	**Frequency**	**%**	**Morphology**	**Frequency**	**%**
Size	pinpoint	9	100%	medium	9	100%
Surface Appearance	mucoid	9	100%	mucoid	9	100%
Color	gray	9	100%	yellow	9	100%
Density	opaque	9	100%	transparent	9	100%
Form	punctiform	9	100%	circular	9	100%
Margin	entire	9	100%	entire	9	100%

Table 1 presents the frequency distribution of the colony morphology of Escherichia coli both in Mung Bean Agar and Trypticase Soy Agar. All the plates in MBA with E. coli showed pinpoint, mucoid, gray, opaque, punctiform, and entire colonies. On the contrary, TSA demonstrated medium, mucoid, yellow, transparent, circular, and entire colonies in all plates.

Table 2 presents the frequency distribution of the colony morphology of the Staphylococcus aureus both in Mung Bean Agar and Trypticase Soy Agar. The replicate plates of MBA with S. aureus displayed pinpoint, smooth, grayish yellow, opaque, punctiform, and entire colonies. Meanwhile, TSA demonstrated small, mucoid, yellow,

transparent, circular, and entire colonies in all plates.

Table 2: Colony Morphology of Staphylococcus aureus in Mung Bean Agar and Trypticase Soy Agar

	Mung Bean Agar			Trypticase Soy Agar		
	Morphology	**Frequency**	**%**	**Morphology**	**Frequency**	**%**
Size	pinpoint	9	100%	small	9	100%
Surface Appearance	smooth	9	100%	mucoid	9	100%
Color	grayish yellow	9	100%	yellow	9	100%
Density	opaque	9	100%	transparent	9	100%
Form	punctiform	9	100%	circular	9	100%
Margin	entire	9	100%	entire	9	100%

Table 3: Colony Morphology of Pseudomonas aeruginosa in Mung Bean Agar and Trypticase Soy Agar

	Mung Bean Agar			Trypticase Soy Agar		
	Morphology	**Frequency**	**%**	**Morphology**	**Frequency**	**%**
Size	pinpoint	9	100%	medium	9	100%
Surface Appearance	smooth	9	100%	rough	9	100%
Color	grayish yellow	9	100%	green	9	100%
Density	opaque	9	100%	transparent	9	100%
Form	punctiform	9	100%	irregular	9	100%
Margin	entire	9	100%	entire	9	100%

Table 3 shows the frequency distribution of the colony morphology of Pseudomonas aeruginosa both in Mung Bean Agar and Trypticase Soy Agar. All nine (9) replicate plates of MBA with P. aeruginosa showed pinpoint, smooth, grayish yellow, opaque, punctiform, and entire colonies. The researchers also noted the color of the MBA culture media with P. aeruginosa colonies were changed from gray into yellow

comparable to that of the Trypticase Soy Agar after 24 hours of incubation. On the other hand, TSA displayed medium, rough, green, transparent, irregular, and entire colonies on all plates.

Similarly, Shareef found that Pseudomonas aeruginosa exhibited prominent characteristics when grown on formulated culture media made of legumes [13]. These characteristics included the formation of large, irregularly shaped colonies with an opaque appearance, accompanied by a sweet odor. These colonies were further distinguished by distinctive pigments, primarily the blue-colored pyocyanin, which spread throughout the culture media.

Table 4: Colony Morphology of Candida albicans in Mung Bean Agar and Trypticase Soy Agar

	Mung Bean Agar			Trypticase Soy Agar		
	Morphology	**Frequency**	**%**	**Morphology**	**Frequency**	**%**
Size	pinpoint	9	100%	small	9	100%
Surface Appearance	smooth	9	100%	mucoid	9	100%
Color	grayish white	9	100%	yellow	9	100%
Density	opaque	9	100%	transparent	9	100%
Form	punctiform	9	100%	circular	9	100%
Margin	entire	9	100%	entire	9	100%

Table 4 shows the frequency distribution of the colony morphology of the Candida albicans both in Mung Bean Agar and Trypticase Soy Agar. All nine (9) replicate plates of MBA with C. albicans showed pinpoint, smooth, grayish-white, opaque, punctiform, and entire colonies. On the other hand, TSA displayed small, mucoid, yellow, transparent, circular, and entire colonies on all plates.

According to the study by Shareef, the colonies of fungi in formulated alternative culture medium, made out of legumes, are smaller in size

as compared to their growth on commercial Potato Dextrose Agar [13]. Additionally, the color of the bacterial colonies was also noted to conform to the color of the formulated culture medium [13].

3.2 Absolute Growth Index

The extent of colonization of the test microorganisms was determined using the four-quadrant streaking method and was expressed as an absolute growth index.

Table 5: Comparison between the of Absolute Growth Index of Test Microorganisms in Mung Bean Agar and Trypticase Soy Agar

Source	Sum of Squares	df	Mean of Squares	F-Value	F-Critical Value	P-Value
Between	1.7882	3	0.5961	1.3651	2.7482	0.2614
Within	27.9444	64	0.4366			
Total	29.7326	67				

Statistically Significant at 0.05 levels

A two-way ANOVA was utilized to compare the absolute growth index of test microorganisms between Mung Bean Agar and Trypticase Soy Agar. The total mean AGI of 3.125 with a standard deviation of 0.75 in MBA is much closer to that of TSA's total mean AGI of 3.25 with a standard deviation of 0.58. Table 5 showed that there is no statistically significant difference between the absolute growth index of TSA and MBA given with the two conditions, the F-value of 1.3651 is lesser than the critical value of 2.7482, and the P-value of 0.2614 is greater than 0.05 level of significance. Given the resulting data presented, the null hypothesis stands accepted. It infers that the mean absolute growth index of test microorganisms in both MBA and TSA does not vary that much. Hence, the environment provided by the MBA for the test microorganisms is comparable to that of TSA in terms of absolute growth index.

As a validation, the study of Arulanantham et al. presents that all the formulated media that utilized legumes as protein sources supported the growth of all test organisms, namely *Bacillus sp.*, *Klebsiella sp.*, *Pseudomonas sp.*, *Staphylococcus sp.*, and *Escherichia coli*. Although *Klebsiella sp.* demonstrated the least growth among the formulated media, the growth of other test organisms, including *Pseudomonas sp.*, *Staphylococcus sp.*, and *E. coli* showed no significant difference when compared to the growth in Nutrient Agar that is utilized as a positive control in the said study [14]. Furthermore, the ability of mung beans to support the development of fungi stands in line with the study of Ilmi et al., which uses mung bean sprouts as an alternative fungal growth medium. The collected results of the researchers of the said study pointed out that the mung bean sprout medium gave a similar growth performance of *Saccharomyces cervesiae, Kluyveromyces marxianus, Aspergillus oryzae* and *Trichoderma viridae* to that of commercial media, which is Potato Dextrose Agar and Malt Extract Agar, in particular [24].

3.3 Cost of the Culture Media

Table 6: Economical Comparison of Culture Media

Cost in ₱/500g	
Trypticase Soy Agar	**Mung Bean Agar**
P3,600.00	P2,564.375

The cost of Mung Bean Agar was initially obtained from the grams of mung bean and agar powder used in the preparation and equated into 500 grams. The calculated price per gram of mung bean (₱0.07/kg) and agar (₱13/g) was then multiplied by the grams used and summed up. On the contrary, the commercial culture media, TSA, was simply recorded by its local price. Table 7 explicitly shows that the preparation of an MBA is less expensive than TSA by approximately ₱1035.63.

Correspondingly, a study in Sri Lanka stated that the formulated alternative culture medium out of legumes costs approximately 300 LKR, or 51 pesos to prepare 1L of the medium while it costs around 400 LKR, or 68.42 pesos, to prepare the commercial Potato Dextrose Agar of the same volume [1]. As a result, the researcher concluded that the said study is feasible and less expensive to use different alternative formulations as culture media in laboratories with basic facilities.

4.0 CONCLUSION

The creation of cost-effective and high-quality cultural media presents huge possibilities for scientific research. The expanding number of studies demonstrating the effectiveness of alternative cultural media implies that they can be just as effective, if not more so, than traditional culture media. Through adopting alternative cultural media, researchers may explore new possibilities and attain comparable or even superior outcomes in their studies [24]. Based on the study's findings, Mung Bean Agar can be used as a potential alternative culture medium for Trypticase Soy Agar. Although most of the colonies in the MBA were pinpoint in size and punctiform, the absolute growth index of the test microorganisms was close to that of TSA. As a result, MBA can provide acceptable environmental conditions for the test microorganisms that have been shown to grow in TSA. Furthermore, the preparation of MBA was also feasible and less expensive compared to that of TSA.

CONFLICT OF INTEREST STATEMENT

The authors have no conflicts of interest to declare and are in agreement with the contents of the manuscript.

ACKNOWLEDGMENTS

The researchers express their utmost gratitude to their research adviser Ms. Chloe Naty Marie Eugenie Siojo for being with them through the whole research process, to Dr. Virginia P. Mesola, Ms. Veronica Fe Isabel O. Cebedo, Ms. Roselita Doming, Mr. Nestor M. Pompa, and Mr.

Karl Christopher Weber, to the University of Cebu-Banilad College of Medical Technology faculty and staff, the Department of Agriculture, Region VII Office, family, friends and above all, to the Almight Father for the success of the study.

5.0 REFERENCES

[1] Uthayasooriyan, M., Pathmanathan, S., Ravimannan, N., & Sathyaruban, S. "Formulation of alternative culture media for bacterial and fungal growth", University of Jaffna, 2016.

[2] *Global Culture Media Market Size and Industry Growth|2022 – 2031. Research Dive* [Online]. Available: www.researchdive.com/413/culture-media-market.

[3] *Prepared Culture Media for Development of Micro- orgaisms – Market Analysis, Forecast, Size, Trends, and Insights. IndexBox. (2023).* Retrieved July 21, 2023 [Online]. Available: https://bit.ly/3OFlDVM

[4] J. Jacobs *et al.*, "Diagnostic bacteriology in district hospitals in sub-Saharan Africa: at the forefront of the containment of antimicrobial resistance," *Front. Med.*, vol. 6, p. 205, 2019.

[5] J. L. Slavin and B. Lloyd, "Health benefits of fruits and vegetables," *Adv. Nutr.*, vol. 3, no. 4, pp. 506–516, 2012.

[6] D. Hou *et al.*, "Mung bean (Vigna radiata L.): Bioactive polyphenols, polysaccharides, peptides, and health benefits," *Nutrients*, vol. 11, no. 6, p. 1238, 2019.

[7] D. Tang, Y. Dong, H. Ren, L. Li, and C. He, "A review of phytochemistry, metabolite changes, and medicinal uses of the common food mung bean and its sprouts (Vigna radiata)," *Chem. Cent. J.*, vol. 8, pp. 1–9, 2014.

[8] Z. Shi, Y. Yao, Y. Zhu, and G. Ren, "Nutritional composition and antioxidant activity of twenty mung bean cultivars in China," *Crop J.*, vol. 4, no. 5, pp. 398–406, 2016.

[9] *Soyabean casein digest agar (tryptone soya agar), HiMedia Laboratories. (2022).* Retrieved December 3, 2022 [Online]. Available: https://bit.ly/3DI39h8

[10] W. K. Fadhilah, H. A. Saputra, and N. Baby, "Mung beans (Phaseolus radiates L.): Utilization as components of the growth medium Bacillus subtilis", *AJHAS*, vol. 1, no. 2, pp. 24–31, Jun. 2022.

[11] C. V Berde, V. B. Berde, and others, "Vegetable waste as alternative microbiological media for laboratory and industry," *World J Pharm Pharmacaeutical Sci*, vol. 4, no. 05, pp. 1488–1494, 2015.

[12] F. P. dos SANTOS, D. C. M. M. de MAGALHÃES, J. dos S. Nascimento, and G. L. de P. A. Ramos, "Use of products of vegetable origin and waste from hortofruticulture for alternative culture media," *Food Sci. Technol.*, vol. 42, p. e00621, 2021.

[13] S. A. Shareef, "Formulation of alternative culture media from natural plant protein sources for cultivation of different bacteria and fungi," *Zanco J. Pure Appl. Sci.*, vol. 31, no. 4, pp. 61–69, 2019.

[14] R. Arulanantham, S. Pathmanathan, N. Ravimannan, and K. Niranjan, "Alternative culture media for bacterial growth using different formulation of protein sources," *J. Nat. prod. Plant resour*, vol. 2, no. 6, pp. 697–700, 2012.

[15] K. Gabunia, H. M. Deslate, and J. Garcia, "Effectiveness of corn husk extract as an alternative culture media for the growth of Escherichia coli and Staphylococcus aureus," *Eff. Corn Husk Extr. as an Altern. Cult. Media growth Escherichia coli Staphylococcus aureus*, vol. 39, no. 2, p. 4, 2019.

[16] B. B. Mohammed, Z. O. Shatti, E. I. Jasim, W. A. Dari, and N. Alfraji, "Local culture medium from the legumes mixture as a novel media for the growth and stimulation of prodigiosin pigment which production from Serratia marcescens that isolated environmentally," *Plant Arch.*, vol. 20, no. 1, pp. 991–1000, 2020.

[17] Raju, K. S., "Alternative culture media for cultivation of bacteria," *International Journal of Science and Research (IJSR)*, vol. 9, no. 3, pp. 1174-1176, 2020.

[18] A. Nurmalasari, L. Marlina, U. Ruhimat, and R. N. Mutmainah, "Almond as Alternative Media for Growth of Staphylococcus aureus and Escherichia coli," *J. Kesehat. STIKes MUHAMMADIYAH CIAMIS*, vol. 9, no. 2, pp. 17–25, 2022.

[19] O. J. Oledibe, I. B. Enweani-Nwokelo, R. N. Okigbo, A. N. Achugbu, and others, "Formulation of Fungal Media from Local Plant Materials," *Adv. Gut & Microbiome Res.*, vol. 2023, 2023.

[20] M. Bonnet, J. C. Lagier, D. Raoult, and S. Khelaifia, "Bacterial culture through selective and non-selective conditions: the evolution of culture media in clinical microbiology," *New microbes new Infect.*, vol. 34, p. 100622, 2020.

[21] J. M. Singer, A. C. Pedroso-de-Lima, N. I. Tanaka, and V. A. González-López, "To triplicate or not to triplicate?," *Chemom. Intell. Lab. Syst.*, vol. 86, no. 1, pp. 82–85, 2007.

[22] *Number of replicates. European Molecular Biology Laboratory. (2023)*, Retrieved March 3, 2024 [Online]. Available: https://bit.ly/3P64nJ8

[23] *Dotmatics. (n.d). Statistics with n=2.* Retrieved March 3, 2024 [Online].

Available: https://bit.ly/49Wib16

[24] M. Ilmi, L. K. Putri, A. A. K. Muhamad, A. Cholishoh, and S. A. Ardiansyah, "Use of mung bean sprout (tauge) as alternative fungal growth medium," in *Journal of Physics: Conference Series*, 2019, vol. 1241, no. 1, p. 12015.

[25] T. Gamit, M. Hajoori, and N. Maisuria, "A Review: Formulation of Alternative Culture Media," *Int. J. Life Sci. Agric. Res.*, vol. 2, no. 8, pp. 206–212, 2023.

HARNESSING THE POWER OF ARTIFICIAL INTELLIGENCE FOR ENHANCED POINT-OF-CARE QUALITY CONTROL IN HEALTHCARE

A.S. Andigema[1,2,3,4,*], N.N. Tania Cyrielle[1,2,3,4,5,*], M.K. Lethicia Danaëlle[3] and E. Ekwelle[6]

[1]Department of Research and Education, Oli Health Magazine Organization, Kigali, Rwanda.

[2]Department of Health and Research, Youth Health Action Network, Douala, Cameroon.

[3]Department of Microbiology, Immunology and Hematology; Faculty of medicine and Pharmaceutical Sciences, University of Dschang, Dschang, Cameroon.

[4]Department of Innovation and Knowledge Dissemination, Bisons' Scholars.

[5]Department of General Medicine, Université Evangélique en Afrique, Democratic Republic of Congo.

[6]Department of Electronics and Electrical Engineering, College of Technology, University of Buea.

[*]Corresponding Author's Email: ngnokamcyrielle@gmail.com, andigemaangyibaserge@gmail.com

Article History: Received January 30, 2024; Revised Febuary 20, 2024; Accepted February 26, 2024

ABSTRACT: Artificial intelligence (AI) is increasingly being used to improve the quality control of point-of-care diagnostics. This is caused by a number of factors, including the following: 1. AI can accelerate and improve testing accuracy. In comparison to humans, AI technology can review data more quickly and precisely, reducing errors and improving overall quality assurance. 2. When it comes to improving POC test findings on healthcare issues such as infectious diseases or medical crises such as heart attacks, AI can be used for sophisticated predictive analytics and modeling that aid in better decision-making. 3. Artificial intelligence facilitates process automation, increasing productivity and lowering labor costs in labor-intensive tasks such

as testing and analyzing samples collected at point-of-care facilities. 4. The use of AI enables organizations implementing these solutions to gain insights from large volumes of raw diagnostic data generated faster and more accurately, allowing them to build solid frameworks around preventive care initiatives and significantly influence public health outcomes.5. Artificial intelligence (AI) has been demonstrated to be a useful tool for real-time monitoring systems that identify any problems with test results early so that they can be corrected before affected patients receive inaccurate diagnoses or treatment plans based on false information provided by diagnostic tests performed at points of care such as clinics or hospitals. Using these technologies would allow healthcare organizations to spend less on labor while still receiving exact diagnoses and rapid treatment delivery at a fraction of the cost that manual approaches required earlier.

***KEYWORDS**: Artificial intelligence (AI); Quality control; Point-of-care diagnostics; Predictive analytics; Process automation.*

1.0 INTRODUCTION

AI has proven to be a long-lasting solution to several problems in laboratory medicine related to precision and accuracy. Artificial Intelligence has gone beyond the human limits to explore invisible errors and loopholes which they human eye passes by but even though has its limitations too [1]. With a focus on laboratory medicine, AI refers to using technology to analyze and interpret health-related data from electronic health records, medical imaging, wearable devices, and other sources and is also used in the developing world to improve diagnosis accuracy, personalize treatment plans, and predict disease outcomes [2].

Point-of-care testing (POCT) refers to medical diagnostic testing performed at or near the site of patient care rather than in a centralized laboratory setting [3] and quality control which is an essential part of it refers to the processes and procedures used to ensure that the results generated by a laboratory are accurate, reliable, and consistent is an aspect which are needed to achieve quality results in the sector of laboratory medicine [4]. POC diagnostic kits are portable, simple-to-use that yield results in a matter of minutes as they make it possible to diagnose and treat infectious diseases outside of lab settings. They are important in rural or resource-constrained locations where it may not

be possible to access advanced laboratory facilities. They can also be utilized in primary care offices, urgent care facilities, and emergency rooms to guarantee that patients receive speedy diagnoses and treatments. They coming of POC diagnostic kits have transformed laboratory medicine and elevated patient care on a global scale [5] but here we are looking at the inclusion of artificial intelligence to step up the accuracy and precision in this POC devices.

2.0 ARTIFICIAL INTELLIGENCE (AI) AND MACHINE LEARNING (ML) ALGORITHMS ON POC DIAGNOSTICS

The introduction of artificial intelligence (AI) and machine learning (ML) algorithms to Point of Care (POC) diagnostics have reshaped the healthcare sector drastically [6]. Point-of-care diagnostic tools offer not only more trustworthy but more accurate and precise and a rapid turnaround time [7]. AI and ML algorithms have proven to be able to process huge information, finding patterns, and spotting anomalies [8] which have been applied to POC diagnostics and have a substantial impact on them. AI algorithms have the ability to lower the likelihood of diagnostic blunders and boost the precision and quality of outcomes. By enabling the POC diagnostic kit to learn from data and adapt its output to each patient's needs, machine learning algorithms can enhance the functionality of the device. The sensitivity and specificity of diagnostic tests can be increased with the aid of AI algorithms. They can also help create personalized POC diagnostic kits in accordance with the requirements of the patient. For instance, AI algorithms can assess a patient's lifestyle, medical history, and other pertinent aspects to assess the possibility of a disease and prescribe certain diagnostic procedures [9].

A smart diagnostic kit that interacts with patients and offers real-time feedback can be created with the aid of ML algorithms. For example, a POC diagnostic kit can assess the patient's breathing patterns using ML algorithms and deliver immediate feedback on how to improve breathing habits. Patients with respiratory conditions like asthma can benefit most from this [10].

Table 1: Floating-point operations necessary to classify a sample

Criteria	Artificial Intelligence (AI)	Machine Learning (ML)
Definition	AI refers to the simulation of human intelligence in machines that are programmed to think and act like humans.	ML is a subset of AI that provides systems the ability to automatically learn and improve from experience without being explicitly programmed.
Scope	AI covers a wide range of capabilities, including problem-solving, speech recognition, planning, and decision-making.	ML focuses on developing algorithms that can learn and make predictions or decisions based on data.
Dependency	AI can work with or without data and depends on pre-defined rules and patterns to make decisions.	ML heavily relies on data to learn and improve its performance, using patterns and structures within the data to make predictions.
Adaptibility	AI can adapt to new environments and tasks by continuously learning and evolving.	ML models are specifically trained for certain tasks and may need retraining if the task changes significantly.
Application	AI applications are diverse, ranging from virtual assistants and autonomous vehicles to medical diagnostics and financial fraud detection.	ML is commonly used in areas like recommendation systems, image recognition, natural language processing, and anomaly detection.

3.0 ENHANCEMENTS IN POC DIAGNOSTICS THROUGH ARTIFICIAL INTELLIGENCE AND MACHINE LEARNING

In every innovation there are always challenges which present itself. These technologies have recently demonstrated significant potential for enhancing POC diagnostics quality control tool. In recent years, artificial intelligence (AI) and machine learning (ML) have emerged as powerful tools that can enhance POC QC processes. This literature review aims to explore the advancements in AI and ML techniques that have improved POC diagnostics and ultimately have the potential to revolutionize healthcare quality control. These technologies have recently demonstrated significant potential for enhancing POC diagnostics quality control.

3.1 Improved Test Accuracy

AI and ML techniques have been applied to POC diagnostics to enhance test accuracy through an automated analysis of test results. Traditional POC tests are often subjective and require manual interpretation, leading to potential human errors or inconsistencies. By leveraging AI and ML algorithms, a consistent and objective analysis can be achieved. For example, they existence of an ML model for diagnosing infectious diseases at POC, achieving an accuracy of 95%, thus outperforming human experts. This demonstrates the ability of AI and ML algorithms to augment human expertise, resulting in improved diagnostic accuracy at the point of care [11, 12].

3.2 Real-Time Decision Support

AI and ML algorithms also provide real-time decision support at the point of care, aiding healthcare workers in making accurate and timely clinical decisions. These algorithms learn from large datasets and generate predictions or recommendations based on the patient's condition, history, and test results. For example, an AI-based decision support system for diagnosing diabetic retinopathy at POC [13,14], allowing non-expert healthcare workers to accurately identify the condition and recommend appropriate interventions. Such real-time support reduces the chances of misdiagnosis and improves patient outcomes.

3.3 Error Detection and Quality Control

AI and ML techniques have shown promise in detecting errors faster and ensuring quality control in POC diagnostics. Errors in test administration, interpretation, or documentation can lead to incorrect diagnosis and subsequent patient harm. By continuously monitoring POC tests, AI algorithms can detect potential errors, alert healthcare workers, and provide suggestions for corrective action. For instance, an AI-based QC system for rapid HIV testing that reduced false-positive rates by 40% [15]. This highlights the potential of AI in improving QC processes and minimizing diagnostic errors.

4.0 EXAMPLES OF POC DIAGNOSTIC KITS THAT HAVE INCORPORATED AI/ML

Some kits which have incorporated AI/ML in their functioning are:

4.1 Flu Detection Kit Powered by AI

An AI-powered flu diagnosis kit has been created by a startup business called Langbo Technologies. It employs deep learning algorithms to examine nose samples from individuals who may be sick with the flu. The kit offers a rapid and reliable detection of the influenza virus, saving healthcare professionals time and lowering the likelihood of prescribing needless antibiotics [16].

4.2 Skin Cancer Biopsy Assessment Tool

An AI-powered tool has been created by a Stanford University research team to evaluate skin samples for the presence of skin cancer. Dermatologists can immediately identify skin cancer and begin treatment since the algorithm can precisely differentiate between benign and malignant lesions [17].

4.3 Organ dysfunction biochemical evaluation

For the early diagnosis of organ dysfunction, numerous AI-powered POC diagnostic kits are being created. For instance, the ASTUTE 140 meter is a POC diagnostic kit that uses AI algorithms to evaluate indicators of kidney and liver function, obviating the need for invasive testing and delivering quick, precise findings [18].

4.4 Tuberculosis diagnosis

An AI-powered POC diagnostic kit that can correctly diagnose TB in patients within an hour has been created by IBM researchers. The kit analyzes samples of patient sputum using machine learning algorithms and gives a real-time diagnosis of TB, allowing medical professionals to rapidly start treatment and stop the spread of the illness [19].

5.0 ADVANTAGES AND LIMITATIONS OF AI/ML USE IN POC DIAGNOSTICS

There are some benefits as well as some drawbacks to the use of

artificial intelligence (AI) and machine learning (ML) in point-of-care (POC) diagnostics. Here are a few of the most typical:

Advantages:

i. Accuracy is improved because AI and ML can evaluate vast volumes of data and spot trends that may be challenging for human therapists to notice. Better patient outcomes and more accurate diagnosis may result from this [8].

ii. Speed: AI systems have a high rate of data processing, which enables quicker diagnosis and treatment [8].

iii. Cost-effectiveness: AI algorithms are particularly cost-effective since they can be employed again without the need for extra resources once they are produced [20].

iv. Greater accessibility to healthcare: POC diagnostics can be employed in rural locations or in regions with few medical resources [21].

Limitations:

i. Regulatory obstacles: Obtaining regulatory authorization for the use of AI and ML in diagnostics can be a time-consuming and expensive procedure. Additionally, regulators can call for continuous evaluation and revision of AI algorithms [22].

ii. Ethical difficulties: Relying on AI for medical diagnosis may raise ethical challenges, such as questions of accountability in the case that the data used to train the algorithm contains errors or prejudice [23].

iii. Privacy issues: Because the application of AI and ML in POC diagnostics necessitates the collecting and analysis of substantial amounts of patient data, privacy issues and the secure management of sensitive data are raised [24].

6.0 CHALLENGES FACED IN IMPLEMENTING AI/ML IN POC DIAGNOSTICS

This section reviews the key challenges faced in implementing AI/ML in POC diagnostics and discusses potential solutions.

6.1 Data quality and availability

One of the primary challenges that have been frequent in trying to implement AI/ML in POC diagnostics is the availability and quality of data. AI algorithms heavily rely on large, diverse, and well-annotated datasets for training. Obtaining such datasets in POC settings can be challenging due to limited resources, small sample sizes, and privacy concerns. Additionally, data quality issues such as missing or biased data can hinder the accuracy and generalizability of AI models [25].

Proposed solutions:

i. Collaborative efforts: Data sharing and collaboration among multiple healthcare institutions can help overcome the issue of limited data availability. Establishing data consortia or networks can enhance the diversity and size of datasets available for training AI models.

ii. Data augmentation techniques: To address limited data samples, techniques such as data synthesis, augmentation, and transfer learning can be employed to enhance dataset size and diversity.

iii. Data quality assurance: Implementing standardized protocols for data collection, annotation, and curation can improve data quality and reduce bias. Regular quality control checks and audits need to be implemented to ensure the accuracy and reliability of the data used for AI training.

6.2 Technical implementation and integration

Integrating AI/ML algorithms into existing POC diagnostic systems is another significant challenge. These systems often have stringent technical requirements, limited computational resources, and may not support real-time analysis. Consequently, implementing AI models that can handle real-time data processing and operate within resource constraints becomes crucial [26].

Proposed solutions:

i. Edge computing: The use of edge computing allows AI algorithms to be run directly on POC diagnostic devices,

reducing the dependence on external computational resources or cloud connectivity. This enables real-time analysis and decision-making at the point of care.

ii. Algorithm optimization: Developing lightweight AI models that require fewer computational resources while maintaining acceptable accuracy levels can facilitate their integration into existing POC diagnostic systems.

iii. Standardization and interoperability: Ensuring compatibility and interoperability between different POC diagnostic systems and AI algorithms is essential to facilitate smooth integration. Standardization efforts that define common protocols and data formats can contribute to the seamless implementation of AI/ML in POC diagnostics.

6.3 Regulatory and ethical considerations

The implementation of AI/ML in POC diagnostics must adhere to regulatory requirements and ethical guidelines, ensuring patient safety, privacy, and data security. Obtaining regulatory approvals and addressing concerns regarding transparency, interpretability, and algorithm bias pose significant challenges [27].

Proposed solutions:

i. Regulatory alignment: Collaborative efforts between regulatory agencies, healthcare providers, and AI researchers can aid in navigating the regulatory landscape, streamlining approval processes, and ensuring compliance with safety standards.

ii. Ethical frameworks: Establishing clear ethical guidelines, such as guidelines on informed consent, data privacy, and algorithm bias, can help address ethical challenges associated with AI/ML implementation in POC diagnostics.

iii. Transparency and interpretability: Developing AI models that provide transparent decision-making processes and can explain their outputs ensures the interpretability of results, which is crucial for clinical acceptance and regulatory requirements.

7.0 CONCLUSION

In conclusion, the use of artificial intelligence (AI) has shown great potential for enhancing point-of-care (POC) quality control in healthcare. AI technology provides various advantages, including improved testing accuracy, predictive analytics for better decision-making, process automation for increased productivity, and the ability to gain insights from large volumes of data. By harnessing the power of AI, healthcare organizations can achieve enhanced diagnostic accuracy, rapid treatment delivery, and cost-effectiveness. Several examples of POC diagnostic kits incorporating AI/ML algorithms have already proven successful in improving diagnostic outcomes. However, there are also limitations and challenges that need to be addressed, such as data quality and availability, technical implementation, and regulatory and ethical considerations. Collaborative efforts, data standardization, and regulatory alignment can help overcome these challenges and ensure the safe and effective implementation of AI/ML in POC diagnostics. Overall, AI has the potential to revolutionize healthcare quality control and significantly improve patient outcomes.

CONFLICT OF INTEREST STATEMENT

The authors have no conflicts of interest to declare and are in agreement with the contents of the manuscript.

ACKNOWLEDGEMENT

The authors acknowledge the infrastructure and support of their respective institutions.

8.0 REFERENCES

[1] S. S. Chanda and D. N. Banerjee, "Omission and commission errors underlying AI failures," *AI & Soc.*, pp. 1–24, 2022.

[2] A. S. Andigema, N. N. T. Cyrielle, K. P. Landry, and A. J. Vladimir, "AI in the Management of HIV: Case Study Cameroon," *Int J Virol AIDS*, vol. 10, p. 89, 2023.

[3] Z. Zhao and D. B. Sacks, "Assay Development in Clinical Pathology,"

in *Pathobiology of Human Disease*, L. M. McManus and R. N. Mitchell, Eds. San Diego: Academic Press, 2014, pp. 3194–3206. doi: https://doi.org/10.1016/B978-0-12-386456-7.06301-2.

[4] Quality Assurance. (2024) *PubMed.* [Online]. Available: https://pubmed.ncbi.nlm.nih.gov/32491435/

[5] S. Nayak, N. R. Blumenfeld, T. Laksanasopin, and S. K. Sia, "Point-of-care diagnostics: recent developments in a connected age," *Anal. Chem.*, vol. 89, no. 1, pp. 102–123, 2017.

[6] M. Martinelli, D. Moroni, A. Prochazka, and M. Strojnik, "Artificial intelligence in point of care diagnostics," *Front. Digit. Heal.*, vol. 5, p. 1236178, 2023.

[7] Larkins, M. C. (2023). *Point-of-Care Testing*. StatPearls - NCBI Bookshelf. [Online]. Available: https://www.ncbi.nlm.nih.gov/books/NBK592387/

[8] G. Krishnan *et al.*, "Artificial intelligence in clinical medicine: catalyzing a sustainable global healthcare paradigm," *Front. Artif. Intell.*, vol. 6, 2023.

[9] N. Ghaffar Nia, E. Kaplanoglu, and A. Nasab, "Evaluation of artificial intelligence techniques in disease diagnosis and prediction," *Discov. Artif. Intell.*, vol. 3, no. 1, p. 5, 2023.

[10] K. C. H. Tsang, H. Pinnock, A. M. Wilson, and S. A. Shah, "Application of machine learning algorithms for asthma management with mHealth: a clinical review," *J. Asthma Allergy*, pp. 855–873, 2022.

[11] M. M. Ahsan, S. A. Luna, and Z. Siddique, "Machine-learning-based disease diagnosis: A comprehensive review," in Healthcare, 2022, vol. 10, no. 3, p. 541.

[12] M. M. Ahsan, S. A. Luna, and Z. Siddique, "Machine-learning-based disease diagnosis: A comprehensive review," in *Healthcare*, 2022, vol. 10, no. 3, p. 541.

[13] R. P. Salongcay et al., "Accuracy of Integrated Artificial Intelligence Grading Using Handheld Retinal Imaging in a Community Diabetic Eye Screening Program," Ophthalmol. Sci., vol. 4, no. 3, p. 100457, 2024.

[14] B. Sheng *et al.*, "An overview of artificial intelligence in diabetic retinopathy and other ocular diseases," *Front. Public Heal.*, vol. 10, p. 971943, 2022.

[15] V. Turbé *et al.*, "Deep learning of HIV field-based rapid tests," *Nat. Med.*, vol. 27, no. 7, pp. 1165–1170, 2021.

[16] R. J. Ward *et al.*, "Flunet: An ai-enabled influenza-like warning system," *IEEE Sens. J.*, vol. 21, no. 21, pp. 24740–24748, 2021.

[17] N. Melarkode, K. Srinivasan, S. M. Qaisar, and P. Plawiak, "AI-powered diagnosis of skin cancer: a contemporary review, open challenges and future research directions," *Cancers (Basel).*, vol. 15, no. 4, p. 1183, 2023.

[18] H. Zhang *et al.*, "Artificial intelligence for the prediction of acute kidney injury during the perioperative period: systematic review and Meta-analysis of diagnostic test accuracy," *BMC Nephrol.*, vol. 23, no. 1, p. 405, 2022.

[19] O. Hrizi *et al.*, "Tuberculosis disease diagnosis based on an optimized machine learning model," *J. Healthc. Eng.*, vol. 2022, 2022.

[20] A. Bohr and K. Memarzadeh, "Chapter 2 - The rise of artificial intelligence in healthcare applications," in *Artificial Intelligence in Healthcare*, A. Bohr and K. Memarzadeh, Eds. Academic Press, 2020, pp. 25–60. doi: https://doi.org/10.1016/B978-0-12-818438-7.00002-2.

[21] B. Heidt *et al.*, "Point of care diagnostics in resource-limited settings: A review of the present and future of PoC in its most needed environment," *Biosensors*, vol. 10, no. 10, p. 133, 2020.

[22] D. B. Larson, H. Harvey, D. L. Rubin, N. Irani, R. T. Justin, and C. P. Langlotz, "Regulatory frameworks for development and evaluation of artificial intelligence--based diagnostic imaging algorithms: summary and recommendations," *J. Am. Coll. Radiol.*, vol. 18, no. 3, pp. 413–424, 2021.

[23] D. D. Farhud and S. Zokaei, "Ethical issues of artificial intelligence in medicine and healthcare," *Iran. J. Public Health*, vol. 50, no. 11, p. i, 2021.

[24] N. Khalid, A. Qayyum, M. Bilal, A. Al-Fuqaha, and J. Qadir, "Privacy-preserving artificial intelligence in healthcare: Techniques and applications," *Comput. Biol. Med.*, p. 106848, 2023.

[25] H. S. Yang, D. D. Rhoads, J. Sepulveda, C. Zang, A. Chadburn, and F. Wang, "Building the model: challenges and considerations of developing and implementing machine learning tools for clinical laboratory medicine practice," *Arch. Pathol. \& Lab. Med.*, vol. 147, no. 7, pp. 826–836, 2023.

OCCUPATIONAL RISK ASSESSMENT AND DETERMINATION OF THE NEED FOR INTERNAL EXPOSURE MONITORING OF RADIATION WORKERS AT INSTITUT KANSER NEGARA

N.K. Zahidi[1*], F. Mohamed[2], M.A. Said[3], U.H. Ibarhim[3], R.A. Mat Salleh[3], N. Abdullah[1], S. Muhd Sarowi[1] and R.Y.T. Loong[1]

[1] Radiation Safety and Health Division, Malaysian Nuclear Agency, Bangi, 43000 Kajang, Selangor, Malaysia.

[2]School of Applied Physics, Faculty of Science and Technology, Universiti Kebangsaan Malaysia, 43600 Bangi, Selangor, Malaysia.

[3]Department of Nuclear Medicine, Institut Kanser Negara, Ministry of Health Malaysia, Putrajaya, 62250, Putrajaya.

[*]Corresponding Author's Email: khairunisa@nm.gov.my

Article History: Received Febuary 26, 2024; Revised March 20, 2024; Accepted March 22, 2024

ABSTRACT: Ionizing radiation exposure is divided into two categories that are external and internal exposure. The annual dose limit for the radiation workers is 20 mSv consists of internal and external exposure. Radiation workers in nuclear medicine are not only exposed to ionizing radiation externally but also internally. The widespread use of unsealed radioactive sources in nuclear medicine poses a potential for internal exposure of radiation workers in the field of nuclear medicine. External radiation monitoring using a dosimeter has been developed in Malaysia since 1985. However, assessment of the need for individual internal dose monitoring has not yet been developed in Malaysia. The purpose of this study is to assess occupational risk and to compare determination value of the need individual internal exposure monitoring of radiation workers in nuclear medicine department at Institut Kanser Negara (IKN). This study involves radiation workers at IKN by observation, survey forms and calculation of decision factor of the need for internal exposure monitoring based on IAEA dose criteria. The results show that the highest risk is during the use of radiopharmaceuticals for diagnosis and treatment of disease through inhalation process for lung scan as well as the preparation and oral

administration to patient, especially radiopharmaceutical containing I-131 and I-124. In addition, a total of 12 out of 16 workers need internal monitoring involving biochemists, pharmacists, and technologists while physicist do not require internal monitoring. Overall, data obtained from this study is the first step in establishing a comprehensive internal exposure framework and promote to more effective and manageable radiation exposure monitoring.

***KEYWORDS**: Internal exposure, decision factor, occupational risk, nuclear medicine*

1.0 INTRODUCTION

Humans can be exposed to external radiation or radionuclides that enter the body (internal exposure) [36]. The basic concept of internal exposure is when radioactive materials enter the body through several main routes, through respiration and wounds [34]. The method used to measure an individual's internal exposure is by directly measuring the radioactivity in the whole body or specific organs by measuring radioactivity through urine and fecal samples [10]. Radiation workers at nuclear medicine department are not only exposed to external ionizing radiation but also internal exposure. Nuclear medicine involves the use of unsealed radioactive materials for diagnosis and treatment of diseases, which can pose significant risks to radiation workers if not properly handled. The work routines of nuclear medicine workers cause them to be exposed to higher radiation doses when compared to other healthcare workers [37], [38]. The assessment of external radiation exposure using dosimeters has been developed in Malaysia since 1985. Currently, radiation worker exposure monitoring in Malaysia is done externally using Optically Stimulated Luminescence Dosimeters (OSLD). Previous studies on internal dosimetry using whole-body gamma counter on nuclear medicine workers from 2 nuclear medicine centres demonstrated no internal exposure found for all monitored radiation workers [1],[39] However, further research is needed to determine if this lack of internal exposure is consistent across all nuclear medicine facilities. Collecting data on the requirements for monitoring the internal dose of radiation workers is the initial step in developing a comprehensive internal exposure monitoring program for radiation workers. The data obtained are precious to authorities in implementing regulations related to routine internal dose exposure monitoring and indirectly assisting employers in ensuring workers' safety, health, and well-being in the workplace.

2.0 METHODOLOGIES

2.1 Sampling location

This study was conducted at the Nuclear Medicine Department of the Institut Kanser Negara (IKN), located in the Federal Territory of Putrajaya, adjacent to Putrajaya Hospital. This department provides diagnostic, therapeutic, Positron Emission Tomography-Computed Tomography (PET-CT) scanning, and cyclotron services. The department began its operations on October 14, 2013, offering radioiodine treatment for hyperthyroid patients and bone scans for external patients. IKN is categorized by the Ministry of Health Malaysia as Level 1 (Diagnostic, External Patient Therapy) and Internal Patient Therapy IKN [21].

2.2 Risk Assessment

The risk assessment used 2 factors in the risk analysis, which are the likelihood or probability of an event occurring and the severity when that event occurs as shown in equation (1). The likelihood is estimated based on work experience, analysis, or measurements, and the range of likelihood scale varies from most likely to inconceivable as shown in Table 1 [9]. The severity level is based on the degree of severity concerning individual health, the environment, or property, and the severity range varies from negligible to extreme as shown in Table 2 [32]. Risk analysis is performed through a qualitative method by expressing the results in a risk matrix as shown in Figure 1, determining the risk level within a range from low to high. The relative risk value is used to prioritize actions that need to be taken to effectively manage workplace hazards. Hazards estimated as "High Risk" require immediate action to mitigate risks to life safety and/or the environment. Risk calculation using the following equation [9]:

$$\text{Relative Risk} = L \times S \quad \ldots (1)$$

Where,

L = Likelihood of an event

S = Severity of an event

Table 1: Likelihood rating

LIKELIHOOD (L)	EXAMPLE	RATING
Most likely	The most likely result of the hazard / event being realized	5
Possible	Has a good chance of occurring and is not unusual	4
Conceivable	Might be occur at some time in future	3
Remote	Has not been known to occur after many years	2
Inconceivable	Is practically impossible and has never occurred	1

Table 2: Severity rating

SEVERITY (S)	EXAMPLE	RATING
Extreme	Fatal / dose > deterministic threshold	5
Major	Major Injury/ dose > legal limits / reportable to HSE	4
Moderate	Three-day injury / dose less than legal limits/ could exceed investigation levels	3
Minor	Minor injury / dose below investigation levels	2
Negligible	Slight chance injury / background radiation dose	1

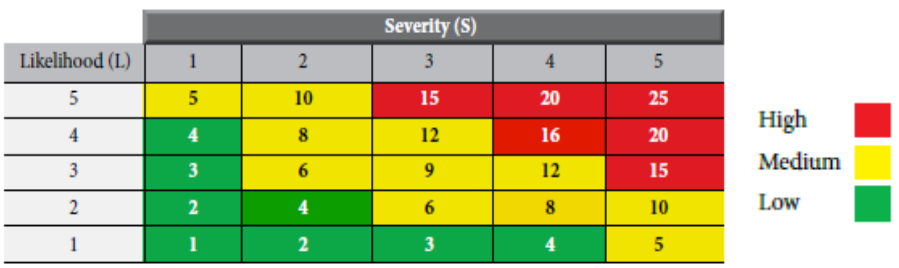

Figure 1: Risk matrix [9]

2.3 Survey Analysis

This study focuses on the factors of knowledge (K), attitudes (A), and practices (P). The study also involves a survey of radiation workers consists of 13 questions with a focus on demographic surveys such as gender, educational background, and work-related information while 16 questions using IAEA documents on safety culture surveys for license holders under the category of attitudes and behaviors [16]. The statistical analysis for survey testing is conducted using SPSS Cronbach's Alpha analysis. This analysis is used to measure internal consistency on a scale of 0 to 1 to assess the reliability of the conducted study [31]. A high reliability value indicates that the study's constructs have acceptable reliability [30] as shown in Table 3. Typically, this Cronbach's Alpha analysis is tested with a small number of

respondents before being applied in a comprehensive study.

Table 3: Cronbach's Alpha score and reliability level [13]

CRONBACH'S ALPHA SCORE	RELIABILITY LEVEL
> 0.9	Excellent
> 0.8	Good
> 0.7	Acceptable
> 0.6	Questionable
> 0.5	Poor
< 0.5	Unacceptable

A descriptive analysis is used to analyze the obtained data, where frequency analysis (mode) is employed to determine demographic information and responses regarding safety in terms of worker behavior.

2.4 Determination of Internal Exposure Requirements

A total of 16 radiation workers who work with unsealed radioactive materials are considered in this determination assessment. This method is used to determine whether radiation workers at the Nuclear Medicine Department of IKN need to undergo internal exposure dose monitoring based on the calculation of dose criteria issued by the IAEA [15] as shown in Equation 2.

$$d_{j\_scenario} = \frac{A_j e(g)_{j,inh} f_{fs} f_{hs} f_{ps}}{0.001} \quad \ldots (2)$$

d_j = decision factor based on operation and radionuclide
A_j = cumulative activity of radionuclide j present in the workplace over the course of the year
$e(g)_{j.inh}$ = dose coefficient (Sv/Bq) for inhalation of radionuclide, j
f_{fs} = physical form safety factor based on the physical and chemical properties of the material being handled
f_{hs} = handling safety factor
f_{ps} = protection safety factor
0.001 = conversion factor from Sv to mSv

The calculation of the final decision factor for each radiation worker is sum of all decision factor, *dj*, obtained for each radiation worker as

shown in Equation 3.

$$D = \sum_{j} d_j \quad \ldots (3)$$

D = final decision factor
d_j = decision factor based on operation and radionuclide

Calculations involving more than one type of radionuclide present in the workplace area, the determination to undergo individual internal exposure monitoring is based on the following criteria [15]:

i. For all radionuclides where the value of $d_j \geq 1$, radiation workers must undergo internal exposure monitoring.
ii. When the value of $D \geq 1$ and the value of $dj \geq 0.3$, radiation workers must undergo internal exposure monitoring.
iii. Internal exposure monitoring is not required if the value of dj is less than 0.1.

3.0 RESULTS AND DISCUSSION

3.1 Risk Assessment

This risk assessment is conducted through observation during the work processes at IKN, starting from the production process to the use of radiopharmaceuticals. Work scenarios are divided into two (2) categories: (i) the production and preparation of radiopharmaceuticals and (ii) the use of radiopharmaceuticals for the diagnosis and treatment of diseases as shown in Table 4 and Table 5. These work scenario categories are carried out based on different scopes of work to facilitate the identification of high-risk levels that need to be prioritized according to more specific work scenarios.

Table 4 : Scenario 1 - Production and preparation of radiopharmaceuticals

1. Identifying Hazards				2. Risk Analysis	
No.	**Work Activity**	**Hazards**	**Potential Consequence**	**Risk Value**	**Risk Level**
1	Distributing radiopharmaceutical vials automatically according to customer requirements	Exposure to external ionizing radiation	Short-term or long-term health effects	10	Moderate
		Spillage or vial breakage	Contamination with radioactive material	12	Moderate
		Ergonomics - object handling, fatigue, pressure, or workplace design errors	Muscle strain/backache	4	Low
2	Transferring containers containing radiopharmaceuticals from an automated machine to lead syringe	Exposure to external ionizing radiation	Short-term or long-term health effects	10	Moderate
		Syringe containing radiopharmaceuticals falls	Radioactive material leakage	6	Moderate
		Ergonomics - object handling, fatigue, pressure, or workplace design errors	Muscle strain/backache	4	Low
		Automated machine malfunctions and requires manual handling	Increased risk of hand extremity dosage	6	Moderate
3	Transferring vials to a dose calibrator for radiopharmaceutical activity measurement	Exposure to external ionizing radiation	Short-term or long-term health effects	10	Moderate
		Contamination on vials	Contamination with radioactive material	12	Moderate
		Spillage or vial breakage	Contamination with radioactive material	12	Moderate
		Ergonomics - object handling, fatigue, pressure, or workplace design errors	Muscle strain/backache	8	Moderate
4	Transportation of	Spillage or vial	Contamination	12	Moderate

	containers containing radiopharmaceuticals in lead containers using a trolley	breakage	with radioactive material		
		Ergonomics - object handling, fatigue, pressure, or workplace design errors	Muscle strain/backache	8	Moderate
5	Quality control - swab test for each vial before transportation process	Exposure to external ionizing radiation	Short-term or long-term health effects	10	Moderate
		Contamination on vials	Contamination with radioactive material	12	Moderate
		Ergonomics - object handling, fatigue, pressure, or workplace design errors	Muscle strain/backache	4	Low
6	Setting for radiopharmaceutical production	Gas usage	Gas leakage	10	Moderate
		Employee work rotation	Self-safety may be compromised	12	Moderate

Based on Table 4, almost all work activities and hazards are at a moderate level because most of the processes involved in the production and preparation of radiopharmaceuticals use automated systems. Adherence to existing regulations and Good Manufacturing Practice (GMP) procedures could further reduce the risk of existing hazards. The IKN facilities also undergo audits [19] and regulatory authorities to ensure that the work processes are in a controlled order. Other factors taken into consideration when determining the moderate risk level include the use of ionizing radiation detectors with warning systems, the use of contamination survey meters, the use of personal protective equipment (PPE) while performing tasks and also failure of quality control of radiopharmaceuticals products where repeated production processes increase the radiation exposure to the workers. Low-risk levels of ergonomic hazards refer to the use of automated equipment that reduces muscle strain and fatigue during the handling of radiopharmaceuticals. There are 2 work activities that have moderate risk levels for physical activities, that are the transport activity by carrying radiopharmaceuticals in lead containers using trolleys and the transfer of vials to the dosimetry

calibrator. The risk levels are based on the handling of the lead containers that are lifted and placed on the calibration counter and trolleys. This ergonomic hazard can give rise to muscle tension or back pain [28]. The maximum weight that can be handled at foot level is 5 to 10 kg [33]. However, the lead containers used at IKN weigh as much as 14 kg, and this can directly have a long-term impact on the body posture of workers. Among the risk controls that can be implemented include using a trolley at the same height as the swab test counter and reducing repetitive operations through job rotation.

Table 5: Scenario 2 - The use of radiopharmaceuticals for diagnosis and treatment of diseases

1. Identifying Hazards				2. Risk Analysis	
No.	**Work Activity**	**Hazards**	**Potential Consequence**	**Risk Value**	**Risk Level**
1	Administration of doses via injection to patients	Exposure to ionizing radiation or radioactive substances	Short-term or long-term health effects	10	Moderate
		Dispersion of radioactive materials in the air and injection room area	Potential for external and internal exposure	6	Moderate
		Patients not following given instructions such as pulling their arm during injection	Contamination of radioactive substances from patient tubes or blood during injection	12	Moderate
		Ergonomics - object handling, fatigue, pressure, or workplace design errors	Muscle strain/backache	8	Moderate
2	Administration of doses via inhalation for lung scans	Exposure to ionizing radiation or radioactive substances	Short-term or long-term health effects	15	High
		Dispersion of radioactive materials in the air and common examination room areas	Potential for external and internal exposure	15	High
		Patients not	Contamination	15	High

		following given instructions such as pulling the mask cover during vapor release	of radioactive substances in the air		
		Ergonomics - object handling, fatigue, pressure, or workplace design errors	Muscle strain/backache	3	Low
3	Preparation and oral administration of doses to patients	Exposure to ionizing radiation or radioactive substances	Short-term or long-term health effects	15	High
		Spillage or leakage in containers containing radioactive liquids or solids	Contamination of radioactive substances in the room environment	15	High
		Patients vomiting after swallowing radioiodine	Contamination of radioactive substances in the room environment	9	Moderate
		Ergonomics - object handling, fatigue, pressure, or workplace design errors	Muscle strain/backache	8	Moderate

According to Table 5, activities such as the administration of doses via inhalation for lung scans and the preparation and administration of oral doses to patients have a high level of risk, particularly for exposure to ionizing radiation and when undesirable events occur. Both processes are carried out in open rooms and can potentially expose workers to internal exposure. The administration of injections to patients is also carried out in open rooms but the risk is at a moderate level due to the radiopharmaceuticals being placed in a lead-shielded syringe. Workers carrying out the injection process in nuclear medicine facilities should go through precaution procedures to prevent exposure [20]. Injection procedures also reduce the risk of internal exposure as the radiopharmaceutical liquid is injected directly into the tube into the patient's blood vessels. Spillage is considered as one of the hazards

where there is a possibility of this happening due to inadequate control of radioactive material sources as well as from the reflex of patients such as withdrawing the arm during injections and removing the face mask during radiopharmaceuticals administration due to discomfort. The risk level for injection spillage is moderate where the radioactivity for each injection is less than 100 mCi (major spill category) [21] while the risk level for oral radio-pharmaceuticals administration spillage is high due to the radioactivity for each sample is exceeding 1 mCi and is categorised as a major spill if occurs [21]. Other than that, the vaporized and oral administration activity using volatile material such as radioiodine and technetium.

3.2 Survey Analysis

3.2.1 Respondent Demography

Table 6 shows the respondent demography based on the data received and majority of the respondents are male aged between 31 to 40 years old.

Table 6 :Analysis of the demographic of survey respondents

Demography	Total	Percentage
Gender		
Male	9	56
Female	7	44
Age		
31-40 years old	13	81
41-50 years old	3	19

Gender and age is one of the aspect that are normally discussed when comes to occupational risk. Female possible to have high risk compared to male in terms of death by receiving same amount dose of ionizing radiation [26], [27]. Relatively female have more reproductive cells compared to male, thus female exposed much more hazard of ionizing radiation due to the reproductive cells radiosensitivity [25]. The International Commission on Radiological Protection (ICRP) also identified differences in radiation risk between males and females, even though ICRP follows a gender-neutral radiation protection policy. In 1990, the ICRP decided that there was no need to differentiate between genders when it comes to controlling occupational radiation exposure. In 2007, the ICRP released specific cancer risk data by gender as a reference, but it is not applicable for general radiation protection purposes [18]. Radiation protection should prioritize workers who are

confirmed to be pregnant, and fetuses should receive radiation protection similar to the general public [18]. Individuals of older age are sensitive to ionizing radiation, where the ability to repair or replace damaged cells due to ionizing radiation decreases [22]. Various other factors also need to be considered when examining the relationship between gender and age with occupational risk, such as a family history of cancer and the individual's lifestyle.

3.2.2 Respondent Education Background and Knowledge

The level of education and work experience is one of the elements considered to assess knowledge about the job to be performed. Theoretical and practical exposure is provided during higher education, while work experience is more related to individual experience. According to Table 7, the majority of respondents have education at the degree level, more than 10 years of work experience, and have attended at least one (1) radiation safety and protection course held internally within the past year. The survey results also indicate that all respondents with a diploma level of education are in the role of technologists, while other positions require either a degree or master's level of education.

Table 7 Analysis of educational level and work experience

Item	Total	Percentage
Education Level		
Diploma	5	31
Degree	7	44
Masters/PhD	4	25
Work experience		
1-3 years	1	6
3-6 years	1	6
6-9 years	5	32
More than 10 years	9	56
Number of trainings on radiation safety and protection in a year		
1 course	12	74
2 course	2	13
More than 3 course	2	13
Level of training		
In-house	16	100

The study on knowledge and awareness of radiation protection

indicates a correlation between work experience (years) and awareness of the hazards of radiation effects [24], [29]. However, specific research through surveys and observations needs to be conducted to assess the knowledge gap regarding radiation protection among IKN workers.

3.2.3 Workers' Behavioral Practices

Based on Figure 2, the majority of workers express positive opinions (agree and strongly agree) regarding the actions taken. However, a minority of workers also provide neutral opinions on the following items:

i. I put in extra effort to improve the safety of the workplace
ii. I voluntarily carry out tasks or activities that help improve safety
iii. I use all the necessary safety equipment to do my job

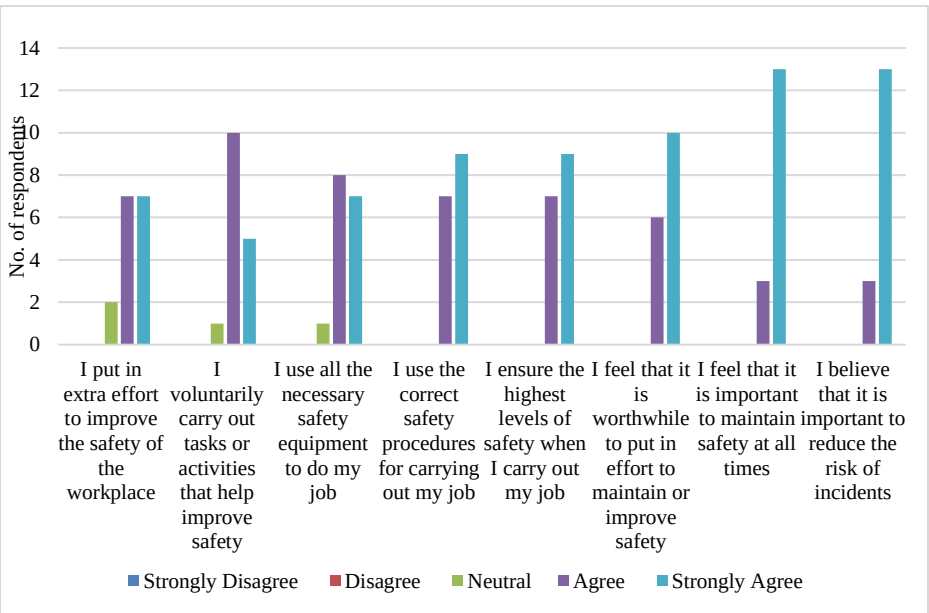

Figure 2: Survey findings on workers' opinions regarding safety aspects

Based on the items mentioned above, respondents who have more experience, specifically 6-9 years and more than 10 years, tend to choose the neutral option. Factors influencing this response may include the individual's perspective or experience, and the selection of a neutral

response does not lean towards agreeing or disagreeing. Respondents who choose the neutral option can be divided into 2 groups: those who genuinely hold a neutral opinion on the statement and those who lack sufficient knowledge or opinion on the statement [23]. This information does not significantly impact the study findings as it represents a minority opinion. In the medical field, ionizing radiation has become an unavoidable tool for the diagnosis and treatment of diseases, along its increased usage has led to both patients and healthcare professionals being exposed to radiation [12].Worker's awareness of the importance of safety aspects in the workplace helps reduce the likelihood of accidents occurring in the workplace [4].

Based on Figure 3, the frequency of workers' behaviours is also considered in this study as an added value to risk assessment. The majority of workers respond with often and very often, indicating a high awareness of safety among colleagues.

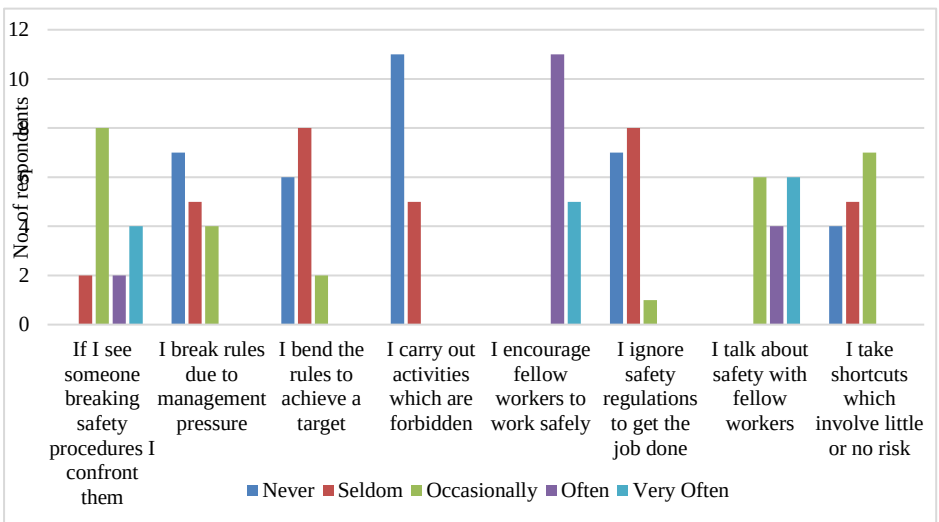

Figure 3: Survey findings on worker's behaviour

However, there are some points to emphasize, as there is a majority response indicating a frequency scale of seldom and occasionally for the following items:

i. If I see someone breaking safety procedures, I confront them
ii. I bend the rules to achieve a target

iii. I ignore safety regulations to get the job done
iv. I take shortcuts which involve little or no risk

Human factor is frequently tends to be one of the causes that can lead to an accidents in the workplace. The concept of human error is often associated solely with individual mistakes, but this issue also needs to be viewed from a new perspective, where individual assessments and actions are based on circumstances [7]. Workers in the healthcare sector provide critical services not only to identify problems but also to help identify the issue behind the problems, whether intentionally or unintentionally [14]. Work procedures need to be updated from time to time, considering the suitability of the work to reduce risks in the workplace.

In addition, there are occasionally and seldom responses, although they are not the majority response, for the following items:

i. I bend the rules to achieve a target

Among the things that can be associated with management pressure and regulatory violations are the pursuit of performance goals, attempts to save one's job and that of others, supervisory pressure, and requests from individuals who support or invest in the organization [11]. Management in any organization is a crucial element where employers in every organization should be responsible for ensuring the safety of every worker, especially when they carrying out their task. It is one of the general obligations of employers under the Occupational Safety and Health Act 1994 (Act 514), where employers are required to provide a safe workplace for their employees and others involved [9]. Therefore, employees and management need to apply the concept of good communication and continuously aim to improve the Occupational Safety and Health Management System (OSHMS). Management needs to design safety behaviour programs that facilitate the safety communication process, safety systems, and training. Employees who perceive that safety communication, safety systems, and training are positive or good are more likely to comply with safety regulations and procedures and voluntarily participate in safety activities [2].

3.3 Determination of Necessity of Internal Exposure

The majority of respondents in this study are pharmacists, while the minority are others, namely biochemist as shown in Table 8. All these workers are involved in various production processes leading to the use of radiopharmaceuticals.

Table 8: List of occupation

Occupation	Total
Pharmacist	5
Physicist	4
Technologist	5
Others (Biochemist)	2

Based on Table 9, there are 12 workers including biochemists, pharmacists, and technologists, who have final decision values, D, exceeding 1 mSv means require individual internal exposure monitoring while four workers including physicists have D values below 1 mSv that do not require individual internal exposure monitoring. Only 1 worker, a pharmacist does not require internal exposure monitoring for the Ga-68 radionuclide due to the assessment value, D, for this radionuclide below 0.1 mSv. In general, 75% of the workers involved in this study need to undergo individual internal exposure monitoring. Similar studies conducted showed that 71.9% and 100% of the workers in their studies [5], [35], respectively, needed individual internal exposure monitoring.

Table 9 Determination value of the necessity among IKN workers

Worker	Radionuclide	Operation	d_j	D
Worker 1 (Biochemist)	F-18	Quality control	1.72	1.72
Worker 2 (Biochemist)	F-18	Quality control	2.03	2.03
Worker 3 (Pharmacist)	Tc-99m	Dose fractionation (syringe)	0.25	27172.30
	Tc-99m	Ventilation study	0.33	
	Tc-99m	Dose administration (injection)	0.30	
	I-131	Dose fractionation (syringe)	266.60	
	I-131	Dose administration (oral)	26901.16	
	I-124	Dose fractionation (syringe)	0.16	
	Lu-177	Dose fractionation (syringe)	3.11	

	Y-90	Dose fractionation	0.38	
Worker 4 (Pharmacist)	F-18	Dose fractionation (vial)	7.61	12.29
	F-18	Dose fractionation (syringe)	1.65	
	Ga-68	Dose fractionation (vial)	0.06	
	Ga-68	Dose fractionation (syringe)	0.06	
	F-18	Dose administration (injection)	2.91	
Worker 5 (Pharmacist)	I-131	Dose fractionation (syringe)	743.73	76685.46
	I-131	Dose administration (oral)	75240.00	
	Tc-99m	Dose fractionation (syringe)	0.34	
	Tc-99m	Ventilation study	0.31	
	I-124	Dose fractionation (syringe)	0.10	
	I-124	Dose administration (oral)	9.97	
	Lu-177	Dose fractionation (syringe)	7.81	
	Lu-177	Dose administration (injection)	683.21	
Worker 6 (Pharmacist)	F-18	Dose fractionation (vial)	6.25	1695.07
	F-18	Dose fractionation (syringe)	0.24	
	Ga-68	Dose fractionation (vial)	0.27	
	Ga-68	Dose fractionation (syringe)	0.04	
	I-131	Dose fractionation (syringe)	14.05	
	I-131	Dose administration (oral)	1674.21	
Worker 7 (Pharmacist)	I-131	Dose fractionation (syringe)	601.19	59888.86
	I-131	Dose administration (oral)	59280.34	
	Tc-99m	Dose fractionation (syringe)	0.33	
	Tc-99m	Ventilation study	0.14	
	Tc-99m	Dose administration (injection)	0.26	
	I-124	Dose administration (oral)	6.61	
Worker 8 (Technologist)	Tc-99m	Dose fractionation (syringe)	0.01	97.30
	Tc-99m	Dose administration (injection)	9.25	
	I-131	Dose administration (oral)	88.04	
Worker 9 (Technologist)	Tc-99m	Dose fractionation (syringe)	0.03	164.16
	Tc-99m	Dose administration (injection)	43.52	
	Tc-99m	Ventilation study	0.30	
	I-131	Dose administration (oral)	119.67	
	F-18	Dose administration (injection)	0.64	
Worker 10 (Technologist)	Tc-99m	Dose fractionation (syringe)	0.04	106.93
	Tc-99m	Dose administration (injection)	19.74	
	Tc-99m	Ventilation study	0.31	
	I-131	Dose administration (oral)	8.58	
	Lu-177	Dose administration (injection)	78.27	
Worker 11 (Technologist)	Tc-99m	Dose fractionation (syringe)	0.02	49.67
	Tc-99m	Dose administration (injection)	12.40	
	Y-90	Dose administration (injection)	37.25	
Worker 12 (Technologist)	Tc-99m	Dose fractionation (syringe)	0.01	94.37
	Tc-99m	Dose administration (injection)	14.26	
	Tc-99m	Ventilation study	0.48	
	F-18	Dose administration (injection)	1.51	
	Ga-68	Dose administration (injection)	0.41	
	Lu-177	Dose administration (injection)	77.72	

Worker 13 (Physicist)	Tc-99m	Quality assurance	0.00	0.00
	F-18	Quality assurance (swab test)	0.00	
Worker 14 (Physicist)	Tc-99m	Quality assurance	0.00	0.00
	F-18	Quality assurance (swab test)	0.00	
Worker 15 (Physicist)	F-18	Quality assurance	0.00	0.14
	F-18	Quality assurance (swab test)	0.00	
	Tc-99m	Dose administration (injection)	0.14	
Worker 16 (Physicist)	Tc-99m	Quality assurance	0.00	0.00
	F-18	Quality assurance (swab test)	0.00	

The decision factors are based on variables such as inhalation dose coefficient for each radionuclide, the type of operation, cumulative annual radioactivity (mCi), and the protective measures used during operations. Pharmacists 3, 5, 6, and 7 have very high values of D from the iodine radiopharmaceutical source through the dose fractionation in the glovebox and the administration of I-131 doses orally in open areas. Although the determination values indicate values exceeding expectations, it still provides an indication that the potential for internal exposure is likely, and these workers require routine individual internal monitoring. The findings of this study are supported by a similar study where individual internal exposure monitoring should be included in the radiation protection plan for workers handling I-131 due to its high risk [6]. The same study has also been carried out in Chile and China, where workers handling I-131 and Tc-99m need to undergo individual internal exposure monitoring [3],[35]. Biochemists have the lowest decision factor. Biochemist also involved in RIA techniques [21], where this process only involves only external radiation exposure. The findings of this study also indicate that all physicist do not require individual internal exposure monitoring as they are not directly involved in the production, preparation, or administration of radiopharmaceuticals. Physicist involved with checking for any contamination on vials before it sent to customers or used by IKN. However, physicist also have the risk of individual internal exposure when there is any contamination during the calibration test. Additionally, the involvement of physicist in radiological emergency response and decontamination activities [17] at IKN could pose a risk of individual internal exposure. Therefore, physicist need to undergo immediate individual internal exposure monitoring when

deemed necessary. Individual internal exposure monitoring is conducted through direct measurements using a thyroid counter (for workers handling I-131) and a whole-body counter for radionuclides emitting gamma radiation [1]. Indirect bioassay measurements using urine samples can also assess internal exposure with low activity. The results of individual internal exposure monitoring need to be recorded in the medical record book (Section B) LPTA/BM/5 [8]. The total external and internal exposure should not exceed 20 mSv per year for these workers.

4.0 CONCLUSIONS

High risk assessments occur during the use of radiopharmaceuticals for the diagnosis and treatment of diseases, especially in the administration of doses through vapor or inhalation for lung scans, as well as the preparation and oral administration of doses to patients, particularly for radiopharmaceuticals containing I-131 and I-124. The behavioral practices survey shows that employees at IKN are aware of safety consciousness in the workplace. However, there are occasionally and seldom responses to the rule violations, lapses in vigilance, and the choice of shortcuts involving minimal risks. Initiatives to improve work procedures in a simpler way may help reduce the likelihood of safety rule violations and work-related risks. The research findings indicating that a total of 12 workers, consisting of biochemists, pharmacists and technologists require individual internal exposure monitoring, while 4 physicist ar exempt. This situation is due to the varying risk levels associated with their roles and potential exposure to hazardous materials. Targeting monitoring efforts towards these at-risk individuals is crucial for effective occupational health and safety management.

CONFLICT OF INTEREST
The authors declare that the research was conducted in the absence of any commercial or financial relationships that could be construed as a potential conflict of interest.

FUNDING
This research did not receive any specific grant from funding agencies in the public, commercial, or not-for-profit sectors.

ETHICAL APPROVAL

The Malaysian Research Ethics Committee and National Medical Research Registry approved this study under the protocol number NMRR ID-22-02767-DRO.

ACKNOWLEDGEMENT

We would like to thank the Director General of Health Malaysia for his permission to publish this article.

5.0 REFERENCES

[1] Abdullah, N., Shuib, N., Zahidi, K., Yapp, R., Loong, T., Ahmad, A. & Sarowi, S. Assessment of Internal Exposure for Radiation Workers Using Whole Body Counter. *Jurnal Sains Nuklear Malaysia*, vol. 32, pp. 31-37, 2020.

[2] Amponsah-Tawaih, K. & Adu, M. A. Work Pressure and Safety Behaviors among Health Workers in Ghana: The Moderating Role of Management Commitment to Safety. *Safety and Health at Work*, vol. 7, no. 4, pp. 340-34, 2016.

[3] Astudillo, R., Hermosilla, A., G.Diaz-Londono & Garcia, M. Assessing the Need for a Routine Monitoring Program in Three Nuclear Medicine Centers in Chile. *Radioprotection*, vol. 50,no. 2, pp. 141-144, 2015.

[4] Bakar, N. S., Yusri, U. N. M., Baharudin, N. A., Bahari, N. F. & Jaafar, S. Kajian Kesedaran Terhadap Faktor Keselamatan Dan Kesihatan Dalam Kalangan Pekerja Sektor Pembuatan. *Journal of Management & Muamalah*, vol. 8, 2018.

[5] Bento, J., Teles, P., Neves, M., Santos, A. I., Cardaso, G., Baretto, A., Alves, F., Guerreiro, C., Rodrigues, A., Santos, J. a. M., Parafita, R. & Matins, B. Study of Nuclear Medicines Practices in Portugasl from an Internal Dosimetry Perspective. *Radiation protection dosimetry*, vol. 149, no. 4, pp. 438-443, 2011.

[6] Dantas, B. M., Lucena, E. a. D. & Dantas, A. L. a. B. Internal Exposure in Nuclear Medicine: Application of IAEA Criteria to Determine the Need for Internal Monitoring. *Archives of Biology and Technology*, vol. 51, 2008.

[7] Dekker, S. *The Field Guide to Human Error Investigations.* Surrey: Ashgate Pub Ltd., 2002.

[8] Department of Atomic Energy. Rekod Perubatan (Seksyen B) Borang-Borang Rekod Dedahan Pekerja (Sinaran) LPTA/BM/5. Malaysia, Lembaga Perlesenanan Tenaga Atom., 1988.

[9] Department of Occupational Safety and Health. Garis Panduan Bagi Pengenalpastian Hazard, Penaksiran Risiko Dan Kawalan Risiko (HIRARC), 2008.

[10] Doerfel, H. R., Andrási, A., Bailey, M. R., Berkovski, V., Blanchardon, É., Castellani, C. M., Cruz-Suarez, R., Etherington, G., Hurtgen, C., Leguen, B., Malátová, I., Marsh, J. W. & Stather, J. W. 1 Rc6 Internal Dosimetry the Science and Art of Internal Dose Assessment., 2008.

[11] ECI. (2020). Pressure and Misconduct Are Linked. Available: 6 August 2023. https://www.ethics.org/pressure-in-the-workplace-risk-factors-and-tips-to-reduce-pressure/.

[12] Frane, N. & Bitterman, A. (2023). Radiation Safety and Protection. Available: 6 July 2023. https://www.ncbi.nlm.nih.gov/books/NBK557499/

[13] George, D. & Mallery, P. *Spss for Windows Step by Step: A Simple Guide and Reference, 11.0 Update*. 4th Edition. Boston: Allyn & Bacon, 2003.

[14] Henriksen, K., Dayton, E., Keyes, M. A., Carayon, P. & Hughes, R. *Chapter 5 Understanding Adverse Events: A Human Factors Framework.* Patient Safety and Quality: An Evidence-Based Handbook for Nurses. Rockville: Agency for Healthcare Research and Quality, 2008.

[15] IAEA. Assessment of Occupational Exposure Due to Intakes of Radionuclides – IAEA Safety Guide No.RS-G-1.2. Vienna, International Atomic Energy Agency, 1999.

[16] IAEA. IAEA Safety Culture Perception Questionnaire for License Holders. Vienna International Atomic Enery Agency**:** 24, 2017.

[17] IAEA. Guidance for Medical Physicists Responding to a Nuclear or Radiological Emergency. Vienna, International Atomic Energy Agency, 2020.

[18] ICRP. (2007). Ethical Foundations of the System of Radiological Protection.Available: 5 July 2023.https://www.icrp.org/consultation_viewitem.asp?guid=%7B5E08F73A-49AD-4644ADC9708029F68F9E%7D

[19] Institut Kanser Negara. (2013). Unit Kualiti. Available: 4 July 2023. https://nci.moh.gov.my/index.php/ms/perkhidmatan/2014-01-27-07-35-07/2014-01-27-07-56-04/unit-kualiti

[20] Ministry of Health of Malaysia. Standard Operating Procedure for Radioactive Contamination in Nuclear Medicine Department, 2017.

[21] Ministry of Health of Malaysia. Operational Policy in Nuclear Medicine Services, Ministry of Health of Malaysia, 2018.

[22] Krasin, M. J., Constine, L. S., Friedman, D. L. & Marks, L. B. Radiation-Related Treatment Effects across the Age Spectrum: Differences and Similarities or What the Old and Young Can Learn from Each Other. *Seminars in Radiation* Oncology, vol. 20, no. 1, pp. 21-29, 2010.

[23] Maness, M., Sheela, P. & Pinjari, S. B. A. When Neutral Responses on a Likert Scale Do Not Mean Opinion Neutrality: Accounting for Unsure Responses in a Hybrid Choice Modeling Framework. ITM, 2018.

[24] Mojiri, M. & Moghimbeigi, A. Awareness and Attitude of Radiographers Towards Radiation Protection. *Archives of Advances in Biosciences* vol. 2, no. 4, 2011.

[25] Narendran, N., Luzhna, L. & Kovalchuk, O. Sex Difference of Radiation Response in Occupational and Accidental Exposure. *Front Genet*, vol. 10, no. 260, 2019.

[26] National Research Council. *Health Risks from Exposure to Low Levels of Ionizing Radiation: Beir Vii Phase 2.* Washington, DC: The National Academies Press, 2006.

[27] Olson, M. Atomic Radiation Is More Harmful to Women. *Takoma Park, MD: Nuclear Information And Resource Service*, 2011.

[28] OSHA. (2022). Ergonomics. Available : 7 July 2023. https://www.osha.gov/ergonomics

[29] Su, W.-C., Huang, Y.-F., Chen, C.-C. & Chang, P.-S. Radiation Safety Knowledge of Medical Center Radiology Technologists in Southern Taiwan. *IRPA-10 Proceedings of the 10th international congress of the International Radiation Protection Association on harmonization of radiation, human life and the ecosystem*, 2000.

[30] Taber, K. S. The Use of Cronbach's Alpha When Developing and Reporting Research Instruments in Science Education. *Research in Science Education* vol. 48, no. 6, pp. 1273-1296, 2018.

[31] Tavakol, M. & Dennick, R. Making Sense of Cronbach's Alpha. *Int J Med Educ* 2(53-55), 2011.

[32] The University of Edinburgh. (2021). Radiation Risk Assessment Template.Available: 19 June 2023. https://www.docs.csg.ed.ac.uk/Safety/rpu/ra/rra.docx

[33] Universiti Malaya. (2022). Getting It Right – Ergonomics in the Workplace. Available: 3 July 2023. https://spm.um.edu.my/2022/10/30/getting-it-right-ergonomics-in-the-workplace/

[34] UNSCEAR. *Sources and Effects of Ionizing Radiation Volume I: Sources Report to the General Assembly Scientific Annexes a and B.* New York: United Nations, 2008.

[35] Wang, H.-B., Zhang, Q.-Z., Zhang, Z., Hou, C.-S., Li, W.-L., Yang, H. & Sun, Q.-F. Necessity of Internal Monitoring for Nuclear Medicine Staff in a Large Specialized Chinese Hospital. *International Journal of Environmental Research and Public Health* vol. 13, no. 418, 2016.

[36] Wrixon, A. D., Shaw, P. & Maslanyj, M. Radiation. Dlm. Ridley, J. & Channing, J. (editor). 7th Edition. *Safety at Work,* pp. 524-525. UK: Elsevier Ltd, 2008.

[37] Krajewska, Grażyna, and Paweł Krajewski. "Evaluation of internal exposure of nuclear medicine staff working with radioiodine in Poland". Int J Occup Med Environ Health. 36 no. 5 (2023): 587-595.

[38] Yazeed Alashban, Nasser Shubayr, Occupational Dose Assessment For Nuclear Medicine and Radiotherapy Technologists In Saudi Arabia, Radiation Protection Dosimetry, vol. 195, no. 1, pp. 50–55, 2021.

[39] Norhayati, A., Suzilawati, M. S., Khairunisa, Z. N., Raymond, Y. T. L., & Azimawati, A. Assessment of internal radiation exposure of nuclear medicine workers using whole body gamma counter. *In Journal of Physics: Conference Serie*s, vol. 1497, no. 1, pp. 012026, 2020.

KIDNEY CANCEROUS TUMOR PREDICTION USING CNN SYSTEM ARCHITECTURE

M.F. Shahoriar Titu[1*], H.M. Emon[1],
S.A. Aumi[1], M.S. Bhuiyan[1],
M.F. Murshid[1], M.R. Rahman[1]

[1]Electrical and Computer Engineering.
North South University, Dhaka, Bangladesh.

*Corresponding author(s). E-mail(s): fahim.shahoriar@northsouth.edu

Article History: Received March 2, 2024; Revised May 20, 2024; Accepted May 23, 2024

ABSTRACT: The study addresses the challenge of interobserver variability in the treatment decisions for kidney cancers, a concern highlighted by the anticipated 73,750 kidney cancer diagnoses in the United States in 2020. This variability often arises due to the subtle differences in imaging characteristics of tumor subtypes. To address this issue, we propose an end-to-end deep learning model leveraging multi-phase CT scans to differentiate between five primary histologic subtypes of kidney cancers, encompassing both benign and malignant tumors. The proposed model demonstrates remarkable precision in identifying kidney cancers, even those of minimal size. In preparing the data for analysis, we divided it into training and validation test sets. The training set was used to employ the random forest method for ranking potential predictors based on their predictive importance. The model's performance was then validated on the test set using leave-one-out cross-validation. This study utilized convolutional and recurrent neural networks to predict kidney cancer outcomes. We used the models to classify adenoma, adenocarcinoma, and non-neoplastic whole slide images (WSIs). The evaluation of our models was conducted using three distinct test sets. The results showed area under the curve scores of 0.97 and 0.99 for distinguishing between cancerous tumors and adenomas and 0.96 and 0.99 for differentiating between kidney cancer and adenomas, respectively. These findings suggest that our models are not only generalizable but also hold significant potential to integrate and deploy into realistic pathological diagnostic workflows of kidney cancer.

KEYWORDS: *Convolution Neural Network, Recurrent Neural Network, Annotations, Augmentations.*

1.0 INTRODUCTION

Kidney disease has affected more than 10% of people worldwide, killing an immense number of people reliably, and innumerable people go through dialysis to stay aware of their lives [1]. Most patients also suffer from fever, erupting, and kidney sufferings, so this disease unfavorably influence the patient's physiology. The objective of therapy is to differentiate minimal cystic renal cell carcinoma from renal injuries, which affects an array of potential treatment plans for patients [2]. Hence, creating a reliable and efficient approach for detecting renal alterations is crucial for patient management. In the medical field, diagnoses of kidney diseases often employ X-rays, CT scans, and B-ultrasounds. CT scans target a specific body area to obtain a cross-sectional or tomographic image of the area under scrutiny. This method can deliver accurate, three-dimensional data of the examined body part, making organs, structures, and injuries easily identifiable. It's ability to be layered is a significant advantage that offers the possibility to reveal more complex information on post-examination [3]. The idea of kidney cancerous tumor prediction employing deep learning techniques was initially proposed by Dong [4]. The authors proposed a non-invasive layer-by-layer planning computation to upgrade the significant development in light of the robust AI network. Profound learning estimations have, furthermore, been extensively used in clinical settings. Tune et al. [5] used the piece fleecy C-infers estimation and the better Grow Cut computation to section kidney pictures, and the customarily delivered seed names raised the division efficiency. Xiang et al. [6] used cortical models and nonuniform advisers to depict the kidney structure in CT pictures. Xiong et al. [7] implemented a disease division system considering flexible distributed level sets, which truly isolated kidney malignant growths in ultrasound pictures. Gao [8] united the level set into picture division to deal with images with unbalanced faint characteristics and achieved extraordinary division results. Hu and his colleagues [9] carried the goalfollowing instrument into the ordinary picture division and achieved incredible division results. These results show the critical advantages of using significant learning-based instruments and work process structures to help clinical analyzers and histopathological characterization, especially concerning extended beginning of screening capability and diminishing logical twofold

examination. Another area for further improvement is the drawn-out course of social occasions, a significant grouping of WSIs with precise pixel-by-pixel remarks, which makes it difficult to set up a managed learning classifier with an alternate plan of pictures. This strategy would require critical development in the number of WSIs and taking care of resources. Based on data from 45,642 WSIs, Campanella et al. [12] employed this technique and obtained terrific results. On a dataset of 45,542 WSIs, significant learning has recently been used to perceive WSIs in kidney and kidney cancer; however, it is on a restricted scale. Sharma et al. [13] endeavored kidney harmful development requests utilizing a [8] WSIs dataset. Profound learning has been used in kidney illness to anticipate general perseverance [14], recognize centres [15], and plan development [7]. In this work, various deep learning models have been applied to portray kidney and kidney cancer-threatening development to assist cautious specialists' standard histology discoveries. We combined two datasets of kidney and kidney growth WSIs, each containing 4,238 and 4,128 WSIs, respectively [16]. This study shows that pre-trained models achieved better exactness and approval exactness. The MobileNetv2 model achieves close to 100% exactness and 96% precision. VGG16 and InceptionV3 gave 98% and 97% exactness individually and accomplished a precision of 96% and 97% separately. ResNet50 gave somewhat less exactness and approval precision, which are 98.8% and 95% apiece. The proposed CNN model got 98% exactness and 97% approval precision. The pre-prepared and custom CNN models gave higher exactness and approval exactness than the past investigations.

2.0 MANUSCRIPT PREPARATION

The dataset employed in this work has been gathered from various reliable opensource destinations and afterward consolidated to make an extensive dataset. The dataset comprises CT pictures of kidney disease positive patients and typical patients. In the applied CNN model, three Conv2D layers, three MaxPooling2D layers, one smoothed layer, two thick layers, and a redressed direct unit enactment capability have been incorporated. The enactment capability utilized for the last thick layer was SoftMax. VGG16, MobileNetV2, InceptionV3, and ResNet50 were utilized for preprepared models, with minor changes in the last layers and a head model obtained from the essential model. Normal pooling, leveling, thick,

and dropout are the adaptable last layers. The CNN model is appropriate for highlight extraction since it removes qualities from provided pictures and learns and recognizes pictures in light of these elements. The intricacy of the learned attributes develops with each layer.

2.1 Materials and Tools

Python libraries are utilized to make AI, information science, information perception, picture and information control, and numerous applications. Given Python's broad library access, profound learning-based issues are especially effective with Python programming. Google Colab was utilized to deal with the vast datasets and prepare the model.

2.2 Dataset Description

The dataset utilized in this study consists of kidney CT pictures of 2,212 images [16]. The dataset has four classes, which are partitioned into an 8:1:1 ratio. The CT images of a Kidney Cancer patient and a normal patient are shown in Figure 1.

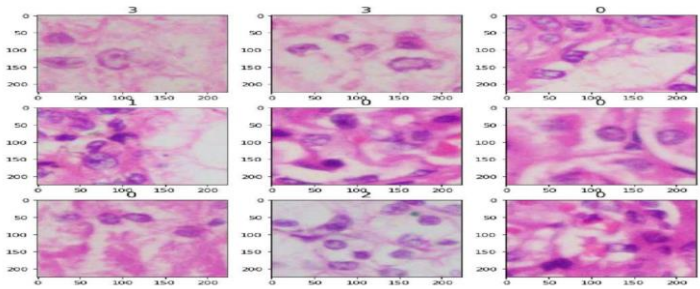

Figure 1: Sample CT images of the employed dataset

Next, the training images was fed traditional preprocessing techniques before fitting into the applied deep learning models, which included bringing in pictures of a particular size, separating the dataset, and using information expansion methodology. The precision was further developed once the model was fitted and hyperparameters were tweaked, employing the validation subset of images.

2.3 System Architecture

There are three channels in the input layer, and the info shape is 224×224. The channel size is 32 with cushioning, the portion size is 3, and the

enactment capability is ReLU in the principal layer of the proposed engineering. The main max- pooling layer follows, which has a pool size of 2 and steps of 1. The following layer is a level layer that joins each of the pooled highlights into one segment. Two thick layers were created eventually. The initiation capability for the primary layer is ReLU, though the enactment capability for the most un-thick layer is SoftMax. Figure 2 illustrates the architecture of the proposed CNN model.

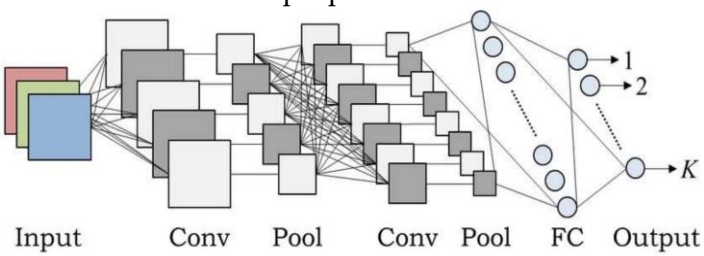

Figure 2: CNN System architecture

2.3.1 Convolutional Layer

The convolutional layer is the essential layer of the CNN. On CNN, it is the center structure block. Most of the calculations happens in this layer. Input information, a channel, and an included application are expected for this layer. In this layer, the information pictures have gone through a channel. The result of similar channels gets the capability map from the convolutional layer. In picture arrangement errands, at least one 2D lattices are viewed as the contribution to the convolutional layer and different 2D frameworks are started as the result. Information and result network numbers might be isolated [17]. The activations of the convolutional layer can be computed by using the following equation:

$$C_{ij} = \theta\left(\sum_{n=1}^{m} W_{n_1 s_1} P_{nt+1-t} + b_i\right) \quad (1)$$

where C_{ij} represents the output of the convention layer for the i^{th} feature map of the j^{th} band, m is the filter scale, W_n, i is the weight vector for the n^{th} band of the i^{th} filter, b_i denotes the bias for the i^{th} feature map, and Θ is the activation function.

2.3.2 Pooling Layer

The pooling layer is another fundamental structure block of CNN. In CNN's layers, the two most normal pooling frameworks are max pooling and normal pooling. The pooling layer eliminates the repetitive elements from the picture and makes the picture all around informed. While utilizing max pooling, the layer takes the limit of a locale from the channel's ongoing perspective each time and assists with the main elements of the picture. The normal pooling layer implies the worth of the ongoing perspective each time. A pooling layer is fundamental for reducing the quantity of element guides and organization boundaries, and a dropout layer forestalls overfitting. The activation of max pooling can be computed as:

$$P_{ij} = max_{k=1}^{t}\left(h_{i,(j-1)}(l+g)\right) \quad (2)$$

In (2), P_{ij} is determined by the i^{th} function map and the j^{th} band of the pooling layer. The pooling scale, represented by t, refers to the total number of bands that are pooled together. Additionally, the subsampling factor, symbolized by l , plays a crucial role in this process

2.3.3 Flattened Layer

After a grouping of convolutional and pooling procedure on the highlights portrayal of the pictures, the Straightened layer is utilized in the result pictures into a solitary long consistent direct exhibit or a vector. The most common way of changing over all the resultant 2D exhibits into a vector is called Leveling. A smoothed layer is ready for the following connected layer of picture grouping by changing over it into a one-layered cluster.

2.3.4 Fully Connected Layer

There are supports of completely associated layers after convolution and pooling layers in the CNN. CNN exceptionally relies upon completely associated layers. In PC vision picture acknowledgment and characterization, completely associated layers have been perceived as exceptionally valuable. The completely associated layer's bits of feedback function as results of the last pooling or convolutional layers, that are leveled and afterward kept in the completely associated layers. For the highest point of these learned elements, completely associated layers function as a categorizer. As a completely associated layer, the ReLU

initiation capability is generally utilized.

2.4 Pretrained Models

In this work, three CNN-based pre-prepared models were utilized, i.e., VGG16, MobileNetv2, and InceptionV3. The CT pictures are the initial step, and the stacking of a pre-prepared model is the second. Three preprepared models are stacked in the subsequent segment. The stacked pre-prepared models were changed involving the accompanying layers in the third part. Finally, the outcome will be introduced as Kidney Sickness contaminated and typical patients in the result area. The convolutional brain network Inceptionv3 has a profundity of 50 layers. With the ImageNet loads, the preprepared form of Inceptionv3 can sort up to 1,000 items. The ResNet50 model was additionally prepared utilizing the ImageNet dataset [19]. MobileNetV2 builds the state-of-the- art execution of adaptable models over a scope of model sizes on various tasks and seat stamps. In each line, MobileNetV2 works as a progression of n rehashing layers [20]. A basic portion can successfully remove the qualities from CT pictures [18]. VGG16 was utilized in this review and a fitting layer was added for the end product.

3.0 Results And Analysis

To conclude, five models had been trained using a trained generator and a validation generator. To train this model, a training and validation dataset was used. Train the custom CNN model and get 98% accuracy and 97% validation accuracy in the final epoch. The total number of epochs was 10. The model achieved satisfactory accuracy from the beginning. In the first epoch, it obtained 86% accuracy and 95% validation accuracy. The pre-trained model VGG16 has 98% accuracy and 96% validation accuracy in the 10th epoch; the training loss and validation loss were 3% and 8%, respectively.

Table 1: Performance Metrics of The Applied Models

Model	Accuracy (%)	Validation Acc (%)	Loss (%)	Validation Loss (%)
Custom CNN	98	97	3	8
MobileNetV2	99	96	14	62
VGG16	98	96	3	8
ResNet50	93	95	20	24
InceptionV3	97	97	32	20

MobileNetV2 secured the highest accuracy among the applied models, which is 99% accuracy and 96% validation accuracy. InceptionV3 has 97% accuracy and 97% validation accuracy. In InceptionV3, 32% training loss and 20% validation loss were observed. The histories of accuracy, validation accuracy, loss, and validation loss of the five models are given in Table 1.

Throughout this research, transfer learning was also used with four pre-trained models. The pre-trained models made much smoother predictions. In the VGG16 model, the accuracy was 98% and the validation accuracy was 96%. In the first epoch of the model, it obtained 92% accuracy and 95% validation accuracy. It gradually increased and obtained 98% accuracy in the 10th epoch. For validation accuracy, it secured 95% in the first epoch, increased to 99% at the 6th epoch, and gradually decreased to 96% at the 10th epoch. The model provided 3% training loss and 8% validation loss. In the first epoch, it provided a 20% training loss, which gradually decreased to 3% in the 10th epoch. For the validation loss, it provided 8% in the first epoch and also in the 10th epoch. In the middle epochs, it gradually decreased. MobileNetV2 provided the highest accuracy among these pre-trained models. It obtained 99% accuracy and 96% validation accuracy. Compared to the VGG16 model's accuracy, it got higher accuracy in the first epoch, which is 94%. Although their validation accuracy for the first epoch was the same, which is 95% for both models, MobileNetV2 has a 14% training loss and a 62% validation loss. In this case, MobileNetV2 did not provide a good validation loss. MobileNetV2's validation loss is 62%, which is the highest validation loss among these four models. The confusion matrix of the custom CNN model is shown in Figure 3.

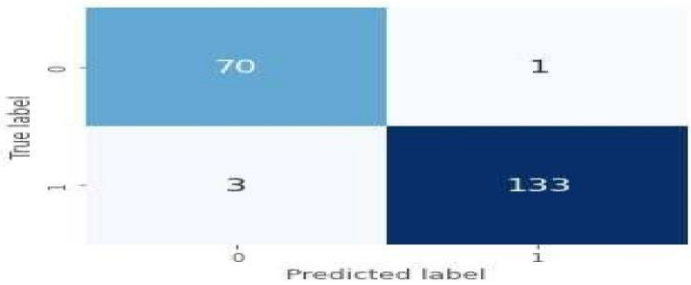

Figure 3: Confusion Matrix of the applied custom CNN model

Predictions, data, and features are the three major terms in error analysis. Error analysis based on prediction can be executed using a confusion matrix, where the percentage can be divided into false positives, false negatives, true positives, and true negatives. The size and nature of the data are also significant for error analysis. The precision of a dataset is defined as the ratio of accurate predictions to provide the total predictions. It can provide us with a brief overview of a model's training quality and potential performance. It does not, however, offer thorough instructions on how to apply it to the issue. When the expense of false positives is substantial, precision—also referred to as PPV—is an appropriate metric to employ. When the cost of false negatives is high, the optimal model is selected using the recall model metric. When the cost of false negatives is significant, recall becomes valuable. When attempting to assess how well recall and accuracy are balanced, an F1-score is required. It is a broad indicator of the correctness of the model. It integrates recollection and accuracy. Low false positives and false negatives are the keys to a high F1-score. During the model evaluation, the test dataset was utilized. This test dataset was created during the dataset split and was reserved solely for testing purposes. This study calculated the precision, recall, and F1-score for all the models utilizing the test dataset. Table 2 demonstrates the precision, recall, and F1-score of the applied VGG16, InceptionV3, MobileNetV2, ResNet50, and Custom CNN models for the proposed kidney cancerous tumor prediction system. It shows that VGG16 and InceptionV3 have the highest F1-score among all these models.

Table 2: Precision, Recall And F1 Score Of The Applied Models

Model	**State**	**Precision**	**Recall**	**F1**
Custom CNN	kidney cancer	0.89	0.97	0.93
Custom CNN	Normal	0.97	0.88	0.93
VGG16	kidney cancer	0.95	0.92	0.94
VGG16	Normal	0.92	0.96	0.94
InceptionV3	kidney cancer	0.96	0.89	0.93
InceptionV3	Normal	0.9	0.96	0.93
MobileNetV2	kidney cancer	0.97	0.88	0.92
MobileNetV2	Normal	0.89	0.97	0.93
ResNet50	kidney cancer	0.87	0.98	0.92
ResNet50	Normal	0.98	0.86	0.91

In this study, testing was conducted by feeding real-time CT images to the trained model. Once training had finished, the model was saved, and separate HDF5 files were generated for each of the four different models. These four files were used to make the predictions. Each model was fed an individual CT image as input, and following the input, the model predicted whether the image indicated kidney cancer or a normal CT image. Figure 4 illustrates the prediction result, indicating whether it belonged to a kidney cancer patient or a normal individual.

In Figure 4, a CT image affected by a kidney cyst was used as an input to the model. The model identified the CT image as a kidney cancer, which was predicted precisely.

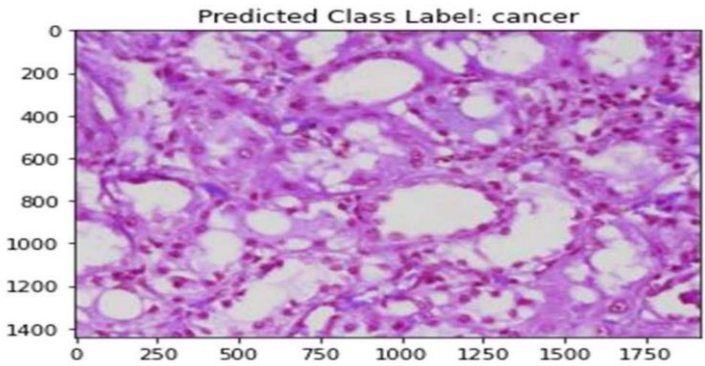

Figure 4: Sample CT image of the Kidney cancer affected result

Following the test, another image was fed as input, and the model correctly predicted it as a tumor-affected CT image. Figure 5 depicts the model's predictions of a tumor-affected CT image.

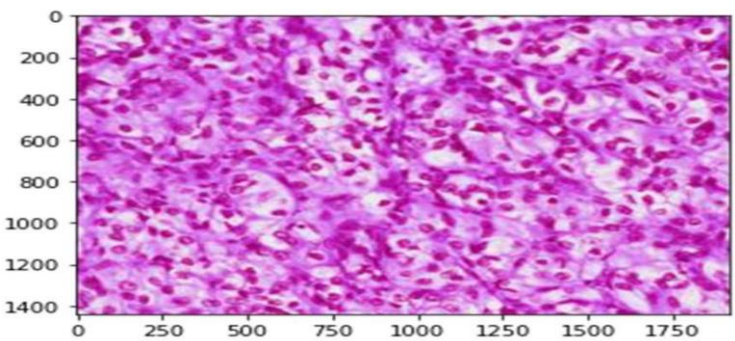

Figure 5: Sample CT image of the Normal result

Table 3 portrays that all the models had an excellent result. Pre-trained models demonstrated higher accuracy compared to the reference models. Comparatively inceptionV3, VGG16 and the custom CNN model had achieved the highest accuracy than the previously studied models. Mobile netV2 had attained the highest accuracy at 99%. VGG16 and InceptionV3 had achieved the level of accuracy respectively 98% & 97%. Which surpassed the accuracies reported in the referenced article (95.9% for VGG16 and 93% for inceptionV3). ResNet50 had achieved excellent accuracy level of 93.8%, Surpassing the performance in previous studies where it achieved 88% [14] and 92.6% [13] accuracy.

Table 3 Comparison Of This Work With Other Similar Systems

Reference	Model Name	Acc (%)	In this study (%)
[10]	VGG16	95.9	98
[12]	MobileNetV2	97.4	99
[11]	InceptionV3	93	97
[14]	ResNet50	88	93.8
[13]	ResNet50	92.6	93.8
[4]	Custom CNN	93	98
[5]	Custom CNN	94.5	98

4.0 CONCLUSION

This research proposes a deep learning technique for CT image-based kidney cancer diagnosis. We employed four pre-trained models and a bespoke CNN model to distinguish between benign and malignant kidney cancers. We demonstrated on a dataset of 2212 CT scans that our models outperformed the earlier techniques. Additionally, we provide some examples of confusion matrices and forecasts. Furthermore, we have identified the difficulties and consequences of our models for future research and clinical practice. We have suggested specific methods to enhance the data quality, incorporate more clinical details, and to expand the application of our models to different cancer types. Our research has attained excellent dependability by utilizing many popular deep-learning models and it has the potential to be the foundation for a system that aids physicians in using CT scans to identify kidney cancer. Future research could improve this system using this method, which might be enhanced by creating a web application and utilizing a larger dataset. This would raise the system's efficacy, accuracy, and outcomes. With further research and development kidney cancer will be diagnosed and identified at the earlier stage. Thus, the patient will get the essential therapy regarding the condition of the kidney cancer. It will help them to cure the cancer earlier and lead them to the sound life.

CONFLICT OF INTEREST STATEMENT

The authors have no conflicts of interest to declare and are in agreement with the contents of the manuscript.

ACKNOWLEDGMENTS

We extend our heartfelt gratitude to our collaborators for their invaluable support throughout this research.

5.0 REFERENCES

[1] R. L. Chevalier, Evolutionary nephrology," *Kidney International Reports*, vol. 2, pp. 302–317, 2017.

[2] J. Eichberger, Kidney symptoms start about five days after exposure, Johns Hopkins study finds — Hub,'' 2020.

[3] Y. M. Bar-On, A. Flamholz, R. Phillips, and R. Milo, Sars-cov-2 (Kidney cancer) by the numbers," *eLife*, vol. 9, 2020.

[4] L. Wang, Z. Q. Lin, and A. Wong, TUMOR-Net: A Tailored Deep Convolutional Neural Network Design for Detection of Kidney Cancer Cases from Kidney X-Ray Images,'' *Scientific Reports*, vol. 10, pp. 1– 12, 2020.

[5] M. Heidari, S. Mirniaharikandehei, A. Z. Khuzani, G. Danala, Y. Qiu, and B. Zheng, Improving the performance of CNN to predict the likelihood of Kidney Cancer using kidney X-ray images with preprocessing algorithms," *International Journal of Medical Informatics*, vol. 144, pp. 104284, 2020.

[6] A. Waheed, M. Goyal, D. Gupta, A. Khanna, F. Al-Turjman, and P. R. Pinheiro, TumorGAN: Data Augmentation Using Auxiliary Classifier GAN for Improved Kidney cancer Detection,'' *IEEE Access*, vol. 8, pp. 91916–91923, 2021.

[7] Q. Li, Z. Yu, Y. Wang and H. Zheng, TumorGAN: Data Augmentation Using Auxiliary Classifier GAN for Improved Kidney cancer Detection," *Sensors*, vol. 20, 2020.

[8] N. Narayan Das, N. Kumar, M. Kaur, V. Kumar, and D. Singh, Automated Deep Transfer Learning-Based Approach for Detection of Kidney Cancer Infection in Kidney X-rays,'' *IRBM*, 2020.

[9] S. Ying et al., Deep learning Enables Accurate Diagnosis of Novel Kidney (Kidney Cancer) with CT images," *medRxiv*, 2020.

[10] A. Shelke et al., Kidney X-ray Classification Using Deep Learning for Automated Kidney Cancer Screening,'' *SN Computer Science*, vol. 2, pp. 1–9, 2021.

[11] L. Gaur, U. Bhatia, N. Z. Jhanjhi, G. Muhammad, and M. Masud, Medical imagebased detection of Kidney Cancer using Deep Convolution Neural Networks," *Multimedia Systems 2021*, vol. 1, pp. 1– 10, 2021.

[12] I. D. Apostolopoulos and T. A. Mpesiana, Kidney cancer: automatic detection from X-ray images utilizing transfer learning with convolutional neural networks,'' *Physical and Engineering Sciences in Medicine*, vol. 43, 20202.

[13] A. M. Ismael and A. S¸engu¨r, Deep learning approaches for Kidney Cancer detection based on kidney X-ray images," *Expert Systems with Applications*, vol. 164, 2021.

[14] A. Uddin, B. Talukder, M. M. Khan, and A. Zaguia, Study on Convolutional Neural Network to Detect Kidney Cancer from Kidney X- Rays,'' *Mathematical Problems in Engineering*, vol. 2021, 2021.

[15] M. Alruwaili, A. Shehab, and S. Abd El-Ghany, Kidney Cancer Diagnosis Using an Enhanced Inception-ResNetV2 Deep Learning Model in X-RAY Images," *Journal of Healthcare Engineering*, vol. 2021, 2021.

[16] KIDNEY CANCER Radiography Database—Kaggle.'' https://www.kaggle.com/datasets/atreyamajumdar/kidney-cancer

[17] R. Nanculef, P. Radeva, and S. Balocco, Training Convolutional Nets to Detect˜ Calcified Plaque in IVUS Sequences," *Intravascular Ultrasound*, pp. 141–158, 2020.

[18] C. Sitaula and M. B. Hossain, Attention-based VGG-16 model for Kidney Cancer kidney X-ray image classification,'' *Applied Intelligence*, vol. 51, pp. 2850–2863, 2020.

[19] K. He, X. Zhang, S. Ren, and J. Sun, Deep Residual Learning for Image Recognition," *Conference on Computer Vision and Pattern Recognition*, vol. 2016, pp. 770– 778, 2015.

[20] M. Sandler, A. Howard, M. Zhu, A. Zhmoginov, and L. C. Chen, MobileNetV2: Inverted Residuals and Linear Bottlenecks,'' *Conference on Computer Vision and Pattern Recognition*, pp. 4510–4520, 2018.

EVALUATION OF ONLINE MEDICAL TECHNOLOGIST TRAINING COURSES CONDUCTED DURING THE COVID-19 PANDEMIC IN 2020 COMPARED WITH FACE-TO-FACE LECTURES IN 2019

K. Goto*

Faculty of Medical Technology, Teikyo University, Tokyo, Japan

*Corresponding Author's Email: gotok@med.teikyo-u.ac.jp

Article History: Received March 18, 2024; Revised April 3, 2024; Accepted April 5, 2024

ABSTRACT: This study compared students enrolled in face-to-face (F/F) lectures in 2019 to those who received online teaching (O/T) during the COVID-19 pandemic in 2020 in terms of class evaluation questionnaires, regular exams scores, and the national medical technologist qualifying examination. A statistical comparison of survey results and grades was conducted with 389 students (first- to fourth-year students) enrolled in the Department of Clinical Laboratory Medicine at Teikyo University's Faculty of Medical Technology in 2019 who received F/F lectures and 403 first- to fourth-year students enrolled in the same department in 2020 who received O/T entirely. Statistical significance was determined using a *t*-test with $p<0.05$ considered statistically significant. The class evaluation questionnaire results showed that students' self-study time, interest in the subject, and sense of achievement were significantly higher for first-, second-, and third-year students in F/F courses than those who received O/T lectures. However, this trend was reversed for fourth-year students. The fourth-year students scored much higher on the national medical technologist examination than the 2020 class. These results indicate that O/T education encourages students to learn independently, leading to improved performance. Therefore, this study suggests that education quality can be improved by combining O/T education with F/F education.

KEYWORDS: *COVID-19; Face-to-Face Lecture; Medical Technologist; Online Teaching; SDG4: Quality Education.*

1.0 INTRODUCTION

Various factors have been cited as problems in clinical laboratory technician education in four-year colleges and universities, including issues with academic performance during college entrance examinations [1] and maintaining motivation for continued learning after enrollment [2]. The COVID-19 pandemic changed social structures worldwide, and higher education was no exception, with face-to-face (F/F) lectures being replaced by online teaching (O/T). In Japan, O/T was practiced on satellite campuses and universities headquartered abroad before 2020. However, due to the pandemic, almost all F/F lectures were replaced with O/T lectures in April 2020. As of late 2020, 59.6% of universities held all lectures in the O/T format, and 19.9% of universities held 50–80% in the O/T format [3]. Although there have been several reports on the validation of O/T in higher education [4-6], few have specifically addressed the validation of O/T outcomes in medical technologist training. In the future, O/T lectures are expected to play an essential role in this area, as well as in venues such as flipped lectures.

Objectively examining the significance of online lectures is vital in unique situations such as the COVID-19 pandemic. In particular, the need for online medical education will increase as medical knowledge continues to expand. This study aims to investigate the usefulness of O/T and examine its associated problems in medical technologist education. This was done by comparing the results of a questionnaire survey and regular exam scores between first- to fourth-year students who were enrolled in F/F courses in 2019 and in O/T courses in 2020. Furthermore, we compared fourth-year F/F and O/T students' national medical technologist licensing exam scores.

2.0 MATERIALS AND METHODS

2.1 Participants

A total of 105 first-, 105 second-, 106 third-, and 73 fourth-year students were enrolled in the Department of Clinical Laboratory Medicine at Teikyo University School of Medical Technology, Japan, in the academic year 2019. A total of 91 first-year, 109 second-year, 105 third-year, and 98 fourth-year

students were enrolled in the same department in the academic year of 2020. Although the cohorts of first-, second-, and third-year students enrolled in 2019 and second-, third-, and fourth-year students enrolled in 2020 belong to the same group, the numbers do not necessarily match because of retention issues.

All department-affiliated students were surveyed, and their participation was voluntary. The questionnaire response rates were 90.8, 58.4, 89.2, 69.8, 56.7, 52.6, 41.0, and 43.9 %, respectively. Despite being assured that non-participation would not disadvantage them, some students did not participate. The reasons students chose not to participate in the survey were unknown. . Lecture Format

All lectures in FY2019 were given in F/F format, and all lectures in FY2020 were given on demand in O/T format using a learning management system (LMS). Regular examinations were conducted in both years in an F/F format and retained the same characteristics as in previous years in terms of timing and method. Each course was held 15 times over six months. In the F/F courses, each lecture lasted for 90 minutes. In the O/T courses, the lectures were conducted in an on-demand style, through which students viewed PowerPoint files with audio, which took approximately 30 minutes to complete.

2.2 Class Evaluation Questionnaire Survey

At the end of the academic year (March 2022 and March 2021), a survey was administered to students in first- to fourth-year students for class evaluation. This study was conducted in accordance with the ethical principles of the Declaration of Helsinki and the Ethical Guidelines for Life Sciences and Medical Research Involving Human Subjects. This study was approved by the Teikyo University Ethical Review Board for Medical and Health Research Involving Human Subjects (Approval No. Tei Rin 23-061). Consideration was given to ensure that the questionnaire responses could not be used to identify individual participants.

Informed consent was not obtained from participants because of the retrospective nature of the study. Although the researcher originally received the questionnaire survey results in a form that did not allow personal identification, the data of those who refused to participate were obtained from the office that conducted the survey. Similarly, the data of those who refused to participate in the study were deleted, and the results were recalculated and used as research data.

The survey items were shown in Table 1.

Table 1. The survey items

Question 1	Time spent preparing for this class in advance (preparation, review of previous classes, etc.). Response options—4: 90 min or more; 3: 30 min or more to less than 90 min; 2: Less than 30 min; 1: Not at all.
Question 2.	Did you read the assigned materials for this class in advance? Response options—4: I read them carefully; 3: I read them; 2: I did not have time to read them; 1: There were no specified materials.
Question 3	Did you achieve the objectives of this class? Response options—5: I achieved all of them; 4: I achieved almost all of them; 3: I achieved about half of them; 2: Not so much; 1: I did not understand the objectives.
Question 4	Did you find the instructor's speaking style clear and easy to listen to? Response options—5: Very clear; 4: Relatively good; 3: Average; 2: Not very good; 1: Poor.
Question 5	Was the instructor's writing style and use of visual aids (e.g., projectors) appropriate? Response options—5: Appropriate; 4: Relatively good; 3: Average; 2: Not very good; 1: Poor.
Question 6	Did you feel that the instructor tried to help you understand the content? Response options—5: Very much; 4: Relatively; 3: Fairly; 2: Not very much; 1: Not at all.
Question 7	Did your knowledge and skills increase after taking this class? Response options—5: Increased; 4: Slightly increased; 3: Cannot say; 2: Did not increase much; 1: Did not increase at all.
Question 8	Was the course designed to allow students to think and discuss among themselves? Response options—5: Agree; 4: Somewhat agree; 3: Neither agree nor disagree; 2: Do not really agree; 1: Do not agree at all.
Question 9	Did the instructors respond appropriately to students' questions and opinions? Response options—5: Agree; 4:

	Somewhat agree; 3: Neither agree nor disagree; 2: Do not really agree; 1: Do not agree at all.
Question 10	Did you find the content of this class interesting? Response options—5: Very interesting; 4: Relatively interesting; 3: Average; 2: Not very interesting; 1: Not interesting.
Question 11	On a scale of 1–5, how would you rate the course? Response options—5: Very good; 4: Somewhat good; 3: Average; 2: Somewhat poor; 1: Poor.

The survey results were presented as averages, with the total score divided by the number of students. The survey results were compared by cross-tabulating the 2019 and 2020 results for the scores on each survey item. Both were tested for significance using the $\chi 2$ test, and the results with $p<0.05$ were considered statistically significant.

The regular exam grades of students enrolled in 2019 and those enrolled in 2020 were compared; the courses for which grades were compared are listed below.

Courses administered in the first year included Basic Medical Theory, Chemistry, Clinical Physiology I, Human Body Structure and Function, Human Communication, Introduction to Medicine, Introduction to Microbiology, and Life Sciences I. The results for the eight subjects were compared. The courses conducted in the second year included Biochemistry, Clinical Laboratory Testing, Clinical Pathology I, Clinical Physiology II, Hematology Informatics, Histocytology, Immunology I, Laboratory Instrumentology, and Microbiology I. The results for the nine subjects were compared. The courses conducted in the third year included Advanced Clinical Examination, Clinical Chemistry II, Clinical Cytology, Clinical Microbiology, Clinical Pathology II, Clinical Physiology III, Genetic Testing, Hematology, Laboratory Management, Medical Electronics, Parasitology, Radiation Science, Special Topics in Pathology, and Team Medicine Exercises. The results for the 14 subjects were compared. The results of the graduation test and nationalexamination by medical technologists were compared for

fourth-year students.

For the above subjects, the total scores in 2019 and 2020 were divided by the number of students to obtain the mean score for each subject, and a *t*-test was used to test for significant differences; $P<0.05$ was considered statistically significant. The SPSS software (IBM SPSS Statistics, ver. 28.0.0.0 IBM Japan, Tokyo, Japan) was used for statistical analysis.

3.0 RESULTS

Table 2 summarizes the results of the class evaluation questionnaires conducted in the 2019 and 2020 academic years which shows the class formats of F/F and O/T, with significantly higher scores. The details of the results can be found in the Appendix section where Figures 1–11 present bar charts that were created based on the cross-table of the results of the class evaluation questionnaires.

In the comparison between F/F and O/T for first-year students, of the 11 questions, only Question 9 (faculty answered students' questions sincerely) was significantly higher in the F/F lecture evaluation. All remaining questions had significantly higher O/T ratings. In the comparison between F/F and O/T for second-year students, five of the 11 questions were rated significantly higher for O/T (Qs 1, 2, 5, 6, and 9), and four were rated significantly higher for F/F (Qs 3, 4, 10, and 11). In a comparison between F/F and O/T for third-year students, no items had significantly higher F/F ratings, and all items had significantly higher O/T ratings, except for Q4 and Q9, where no difference in ratings was found. However, a comparison between F/F and O/T for fourth-year students showed no items with significantly higher O/T ratings or significantly higher F/F ratings for Qs 4, 6, 9, and 11, but no differences in ratings for the other items.

Table 2. Highly rated face-to-face lectures held in 2019 and online teaching held in 2020

A summary of Figures 1–11

	Fiscal Year with Significantly High Evaluations for Each Question Item			
	1st-year student	2nd-year student	3rd-year student	4th-year student
Q1	O/T*	O/T	O/T	=**
Q2	O/T	O/T	O/T	=
Q3	O/T	F/F***	O/T	=
Q4	O/T	F/F	=	F/F
Q5	O/T	O/T	O/T	=
Q6	O/T	O/T	O/T	F/F
Q7	O/T	=	O/T	=
Q8	O/T	=	O/T	=
Q9	F/F	O/T	=	F/F
Q10	O/T	F/F	O/T	=
Q11	O/T	F/F	O/T	F/F

O/T*: The evaluation of remote lectures held in 2020 was significantly higher compared with the evaluation of face-to-face lectures held in 2019 ($P<0.05$).

(=)**: There was no significant difference between the evaluations of remote lectures held in 2020 and the evaluation of face-to-face lectures held in 2019 ($P>0.05$).
F/F***: The evaluation of the face-to-face lectures held in 2019 was significantly higher than the evaluation of the remote lectures held in 2020 ($P<0.05$).

The results of the regular test scores for F/F and O/T students received are listed in Table 3. Students who received O/T had significantly higher scores than those who received F/F lectures in five of the eight first-year courses

(Chemistry, Clinical Physiology I, Human Communication, Introduction to Microbiology, and Life Science I). Furthermore, the scores of students who took the F/F course were significantly higher than those of students who took the O/T course alone. The remaining six courses (Basic Medical Theory, Clinical Physiology I, Human Communication, Introduction to Microbiology, Human Body Structure and Function, and Introduction to Medicine) showed no difference in scores between the two groups, and none of the courses were scored higher by the F/F students. Of the nine courses offered in the second year, six (Biochemistry, Clinical Laboratory Testing, Clinical Pathology I, Clinical Physiology II, Immunology I, and Laboratory Instrumentology) scored significantly higher for students who took O/T courses, and one (Histocytology) scored significantly higher for students who took F/F courses. The remaining two courses (Hematology Informatics and Microbiology I) showed no differences. Five of the 14 third-year courses (Clinical Microbiology, Clinical Pathology II, Genetic Testing, Medical Electronics, and Radiation Science) had significantly higher scores among O/T students, and one course (Special Topics in Pathology) had significantly higher scores among F/F students. In the remaining eight courses (Advanced Clinical Examination, Clinical Chemistry II, Clinical Cytology, Clinical Physiology III, Hematology, and Laboratory Management), although there was no difference between the two groups regarding their scores on the fourth-year graduation examinations, the O/T students performed significantly better on the national medical technologist examination taken after graduation, as shown in Figure 12.

Table 3. Comparison of test scores for each subject in face-to-face lectures (F/F) in 2019 and online teaching (O/T) in 2020

Subject	Course year	F/F (2019)				O/T (2020)				t-test	
		Score (/100 score) except "*"	SD	n		Score (/100 score) except "*"	SD	n		P*	
Basic Medical Theory	1	83.32	12.59	101		83.58	10.21	90		0.876	
Chemistry	1	76.58	17.34	105		92.68	8.41	90		0.010	**
Clinical Physiology I	1	60.15	13.51	105		69.08	12.49	89		0.010	**
Human Body Structure and Function	1	72.14	19.79	102		72.68	17.68	87		0.840	

Human Communication	1	86.68	9.39	103		90.17	5.29	90		0.002	**
Introduction to Medicine	1	71.93	15.63	105		74.66	8.81	90		0.129	
Introduction to Microbiology	1	75.62	18.75	101		91.11	74.76	90		0.046	**
Life Science Ⅰ	1	77.42	10.23	105		83.81	8.50	90		0.010	**
Biochemistry	2	64.00	8.7	101		67.19	10.90	68		0.010	**
Clinical Laboratory Testing	2	67.87	12.51	101		74.21	13.62	68		0.002	**
Clinical Pathology Ⅰ	2	70.34	12.53	102		79.29	10.52	68		0.010	**
Clinical Physiology Ⅱ	2	59.22	11.81	104		65.09	12.47	66		0.002	**
Hematology Informatics	2	69.36	18.44	102		64.53	18.62	68		0.097	
Histocytology	2	71.88	15.75	102		67.16	12.34	67		0.031	***
Immunology Ⅰ	2	64.47	16.61	103		74.84	14.6	67		0.003	**
Laboratory Instrumentology	2	63.34	14.9	103		73.91	8.97	68		0.010	**
Microbiology Ⅰ	2	67.33	21.19	102		60.78	21.76	68		0.052	
Advanced Clinical Examination (/200 score)	3	129.84*	27.72	100		126.08	25.84	100		0.320	
Clinical Chemistry Ⅱ	3	65.78	10.43	104		67.90	10.99	102		0.156	
Clinical Cytology	3	79.39	13.17	104		80.43	11.11	102		0.540	
Clinical Microbiology	3	62.19	19.09	104		77.38	18.76	102		0.010	**
Clinical Pathology Ⅱ	3	70.04	12.66	98		75.22	11.35	98		0.003	**
Clinical Physiology Ⅲ	3	71.70	10.99	98		70.82	11.11	97		0.580	
Genetic Testing	3	71.24	8.96	104		80.55	10.56	102		0.010	**
Hematology	3	65.95	17.28	104		69.51	17.89	102		0.148	
Laboratory Management	3	72.85	9.56	102		75.26	10.69	97		0.090	
Medical Electronics	3	63.88	13.55	104		75.15	13.74	103		0.010	**

Parasitology	3	69.79	16.45	104		67.41	14.66	102		0.275	
Radiation Science	3	76.88	12.22	104		82.65	12.10	103		0.010	**
Special Topics in Pathology	3	85.42	1.39	96		80.29	6.15	104		0.010	***
Team Medicine Exercise	3	61.83	12.97	97		56.62	11.92	99		0.210	
Graduation test (/200 score)	4	125.12*	18.86	73		130.08	19.03	96		0.094	
National examination (/200 score)	4	140.5*	11.69	60		146.02	14.76	90		0.016	**

*:Scores/200, **:Score of O/T (2020) is significantly higher than that in 2019, ***:Score of F/F (2019) is significantly higher than that in 2020.

*:Scores/200, **:Score of O/T (2020) is significantly higher than that in 2019, ***: Score on F/F (2019) was significantly higher than that in 2020.

4.0 DISCUSSION

The COVID-19 pandemic had a significant impact on Japan. It impacted not only economic activities but also the education system, as most F/F classes have been replaced by O/T formats [7,8]. One major difference created by the pandemic, as revealed by the survey results, was that the average amount of time students spent on prior learning during O/T courses was significantly higher than that in F/F courses for students in all years except the fourth. Specifically, in the first year, 2.4% and 1.4% of students spent more than 90 minutes per day, 13.6% and 21.7% spent between 30 and 90 minutes per day, 38.9% and 51.0% spent less than 30 minutes per day, and 44.1% and 26.0% did not study on their own at all in 2019 and 2020, respectively.

Japanese university students tend to have less time to study at home; however, the implementation of O/T forces them to do so. The fourth-year students tended to voluntarily study at home for national examinations, even when enrolled in F/F courses. Prior research has shown that, regardless of the COVID-19 pandemic, 58.4% of students in the United States spend more than 11 hours per week on practical training [9], far more than Japanese students.

Students' final evaluations of lectures at the end of the school year (Q11) tended to be higher in 2020 for first- and third-year students, but in 2019 for second- and fourth-year students (first-year score average 2019 vs. 2020 = 3.73 vs. 4.25, second-year 3.69 vs. 3.90, third-year 3.78 vs. 3.77, fourth-year 3.94 vs. 3.52) (Figure 11). The results also indicated that second-year students, who are about to start their specialized education, need more detailed guidance through F/F education and that fourth-year students, who are about to take the national examination, need more guidance than second-year students receive through O/T, as do second-year students. This is a general tendency among the survey items. Second-year students tended to rate approximately half of the items higher in 2019.

Grades generally tended to be higher for students in 2020; that is, those who had experienced O/T. This phenomenon appears to be influenced by the longer time allocated to independent studies. Although there was no difference in graduation exam scores between the students enrolled in the F/F and O/T courses, the performance of 2020 students

on the national exam was higher than that of 2019 students, suggesting that O/T education is effective when simply focusing on passing the national exam. Incidentally, the national exam pass rates for new graduates were 86.5% in 2019 and 83.1% in 2020 [10], indicating no significant difference in the difficulty of the national exam.

Hospital training is required at medical universities, including medical technologist training universities. In FY2020, hospital training was either conducted in an observation-only format or consisted of O/T-based visual training. Although this study did not examine the impact of O/T on practical training, it was inferred that O/T lectures encouraged students to study independently and contributed to higher grades when focusing only on the national examination scores in 2020. Allowance for hospital training in O/T should be considered in the future [11]. Continuing online medical education, including practice, has the potential to improve the satisfaction, knowledge, and practice of general practitioners [12]. In the future, the quality of clinical technologist training could be improved by combining O/T education, which promotes students' independent study, with F/F [13].

5.0 CONCLUSION

O/T education is useful because it emphasizes student autonomy. Our results indicated that students who engaged in O/T learning scored higher than F/F-educated students in most courses offered on campus and the national exam for clinical laboratory technician certification. However, it is difficult to provide experience-based education through O/T learning. Based on these points, we believe that the quality of student education can be improved by combining O/T education, which encourages independent learning, with F/F education, which is advantageous for practical purposes. While O/T was found to be beneficial for improving student performance, this study did not consider its effects on creativity, independence, or discussion skills. Because one of the goals of undergraduate medical students is to obtain certification, future research should examine whether O/T plays a beneficial role in achieving these goals in higher education.

ACKNOWLEDGMENTS

I would like to thank Editage (www.editage.jp) for their English language editing.

Statements and Declarations

Funding: The authors did not receive support from any organization for the submitted work.

Data Availability Statement: Not applicable.

Author Contributions: The author confirms sole responsibility for the study conception and design, data collection, analysis and interpretation of the results, and manuscript preparation.

Compliance With Ethical Standards

Disclosure of Potential Conflicts of Interest: The authors have no relevant financial or nonfinancial interests to disclose.

Research Involving Human Participants and/or Animals: This study was conducted according to the ethical principles of the Declaration of Helsinki and the Ethical Guidelines for Life Sciences and Medical Research Involving Human Subjects. This study was approved by the Teikyo University Ethical Review Board for Medical and Health Research Involving Human Subjects (Approval No. Tei Rin 23-061).

Informed Consent: Informed consent was not obtained from any participants because of the retrospective nature of this study.

Consent to Publish: Not applicable.

6.0 REFERENCES

[1] K. Goto, "Measuring academic achievement using selected exam subjects", *Medical Technologies Journal*, vol. 3, no. 4, pp. 455-73, 2019.

[2] K. Goto, "Predicting failure to pass medical college graduation exam: Prediction of senior year medical students who do not pass the graduation exam by logistic analysis using data on gender, experience of repetition, and results of previous exams", *Medical Technologies Journal*, vol. 4, no. 1, pp. 497-503, 2020.

[3] Ministry of Education, Culture, Sports, Science and Technology. *Students and others affected by the new coronavirus infection Survey on Student Life (Results*) [Online]. In Japanese. Available: https://mext.go.jp/content/20210525-mxt_kouhou01-000004520_1.pdf.

[4] M. Riedel, G. Eisenkolb, N. Amann, A. Karge, B. Meyer, M. Tensil,

F.Recker, A.Dobberkau, F.Riedel, B.Kuschel, E.Klein. Experiences with alternative online lectures in medical education in obstetrics and gynecology during the COVID-19 pandemic-possible efficient and student-orientated models for the future?" *Archives of Gynecology and Obstetrics*, vol. 305, no. 4, pp. 1041-1053, 2022.

[5] J. Svatos, J. Holub, J. Fischer, J. Sobotka, "Online teaching of practical classed under the COVID-19 restrictions", *Measurement: Sensors*, vol. 22, 100378, 2022.

[6] T. Totlis, M. Tishukov, M. Piagkou, M. Kostares, K. Natsis, "Online educational methods vs. traditional teaching of anatomy during the COVID-19 pandemic", *Anatomy & Cell Biology*, vol. 54, no. 3, pp. 332-339, 2021.

[7] A. Naciri, M. Radid, A. Kharbach, G. Chemsi, "E-learning in health professions education during the COVID-19 pandemic: A systematic review", *Journal of Educational Evaluation for Health Professions*, vol. 18, p. 27, 2021.

[8] Q. Fan, H. Wang, W. Kong, W. Zhang, Z. Li, Y. Wang, "Online learning-related visual function impairment during and after the COVID-19 pandemic", *Frontiers in Public Health*, vol. 9, 645971, 2021.

[9] Ministry of Education, Culture, Sports, Science and Technology. *Current status of student study hours* [Online]. In Japanese. Available: https://www.mext.go.jp/b_menu/shingi/chukyo/chukyo4/siryo/attach/__icsFiles/afieldfile/2012/07/27/1323908_2.pdf.

[10] Ministry of Health, Labour and Welfare. *Announcement of successful completion of the National Examination for Clinical Laboratory Technicians.* In Japanese. Available: https://www.mhlw.go.jp/general/sikaku/successlist/2019/siken07/about.html.

[11] A. Alsoufi, A. Alsuyihili, A. Msherghi, A. Elhadi, H. Atiyah, A. Ashini, A.Ashwieb, M.Ghia, H.Ben Hasan, S.Abudabuos, H.Alameen, T.Abokhdhir, M.Anaiba, T.Nagib, A.Shuwayyah, R.Benothman, G.Arrefae, A.Alkhwayilai, A.Aihadi, A.Zaid, M.Eihadi. "Impact of the COVID-19 pandemic on medical education: Medical students' knowledge, attitudes, and practices regarding electronic learning", *PloS One*, vol. 15, no. 11, e0242905, 2020.

[12] I. Thepwongsa, C.N. Kirby, P. Schattner, L. Piterman, "Online continuing medical education (CME) for GPs: Does it work? A systematic review", *Australian Family Physician*, vol. 43, no. 10, pp. 717-721, 2014.

[13] M. Mortagy, A. Abdelhameed, P. Sexton, M. Olken, M.T. Hegazy, M.A. Gawad, F.Senna, I.A.Mahnoud, J.Shah, Egyptian Medical Education

Collaborative Group (EGY MedED), H.Aiash. "Online medical education in Egypt during the COVID-19 pandemic: A nationwide assessment of medical students' usage and perceptions", *BMC Medical Education*, vol. 22, no. 1, p. 218, 2022.

FIGURE LEGEND

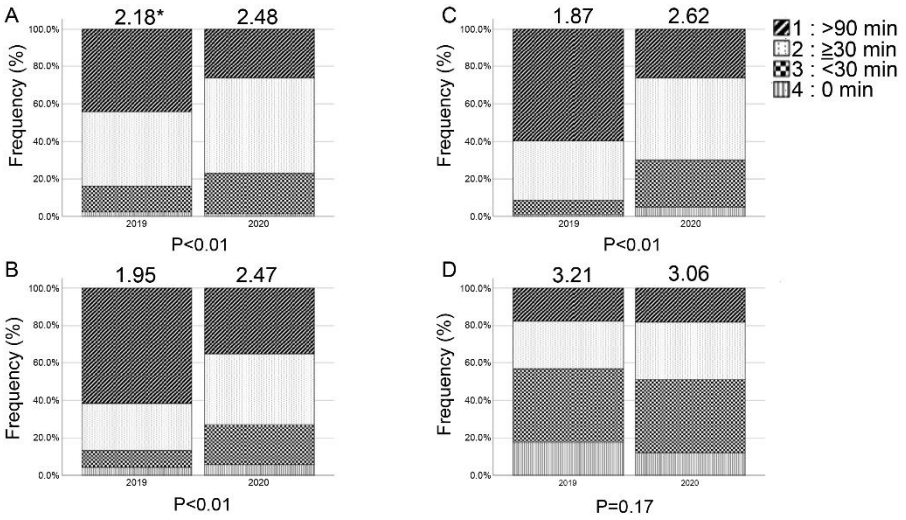

Figure 1: Custer bar graph of self-study time at home for first- through fourth-year students enrolled in 2019 and 2020. The length of self-study time was categorized as 4: *>90 minutes*, 3: *>30 minutes*, *<90 minutes*, 2: *<30 minutes*, and 1: *0 minutes*. Significant differences (p-values) in both years were determined by the $\chi 2$ test of cross-tabulation: A represents first-year, B represents second-year, C represents third-year, and D represents fourth-year students.

* Mean scores are shown.

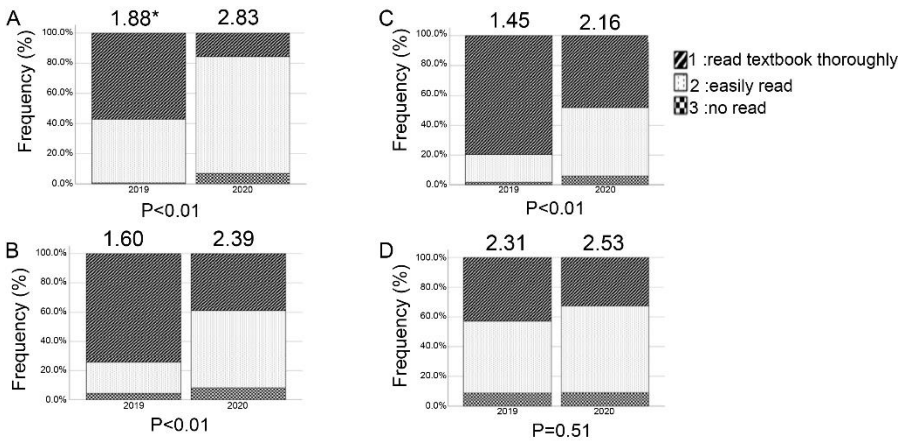

Figure 2: Cluster bar graph of whether students in years one to four enrolled in 2019 and 2020 read the textbook in advance, categorized as 3: *Read carefully*, 2: *Skimmed through*, and 1: *Did not read*. Significant differences (p-values) in both years were determined by the $\chi 2$ test of cross-tabulation: A represents first-year, B represents second-year, C represents third-year, and D represents fourth-year students.

* Mean scores are shown.

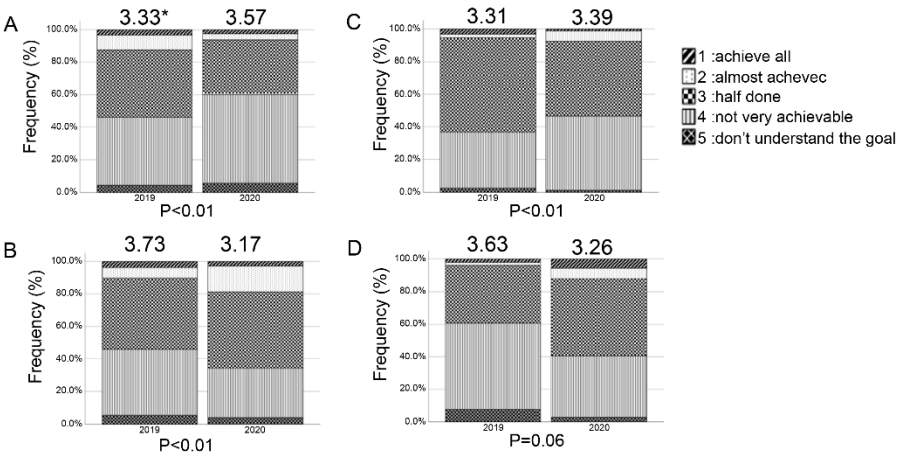

Figure 3: Cluster bar graph of first through fourth-year students enrolled in the 2019 and 2020 academic years asking if they were able to meet the achievement goals of the course, categorized as 5: *I met all goals*, 4: *I met most goals*, 3: *I met about half goals*, 2: *I did not meet many goals*, and 1: *I did not understand the achievement goals*. Significant differences (p-values) between the two years were determined by the $\chi 2$ test of cross-tabulation: A represents first-year, B represents second-year, C represents third-year, and D represents fourth-year students.

* indicates mean score.

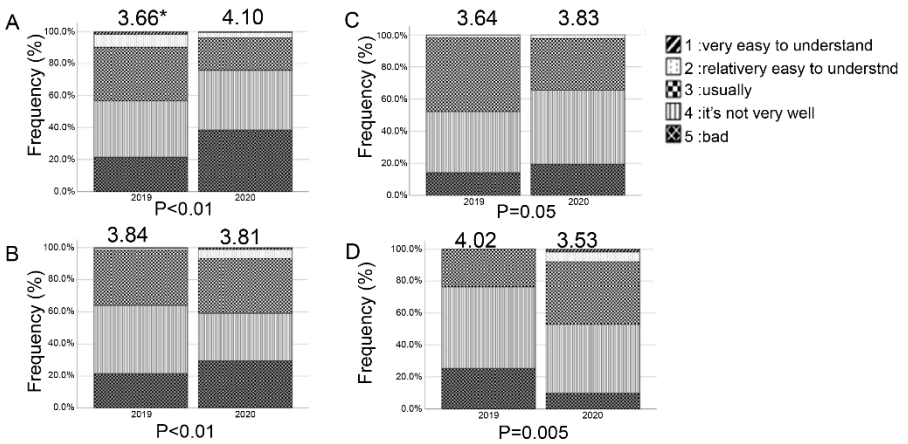

Figure 4: Cluster bar graph of responses to the question of whether the teacher's speech was clear and easy to listen to for first- through fourth-year students enrolled in 2019 and 2020, categorized as 5: *Very clear*, 4: *Relatively good*, 3: *Average*, 2: *Not very good*, 1: *Poor*. Significant differences (p-values) between years were determined by the $\chi 2$ test of cross-tabulation: A represents first-year, B represents second-year, C represents third-year, and D represents fourth-year students.

* Mean scores are shown.

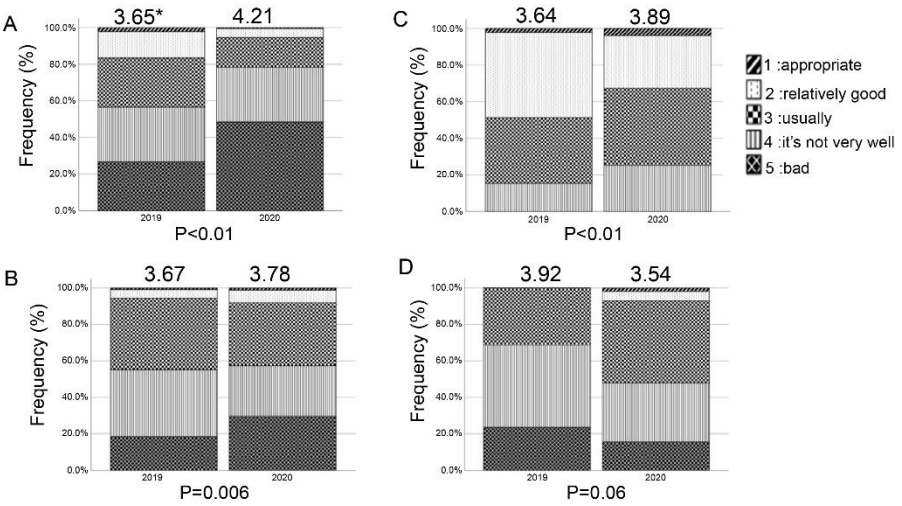

Figure 5: Cluster bar graph of responses to the question of whether the teacher's writing style and use of visual aids (e.g., projector) were appropriate for first- through fourth-year students enrolled in 2019 and 2020, categorized as 5: *Appropriate*, 4: *Relatively good*, 3: *Average*, 2: *Not very good*, 1: *Poor*. Significant differences (p-values) between the two years were determined by the $\chi 2$ test of cross-tabulation.

* indicates mean score.

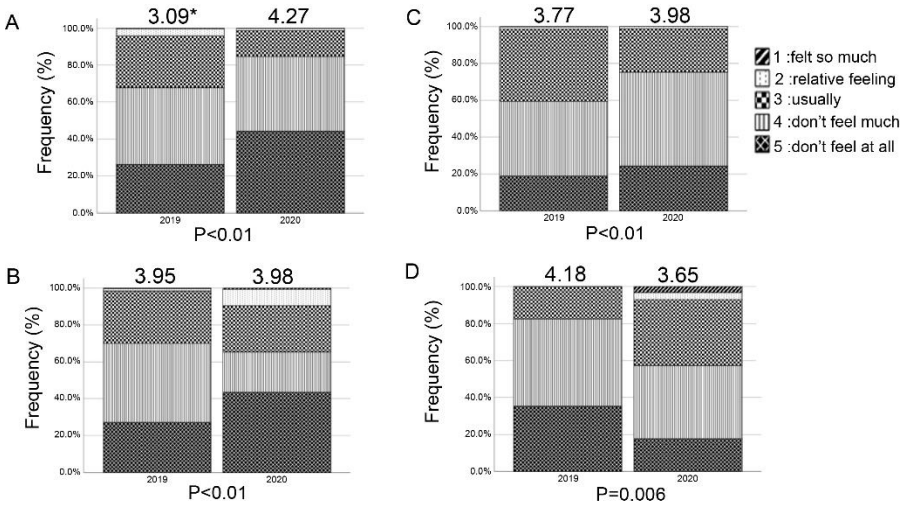

Figure 6: Cluster bar graph of responses to the question of whether teachers made an effort to make students understand the content in first- through fourth-year students enrolled in 2019 and 2020, categorized as 5: *Very much*, 4: *Relatively much*, 3: *Fairly much*, 2: *Not much*, 1: *Not at all*. The cross-tabulation was classified as follows. Significant differences (p-values) between the two years were determined by the $\chi 2$ test of cross-tabulation.

* Mean scores are shown.

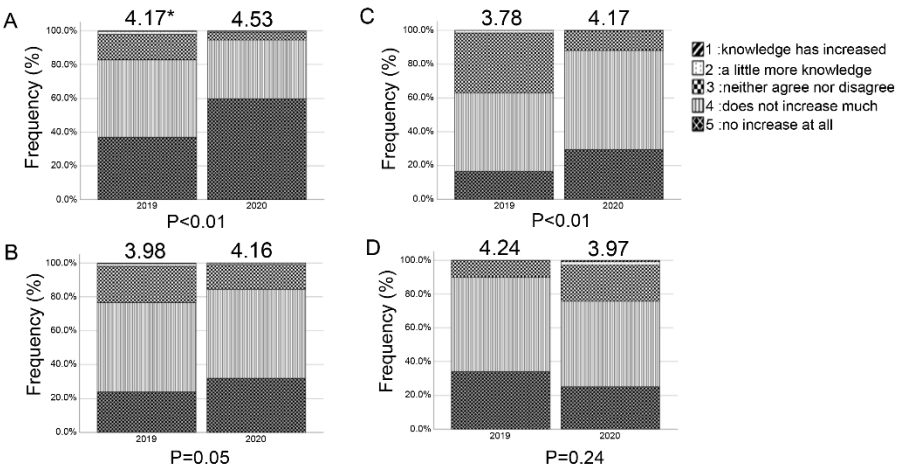

Figure 7: Cluster bar graph of responses to the question of whether knowledge and skills increased before and after taking this class for first- through fourth-year students enrolled in 2019 and 2020, categorized as 5: *Increased*, 4: *Increased somewhat*, 3: *Undecided*, 2: *Did not increase much*, 1: *Did not increase at all*. Significant differences (p-values) between the two years were determined by the $\chi 2$ test of cross-tabulation.

* indicates mean score.

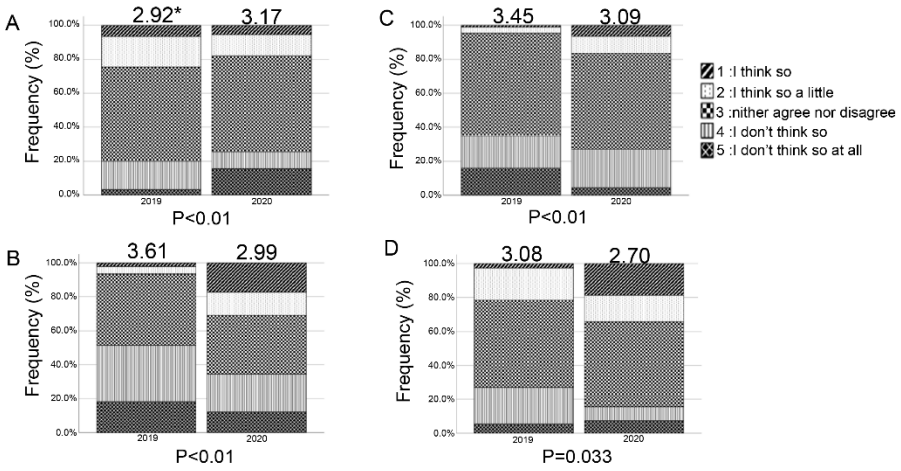

Figure 8: Cluster bar graph of responses to the question of whether students were encouraged to think and discuss issues on their own for first- through fourth-year students enrolled in 2019 and 2020, categorized as 5: *Agree*, 4: *Somewhat agree*, 3: *Undecided*, 2: *Do not really agree*, 1: *Do not at all agree*. Significant differences (p-values) between the two years were determined by the $\chi 2$ test of cross-tabulation.

* Mean scores are shown.

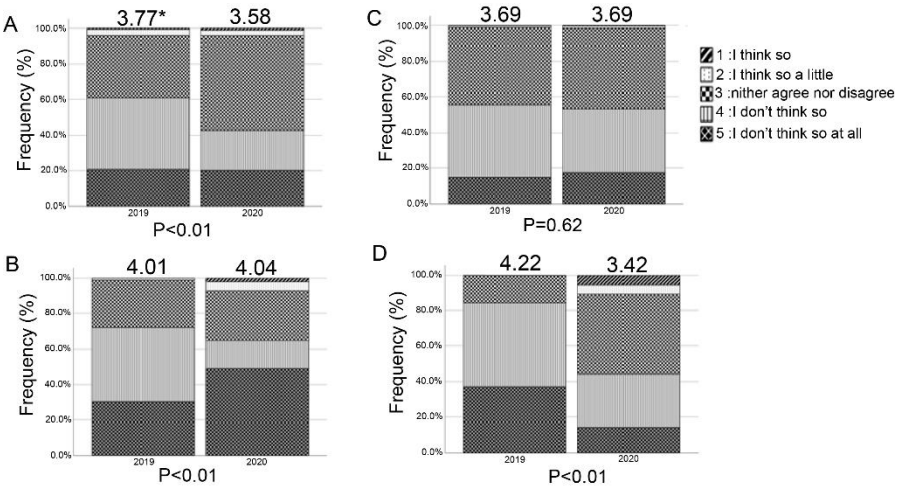

Figure 9: Cluster bar graph of responses to the question of whether faculty members responded appropriately to students' questions and opinions for first- through fourth-year students enrolled in 2019 and 2020, categorized as 5: *Agree*, 4: *Somewhat agree*, 3: *Neither agree nor disagree*, 2: *Do not agree*, 1: *Do not agree at all*. Significant differences (p-values) between the two years were determined by the $\chi 2$ test of cross-tabulation.

* indicates mean score.

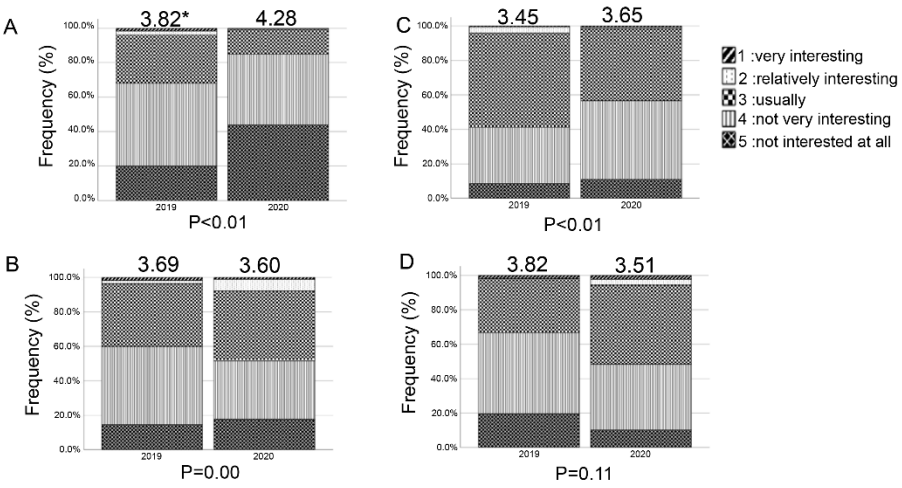

Figure 10: Cluster bar graph of responses to the question of whether first- through fourth-year students enrolled in 2019 and 2020 found the content of this course interesting, categorized as 5: *Very interesting*, 4: *Relatively interesting*, 3: *Normal*, 2: *Not very interesting*, or 1: *Not interesting*. The cross-tabulation $\chi 2$ test was performed. Significant differences (p-values) between years were determined by the $\chi 2$ test of cross-tabulation.

* Mean scores are shown.

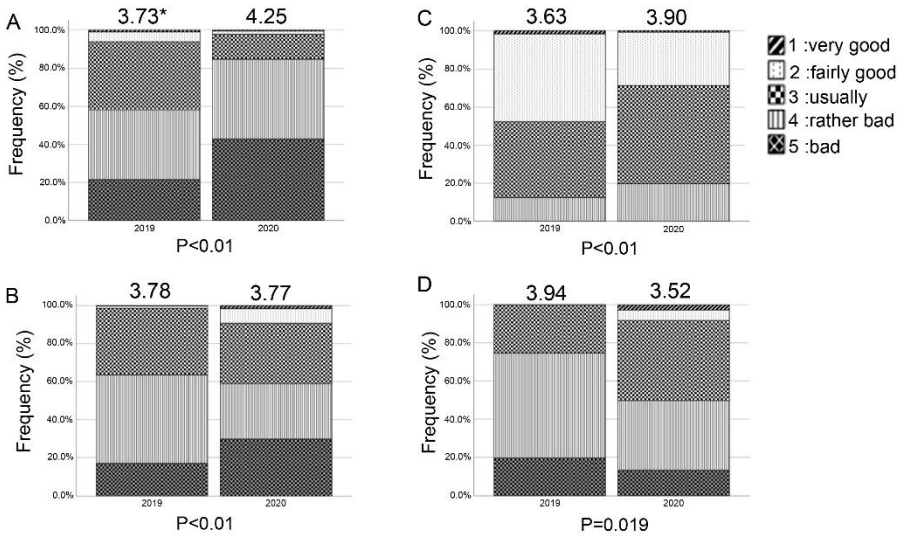

Figure 11: Cluster bar graph of responses to overall lecture evaluations for first- through fourth-year students enrolled in 2019 and 2020, categorized as 5: *Very good*, 4: *Somewhat good*, 3: *Average*, 2: *Somewhat poor*, 1: *Poor*. Significant differences (p-values) between the two years were determined by $\chi 2$ test of cross-tabulation: A represents first-year, B represents second-year, C represents third-year, and D represents fourth-year students.

* Mean scores are shown.

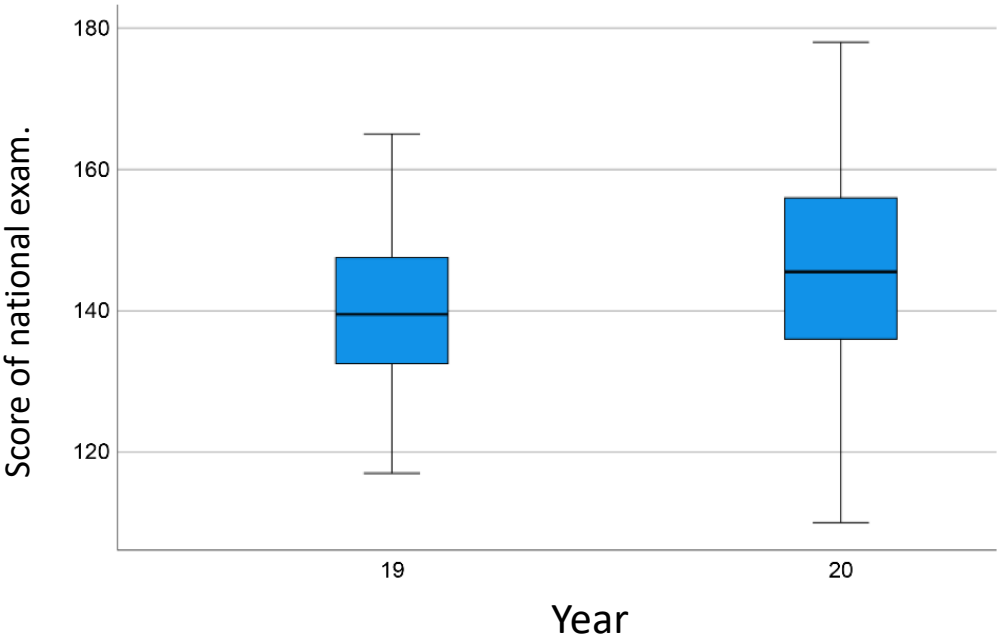

Figure 12: National Clinical Laboratory Technician National Examination scores in 2019 and 2020; the score for 2019 was 140.50 and for 2020 was 146.02 (out of 200), with the score for 2020 being significantly higher (P = 0.01).

DOSIMETRIC CHARACTERISATION OF THE NANODOT OPTICALLY STIMULATED LUMINESCENT DOSIMETER FOR USE IN NATIONAL ELECTRON BEAM DOSIMETRY AUDIT SERVICES FOR RADIOTHERAPY FACILITIES

N. Abdullah[1,2,*], N. Mohd Noor[1,3,*], Z. Kamarul Zaman[4], M. Mohammad Zahid[5], N.M Ung[6]

[1]Medical Physics Laboratory, Department of Radiology, Faculty of Medicine and Health Sciences, Universiti Putra Malaysia, 43400 Serdang, Selangor, Malaysia
[2]Medical Physics Laboratory, Radiation Metrology Group, Malaysian Nuclear Agency, 43000 Kajang, Selangor, Malaysia
[3]Medical Physics Unit, Hospital Sultan Abdul Aziz Shah, Universiti Putra Malaysia, 43400 Serdang, Selangor, Malaysia
[4]Department of Medical Physics, University of Malaya Medical Centre, 59100 Kuala Lumpur, Malaysia
[5]Department of Radiotherapy and Oncology, National Cancer Institute, 62250 WP Putrajaya, Malaysia
[6]Dean Office, Faculty of Medicine, University of Malaya, 59100 Kuala Lumpur, Malaysia

[*]Corresponding Authors' Email: [1,2]hayatie@nm.gov.my; [1,3]noramaliza@upm.edu.my

Article History: Received April 24, 2024; Revised May 14, 2024; Accepted May 17, 2024

ABSTRACT: The Malaysian Nuclear Agency's secondary standard dosimetry laboratory (SSDL) aims to establish a national dosimetry audit service for radiotherapy facilities. For this purpose, a nanoDot optically stimulated luminescent dosimeter (OSLD) was

selected as the transfer dosimeter for the audit program. The study aims to establish the basic dosimetric characteristics and associated correction factors of nanoDot OSLD for use in electron beam dosimetry audits. An investigation of the dosimetric characteristics of the nanoDot, comprising the sensitivity correction factor (SCF), dose-response linearity, beam energy dependency, signal depletion per readout, and signal fading when subjected to electron beams, was conducted. A preliminary electron beam dosimetry audit using nanoDot OSLD was performed for two radiotherapy facilities under both reference and non-reference conditions. The measurement uncertainty of the absorbed dose for the nanoDot OSLD was also estimated. The mean SCF of the 91 nanoDot OSLD was 1.001 ± 0.25%. The dose-response curves for the 6 MeV and 9 MeV beams exhibited linear characteristics, with a determination coefficient of 0.9982 for the dose range of 50–300 cGy. However, a high energy dependency was observed at 12 MeV, resulting in a deviation of 4.08% compared to that at 6 MeV. The nanoDot signal decreased by 0.03% after 100 readouts and faded by 3.20% at 70 days post-irradiation. It is noteworthy that all audit results from the six electron beams were in compliance with the tolerance limit of ± 5%, with mean dose deviations of -1.66% ± 0.81% and -1.37% ± 0.65% for the reference and non-reference conditions, respectively. The combined uncertainty was estimated to be ± 1.41% (coverage factor, k = 1). National electron beam dosimetry audits using nanoDot OSLD can now be implemented as a regular service.

KEYWORDS: *radiotherapy dosimetry audit; electron beam; optically stimulated luminescent dosimeter; nanoDot OSLD.*

1.0 INTRODUCTION

Safe and effective radiotherapy relies on the accuracy of dose delivery to the target volume in the patient, which is typically within ± 5% of the prescribed dose at a 95% confidence level, as recommended by the International Commission on Radiation Units and Measurements (ICRU)[1]. Any errors in radiotherapy dosimetry can lead to radiation injuries and severe complications [2]. To prevent such errors, dosimetry audits are conducted at the national or international level as part of the quality assurance program (QAP) in radiotherapy. These audits have been successful in identifying errors, providing support for identifying the sources of errors, and rectifying them [3], [4]. The audit also serves as an early error detection mechanism, which is essential for taking prompt corrective action to safeguard patients from potential harm. This practice will improve dosimetry practices and reduce the likelihood of errors occurring, ultimately affecting patient health [5]. According to D. Van Der Merve [6], an independent dosimetry audit should be performed for every new installation and regularly. This is crucial because dosimetry audits provide medical physicists with confidence in applying new radiotherapy modalities and techniques [7].

In keeping with the International Atomic Energy Agency (IAEA) guidelines, Malaysian radiotherapy facilities have actively participated in IAEA/World Health Organization (WHO) postal radiotherapy dosimetry audits since 2011, with a focus on assessing the absorbed dose of water from photon beams under reference conditions [8]. Presently, there are 35 radiotherapy centres in the country, comprising seven government hospitals and 28 private facilities [9]. One government-funded radiotherapy service was provided through a contract with a private

institution. In total, 93 radiotherapy modalities are available, including 57 medical linear accelerators (linac), 19 brachytherapy, 7 intra-operative radiotherapy (IORT), 5 tomotherapy, 3 gamma knife, and 2 cyberknife [10]. On average, seven radiotherapy centres in Malaysia participate in the IAEA audit annually, with the highest participation reaching 12 centres in 2022. The IAEA audit results from 2011 to 2022 found that out of 202 beams checked, the majority (93%) were satisfied with an acceptance limit of ±5%, except for 13 photon beams (6%) and three electron beams (2%) [11]. Despite the low failure rate, this situation poses a severe risk of radiation injuries and, in extreme cases, death if not addressed promptly. Until recently, no national remote dosimetry audits had been conducted in Malaysia, as a national dosimetry audit network (DAN) has not yet been established. An international review of remote dosimetry audits indicated that electron beams are more susceptible to errors than photon beams [12], [13]. In 2021, the International Atomic Energy Agency (IAEA) initiated the Electron Audit Service for its member states, with one facility from Malaysia participating [14]. Therefore, establishing a national dosimetry audit for electron beams is crucial because of insufficient access to radiotherapy centres for IAEA audits, as priority is given to new linac installations.

Generally, electron remote dosimetry audits are limited to the measurement of the electron beam output under reference conditions [15], [16], with some additional parameters tested for on-site audits [17], [18], [19]. For this purpose, various detectors have been employed, including alanine, ionisation chambers, and radio photoluminescent glass dosimeters (RPLD). Each dosimeter has exclusive advantages; however, the nanoDot optically stimulated luminescent dosimeter (OSLD), one of the most versatile dosimetry systems with great dosimetric characteristics and convenience of use for a large-scale audit, is preferable for remote dosimetry audits [20], [21]. Several studies have

described the dosimetric characteristics of nanoDot OSLD for radiotherapy dosimetry applications [22], [23], [24], [25]. However, this study is the first to present the establishment of dosimetric characteristics and their associated correction factors for nanoDot OSLDs for remote radiotherapy dosimetry audits using electron beams for reference and non-reference conditions. These characteristics include (i) dosimeter sensitivity, (ii) dose-response linearity, (iii) beam energy dependency, (iv) signal depletion, (v) signal fading, and (vi) readout reproducibility. This was followed by the fabrication and testing of the newly fabricated nanoDot OSLD holder for electron beam audit, implementation of a preliminary dosimetry audit for electron beams in reference and non-reference conditions, and relevant measurement uncertainty of the absorbed dose from nanoDot OSLD.

2.0 METHODOLOGY

2.1 NanoDot optically stimulated luminescence dosimetry system

This study utilized a nanoDot optically stimulated luminescence (OSL) dosimetry system procured from Landauer Inc. (Gleenwood, USA). The nanoDot OSL material was made of Aluminum Oxide doped with Carbon (Al_2O_3:C) and has a thickness of 0.12 cm and a diameter of 0.5 cm. It is encased in a 1 cm × 1 cm × 0.18 cm light-tight plastic case with a mass density of 1.03 g/cm^3 to protect it from light-induced signal fading. The OSL material in the disc can easily slide out of its plastic casing during the readout and optical bleaching processes. The nanoDot was read using an InLight MicroStar system installed with MicroStar software version 4.3. During the readout process, the OSL material was exposed to green light (540 nm wavelength). This process triggered the dosimeter to emit blue light with a wavelength of 430 nm,

and the light signals were counted using a photomultiplier tube (PMT). The OSL signals were then converted to the actual absorbed dose in Gray by multiplying with the relevant correction factors.

To minimise errors due to accumulative background signals, pre-irradiation OSL signals were recorded by reading the nanoDot within one day before irradiation. Between the irradiation and readout periods, the nanoDots were kept in a closed cabinet at room temperature to minimise sensitivity and optical fading [26]. The nanoDots can be read 10 min post-irradiation to allow stabilisation of the OSL signals [27], [28]; however, in this study, the irradiated nanoDots were read not earlier than 24 h after irradiation to acquire post-irradiation OSL signals. When necessary, the net OSL signal was calculated by subtracting the pre- and post-irradiation signals. At least three nanoDots were used for all measurements, which were read more than five times sequentially to provide reliable mean values and a smaller margin of error.

2.2 Optical annealer

The OSL signals were bleached using an light emission diode (LED) X-ray illuminator (MST-4000, Minston, China). The annealer was made of a 20 W LED light panel with a luminance of 5500 cd/m^2. This optical bleaching process requires manual sliding of the OSL disc out of the plastic case. The OSL disc was continuously exposed to light from the optical annealer for at least three days until the residual signal was nearly identical to the background signals (< 200 counts). Background subtraction was not performed if the background signals were minimal compared to the OSL signals (> 100,000 counts).

2.3 Electron beam irradiation using a linac

A linac Novalis Tx linear accelerator (Varian Medical Systems, Palo Alto, CA, USA) at the University Malaya Medical Centre (UMMC) was used to establish the dosimetric characteristics and relevant correction factors of the nanoDot subject to electron beams. To minimise the air gap during irradiation, the nanoDot was placed inside a polymethyl methacrylate (PMMA) slab phantom with dimensions of 30 cm × 30 cm × 0.7 cm that was designed with a slot to accommodate the nanoDot tightly. A 10 cm thick solid water phantom (type 457, Gammex RMI, USA) with dimensions of 30 cm × 30 cm was placed below the PMMA slab phantom to provide a full-scatter condition. The nanoDots were irradiated at the intended dose, delivered at a rate of 400 cGy/min at 100 cm source-surface distance (SSD) with a 10 cm × 10 cm field size at scaled depth in a PMMA slab phantom, Z_{PMMA} for 6 and 9 MeV electron beams. Considering the density of the PMMA slab phantom, ρ_{PMMA} of 1.19 g/cm^3 and depth scaling factor, C_{PMMA} of 0.941 [29], the Z_{PMMA} and measurement depth equivalent in water, Z_{water} was estimated as presented in Table 1. These experimental setups were the same for all dosimetric measurements unless otherwise mentioned.

Table 1: Measurement setup of nanoDot in PMMA slab phantom for electron beam irradiation.

Beam energy (MeV)	6	9
Beam quality, $R_{50,water}$ (cm)	2.47	3.68
Reference depth in water, Z_{ref} (g/cm^2)	1.38	2.11
Measurement depth in PMMA, $Z_{measured}$ (cm)	1.05	1.50
Scaled depth in PMMA, Z_{PMMA} (g/cm^2)	1.25	1.79
Measurement depth equivalent in water, Z_{water} (g/cm^2)	1.18	1.68
Percentage depth dose, PDD (%)	99.65	99.36

To determine the calibration coefficient, the nanodots were calibrated in terms of the absorbed dose to water under reference conditions in 6 and 9 MeV beams. A calibrated 0.4 cm^3 plane parallel ionisation chamber, type PPC40 (IBA

Dosimetry GmbH, Germany), connected to a PTW Unidos E electrometer, type T10009 (PTW Freiburg, Germany), was used to measure the absorbed dose to water. The absorbed dose to water was determined according to IAEA's Technical Report Series (TRS) No. 398 [29]. Detailed procedures are discussed in Abdullah et al.(2023). The calibration coefficient of the nanoDot OSLD dosimetry system was calculated as the ratio of the absorbed dose in water measured using an ionisation chamber, in cGy, and the corrected OSL readings of the nanoDot, in nC.

2.4 Dosimetric characteristics and relevant correction factors

2.4.1 NanoDot sensitivity correction factor

The inhomogeneous composition of the OSL material in the nanoDot produced variability in the sensitivity required for the individual sensitivity correction factor (SCF). In this study, 93 nanoDots were examined for their SCFs. Before irradiation, the pre-irradiation signal (initial background) was measured for each nanoDot. The nanoDots were then irradiated with 50 cGy under conditions of 20 cm × 20 cm field size (FS) and 100 cm SSD for a 6 MeV electron beam. A 0.5 cm bolus and a 1.0 cm slab phantom were placed above the nanoDots to provide a flat beam at the reference depth of 1.5 cm. After removing the outliers (nanoDots whose background corrected signal was outside three times the standard deviation), the SCF was calculated by taking the ratio of the average net OSL signal of all nanoDots and the net OSL signal of each nanoDot. The data were further assessed using a one-sample t-test using IBM SPSS Statistics Version 29.

2.4.2 Linearity of dose with OSL signal

To investigate the OSL signal response as a dose function, three nanoDots were irradiated for each planned dose within 50–300 cGy at 25 cGy intervals for both 6 MeV and 9 MeV beams. The linearity curves of the OSL signals against dose were plotted with linear functions fitted to the data to obtain the determination coefficients (R^2). The corresponding dose-response linearity correction factor, k_{lin} for each beam energy was calculated as the ratio of the OSL signal at 100 cGy to other doses. A graph of k_{lin} versus dose was plotted, with the linear functions fitted to the data to obtain a linear equation model. Finally, simple linear regression statistical tests were conducted to predict the value of k_{lin} based on the dose for each beam energy.

2.4.3 Beam energy dependency

The beam energy dependency of nanoDots was quantified for the most commonly used radiotherapy treatment beams: 6, 9, and 12 MeV. The nanoDots were irradiated under the reference conditions using a fabricated PMMA OSLD holder (Figure 1) following TRS-398 [29]. The energy correction factors, k_{energy} were subsequently determined based on the ratio of the OSL signal emitted by the nanoDots in a 6 MeV beam relative to the other beams.

2.4.4 Signal depletion per readout

The OSL signal in the nanoDot could be read repeatedly, but with partial signal loss. To study the signal depletion per readout, the nanoDots were exposed to 200 cGy with 6 MeV and 9 MeV beams. Without repositioning the nanoDot in the reader, signal depletion of nanoDot was observed by reading the nanoDots 100 times successively with a 10-second reading cycle. A graph of the signal

depletion versus the sequential reading number was plotted, and a linear function was fitted to the data.

2.4.5 Signal fading over time

The decay in the OSL signal as a function of time post-irradiation was assessed by exposing the nanoDots to 200 cGy with 6 MeV and 9 MeV beams. A total of 17 nanoDots were prepared, of which 15 nanoDots were exposed to the corresponding beams, and the remaining dosimeters were used for background radiation monitoring. The first OSL reading was taken 24 h after irradiation to allow for decay of the phosphorescence signals observed immediately after irradiation [31]. The irradiated nanoDots were then read once per week for ten weeks. Simultaneously, two control nanoDots were read to monitor the accumulated background radiation. Each data point was corrected using a signal depletion correction factor and accumulated background radiation. A graph of the normalised OSL signal against days post-irradiation was plotted. A logarithmic function was fitted to the data, and the standard uncertainty was calculated.

2.4.6 Reproducibility of OSL readout and dosimeter

The reproducibility of the OSL readout was evaluated by randomly taking five nanoDots and delivering them at 200 cGy with 6 MeV and 9 MeV beams. The standard uncertainty provided by each dosimeter for various numbers of readings was compared to determine the readout reproducibility. In this study, the nanoDots were reused multiple times after bleaching as opposed to a single use. Therefore, the dosimeter reproducibility after long-term reuse of nanoDots was evaluated. To test this, the SCF for all nanoDots, except for four nanoDots used for the long-term stability of the OSL reader, was determined again following the method described in 2.4.1.

A paired sample t-test was used to evaluate the differences in the data of old and new SCF for statistical significance.

2.4.7 Fabrication and test of nanoDot OSLD holder for remote dosimetry audit

The OSLD holder for the electron beam dosimetry audit was fabricated using PMMA with a density of 1.190 g/cm^3. The complete set of holders consisted of a stand, nanoDot OSLD disc, rod spacers, ring spacers, and screws (Figure 1). The stand was fabricated following the IAEA TLD standard stand [32] with a lead base to provide weight in water. The OSLD disc was designed with a 10 mm × 10 mm × 2 mm groove to fit into a single nanoDot and a watertight lid. Various ring spacer thicknesses (1, 2, and 10 mm) were used to adjust the irradiation depth of the nanoDots to correspond to the beam energy used. Two metal screws were used to open the nanodot disc lid. The scatter influence of the fabricated holder was investigated experimentally using the EBT 3 film by comparing the results to the IAEA standard holder for beams with energies of 6, 9, and 12 MeV.

2.5 OSL reader stability

The OSL reader was warmed for 30 min to ensure system stability before use. Following this, the readers' performance was monitored according to the established measurement standards. The measurement includes dark counts from the PMT tube (DRK), count calibration using a built-in Carbon-14 (^{14}C) radioactive source (CAL), and beam intensity from the LED. The measurement standard results were checked to ensure that they were within the specified limits for the DRK (less than 30 counts), CAL, and LED (within ± 10% of the average value).

Additionally, a quality control (QC) test using standard nanoDots irradiated with a Srontium-90 beta source (^{90}Sr) was performed to determine the long-term stability of the reader.

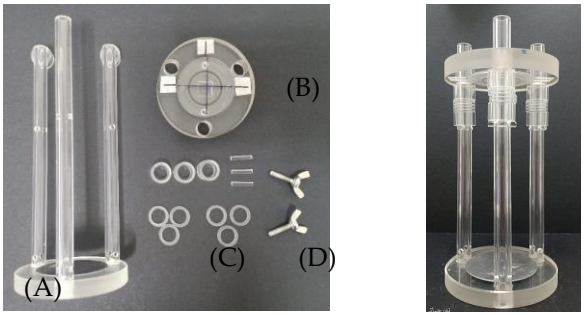

Figure 1: The PMMA OSLD holder for the electron beam audit. It consists of (A) a stand; (B) an nanoDot OSLD disc; (C) rod and ring spacers; (D) screws.

2.6 Preliminary dosimetry audit of electron beams

The primary objective of the dosimetry audits was to assess the accuracy of the absorbed dose delivered by the linac for electron beams under both reference and non-reference conditions. The audits involved six electron beams produced from four linacs at two radiotherapy centres. Prior to the audit, each centre received a set of instructions and materials including the irradiation procedure and form, a specified quantity of nanoDots for each beam (eight for irradiation and one for control), and a fabricated OSLD holder set. The centres were requested to irradiate the nanoDot in a water phantom using an OSLD holder at an absorbed dose of 100 cGy for the following conditions: (i) reference condition as defined by TRS 398, and (ii) non-reference condition at the beam's central axis with FS of 6 cm × 6 cm, 10 cm × 10 cm, and 15 cm × 20 cm at a depth of maximum dose, Z_{max} and SSD greater than 105 cm.

The measured absorbed dose (D) was calculated from the OSL signals using the following equation:

$$D = M \times SCF \times N \times k_{lin} \times k_{energy} \times k_{fade} \times k_{holder} \quad (1)$$

where M is the mean of the net OSL signals from the two nanoDots, SCF is the nanoDot sensitivity correction factor, N is the dosimetry system calibration coefficient of 0.001712 cGy ± 0.82%, k_{lin} is the dose-response linearity correction factor, k_{energy} is the energy correction factor, k_{fade} is the fading correction factor, and k_{holder} is the holder correction factor.

The audit results were expressed as the percentage deviation between the dose delivered by the radiotherapy centres and the absorbed dose measured from the nanoDots.

2.7 Estimation of measurement uncertainty

In accordance with Equation 1, an uncertainty analysis of the measured absorbed dose from nanoDots was carried out utilising the guidelines outlined in the "Guide to the expression of uncertainty in measurement" [33]. The sources of uncertainty and the corresponding numerical values of the random (Type A) and systematic (Type B) uncertainties were determined. The total combined standard uncertainty was calculated by summing the Type A and Type B uncertainties using a quadratic method.

3.0 RESULTS AND DISCUSSION

2.8 Establishment of dosimetric characteristics and correction factors

2.8.1 Sensitivity correction factor of nanoDot

Figure 2 shows the distribution of the SCFs of nanoDots subjected to a 6 MeV electron beam. After eliminating the two outliers, the SCFs ranged from 0.946 to 1.060, with a mean of 1.001 ± 0.25%. The nanoDots used in this study were obtained from the manufacturer and were pre-screened to ± 5% uniformity of sensitivity; however, the results revealed that 86 (94%) nanoDots were within this range. These findings are comparable with the published data by Retna Ponmalar et al. (2017), who reported the SCF distribution between 0.90 and 1.07, with 90% of the 200 nanoDots falling within that acceptance limit. Another study reported that 97% of 1000 nanoDots were within the acceptable limit, and the SCF distribution was between 0.930 and 1.134 [22]. These results help to justify that instead of using the SCFs provided by the manufacturer that were irradiated with Cesium-137 (^{137}Cs), users should determine the SCF experimentally for their applications. To minimise the uncertainty due to SCFs, selected nanoDots with sensitivities of ± 5% (ICRU 24, 1976) and ± 3% were subsequently utilised in the dosimetric characteristic study and electron beam dosimetry audit. Five nanoDots with SCF outside the acceptance limit were used for background radiation monitoring. Further analysis using a one-sample t-test was performed to assess whether the mean SCF in these nanoDots differed from the normal SCF, which was defined as 1.000. The assumption that the SCFs were normally distributed was met, as assessed by the Shapiro-Wilk test ($p = 0.811$). The mean SCF of 1.001, with a standard deviation of 0.024, was slightly higher than the normal SCF of 1.000; however, the difference was not statistically significant ($t(90) = 0.213$, $p = 0.831$). To achieve high dosimetry accuracy, SCF was required for each nanoDot in the following measurements.

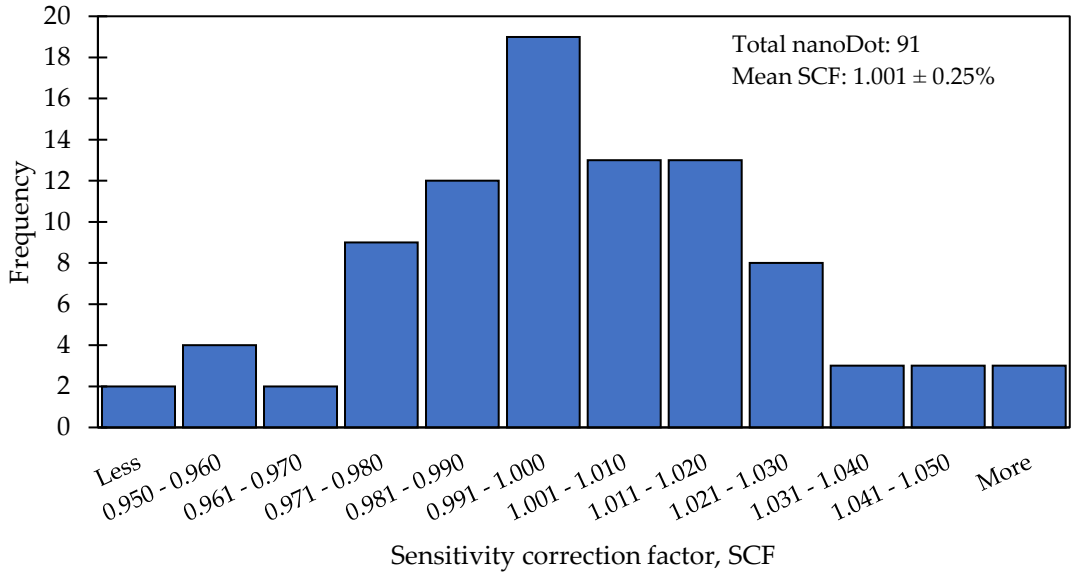

Figure 2: Histogram of the distribution of sensitivity correction factors of nanoDots subject to a 6 MeV electron beam.

2.8.2 Linearity of OSL signal with absorbed dose

The linearity of the OSL signal within a dose range of 50 cGy – 300 cGy for 6 MeV and 9 MeV was established. Overall, a gradual increase in the OSL signal was observed, with averages of 21.30% ± 4.49% and 20.80% ± 4.93% for each 25 cGy dose increment from 50 cGy – 300 cGy subject to the 6 MeV and 9 MeV beams, respectively. The results showed a linear OSL signal for the intended dose range, with an R^2 value of 0.9982 for both beams (Figure 3). Similar observations have been reported, in which the OSL signal was linear from 50 cGy – 300 cGy, with R^2 values ranging from 0.997 to 0.998 for 6 to 20 MeV beams [34]. According to previous studies, these results are comparable to those of photon beams, in which the

OSL signal has a dose linearity of up to 400 cGy [35], [36], [37]. To obtain better accuracy in dose measurement, the values of k_{lin} over the dose range of 50 cGy to 200 cGy, normalised to 100 cGy, which is the reference dose used in the audit program, were determined (Figure 4). The k_{lin} values were 0.966 – 1.139 and 0.995 – 1.199 at 6 MeV and 9 MeV, respectively. From the SPSS output, the assumptions of a linear relationship between the absorbed dose and k_{lin} for each energy were met, as observed from the simple scatter plots. The linear regression models showed that there was a statistically significant difference between the absorbed dose and k_{lin} for 6 MeV and 9 MeV, with (R^2 = 0.850, F(1,5) = 28.422, p = 0.003) and (R^2 = 0.646, F(1,5) = 9.134, p = 0.029), respectively. These results indicate that the linear equations presented in Figure 4 must be applied to improve the accuracy of the dose calculation for the relevant nominal beam energies.

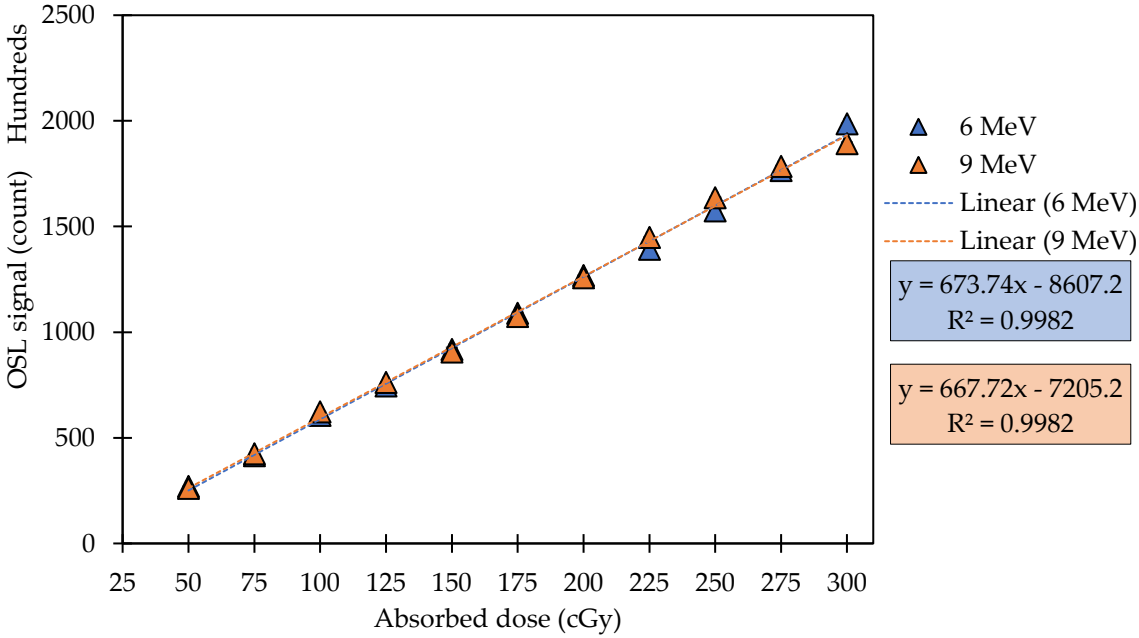

Figure 3: Linearity of the OSL signal for an absorbed dose range from 50 cGy – 300 cGy subjected to 6 MeV and 9 MeV electron beams. The dotted lines are linear function fits to the data, obtaining an R^2 of 0.9982 for both beams. The error bars were less than 955 counts, that is, smaller than the data points, so they do not appear in the graph.

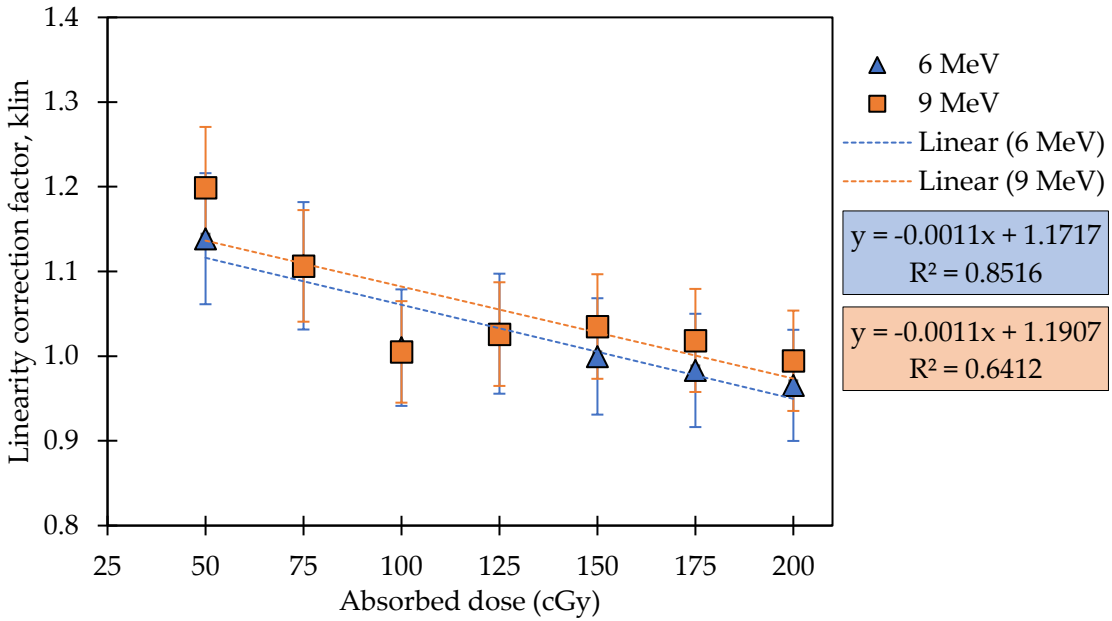

Figure 4: Linearity correction factors of nanoDots subjected to 6 MeV and 9 MeV electron beams for a dose range from 50 cGy – 200 cGy, normalised to 100 cGy. The dotted lines are linear functions that fit the data. Error bars represent standard uncertainty (k=1).

2.8.3 Beam energy dependency

The results for k_{energy} in comparison with those at 6 MeV are presented in Table 2. The nanoDot demonstrated high-energy dependency, particularly at a higher beam energy of 12 MeV, with a significant deviation of 4.08% compared to that at 6 MeV. This effect is precisely due to its non-tissue equivalent material (Al_2O_3:C) having a highly effective atomic number, Z_{eff} of 11.28, which makes it sensitive to different beam qualities. These findings are in line with those reported in the literature, where nanoDots exhibited a relative energy-dependent response for both photon and electron beams [23], [34], [38]. For radiotherapy dosimetry, the dosimetric material should have a Z_{eff} close to that of water or tissue (Z_{eff} = 7.4), and lithium fluoride doped with magnesium and titanium (LiF:Mg, Ti) with Z_{eff} ~ 8.2, is commonly used for this reason [39], [40]. However, the non-tissue equivalent of nanoDot is not an issue in radiotherapy dosimetry, as long as the k_{energy} for each beam energy is considered carefully in the dose calculation.

Table 2: Beam energy correction factor, k_{energy} in comparison with the 6 MeV beam.

Nominal electron beam energy (MeV)	Beam quality, R_{50} (cm)	k_{energy} in comparison with 6 MeV
6	2.47	1.000 ± 0.004
9	3.68	1.013 ± 0.005
12	5.02	1.041 ± 0.003

2.8.4 OSL signal depletion

After 100 consecutive readings, small signal reductions of 6 MeV and 9 MeV were observed for a dose of 200 cGy, with a similar value of 0.03% per reading (

Figure 5). These results indicate that the depletion rates were independent of the beam energy. In contrast,

Ponmalar et al. (2017) reported a slight difference in the depletion rate of energy from 6 MeV to 20 MeV, where the percentage reduction in the signal for the same dose was 0.04% and 0.05% after 200 readings, respectively. The results are also comparable to previous findings by Dunn et al. (2013) and Wesolowska et al. (2017), where a signal depletion of 0.03% and 0.04% per reading in response to photon beams was reported. Where applicable, the linear equations presented in

Figure 5 were used to correct the repeated readings in the following measurements, especially for signal fading and long-term stability of the OSL reader studies.

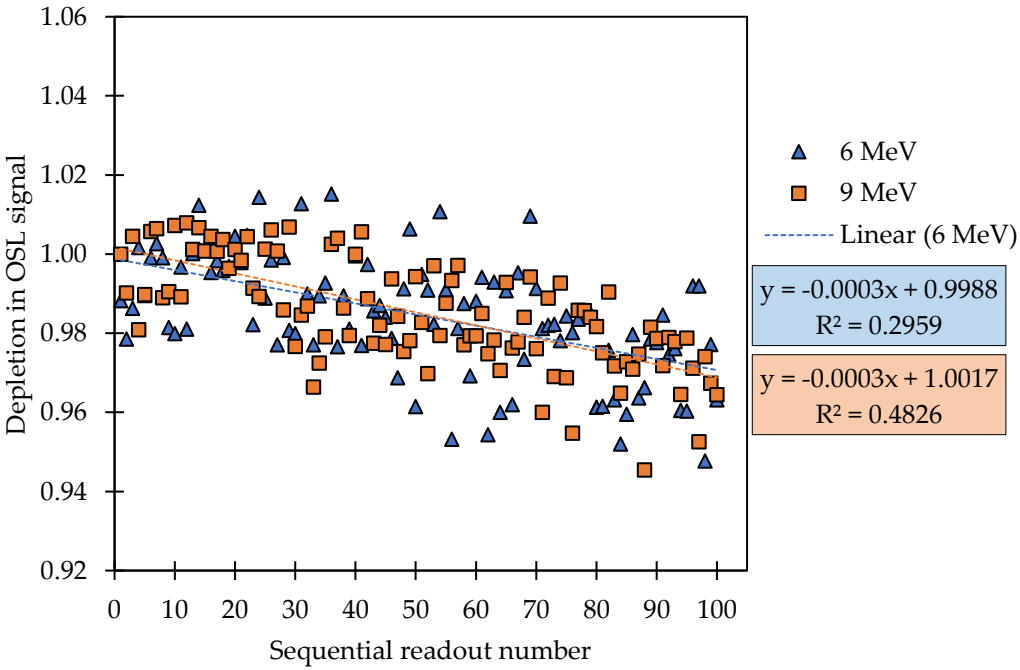

Figure 5: Signal depletion per readout for nanoDot subject to 6 MeV and 9 MeV beams. The dotted lines are linear functions that fit the data.

2.8.5 Signal fading over time

Figure 6 illustrates that OSL signal fading occurs logarithmically with time. The OSL signal fading was most noticeable within ten days of irradiation. After more time passes post-irradiation, the effect of OSL fading becomes more stable. The OSL fading exhibited a similar trend for all beams, regardless of the energy involved during irradiation. Over 70 days, the nanoDot signals exposed to 6 MeV and 9 MeV dropped by approximately 3.0% and 3.2%, respectively, with normalisation to day one post-irradiation. For comparison, the nanoDot fading reported by Dunn et al. (2013) was 3.5% six months after irradiation, normalised to the first day. Long-term fading of the OSL signal is an essential parameter in dosimetry audits, considering the one-month time frame required to complete the audit process. Therefore, a signal fading correction factor, k_{fading} (1/normalized OSL signal) should be applied in the dose calculation.

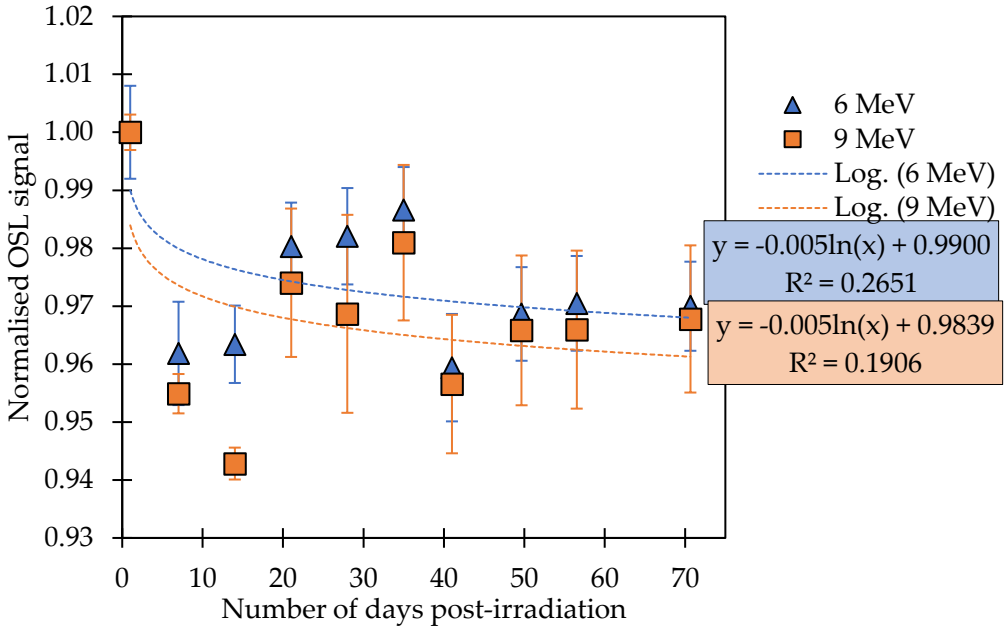

Figure 6: OSL signal loss over time normalised to day one post-irradiation of nanoDot subjected to electron beams with a constant absorbed dose of 200 cGy. The dotted lines are logarithm functions that fit the data. Error bars represent the standard uncertainty of 25 OSL readings, with the highest value of 0.017.

2.8.6 OSL readout and dosimeter reproducibility

The nanoDots showed consistent reproducibility for the readout and dosimeter. When the number of readings increased from 8 to 40, the readout reproducibility improved significantly, from 0.95% – to 0.51%. After five irradiation cycles, the dosimeter reproducibility was maintained at 0.72%. These results comply with the tolerance limit of ± 2% associated with a reliable dosimeter [41]. Overall, reproducibility can be better with multiple

readings, and thus contributes to a smaller standard uncertainty of measurement. To achieve a standard uncertainty owing to a readout reproducibility of less than 1.0%, it is recommended to repeat the readings at least four times. In addition, the results of SCF reproducibility from a paired samples t-test demonstrated that there was no significant difference between old SCF (mean = 1.000, standard deviation = 0.023) and new SCF (mean = 1.002, standard deviation = 0.048); t(88) = -0.568, p = 0.572. Considering the changes in the nanoDot sensitivity after an accumulated dose limit of 10 Gy [26], [42], a new SCF should be implemented.

2.8.7 Holder correction factor

The result of the scattering influence showed no significant variation in response to the dose for the fabricated PMMA OSLD holder and IAEA TLD standard holder, with 0.29%, -0.32%, and 0.05% for the 6, 9, and 12 MeV beams, respectively. Therefore, the PMMA TLD holder correction factor, k_{holder} established by the IAEA was applied in the dose calculation. The k_{holder} for electron beams was calculated by Monte Carlo simulation and was essentially constant at 1.0019 ± 0.0008 for all 6 MeV – 20 MeV beams [32].

2.9 Stability of OSL reader

Throughout the study, the stability of the OSL reader was checked using the following parameters: The consistency of the dark current was (3.53 ± 0.25) counts, within the acceptance limit of less than 30 counts. The energy calibration and light intensity consistency from the LED were (4.21 ± 3.25) % and (1.68 ± 0.31) %, respectively, within the acceptable limit of ± 30%. The long-term stability of the OSL reader using standard nanoDots

provided consistent data, with an average of − 0.85% and a standard uncertainty of 0.82%.

2.10 Preliminary audits for electron beams under reference and non-reference conditions

The results of the preliminary audit of the electron beams from the two radiotherapy centres are presented in Table 3. These results are well within the tolerance of ± 5%, as recommended in ICRU Report No. 24, except for two beams from Linac 2 for a non-reference condition of 6 cm × 6 cm FS. After the investigation, the cause of the deviation for Linac 2 was identified as a mistake in the positioning of the nanoDots at different irradiation depths. After follow-up irradiation, the results of Linac 2 were improved to 3.93% and 3.65% for 6 MeV and 8 MeV, respectively. Overall, the mean distribution of percentage deviations after follow-up irradiation was -1.66% ± 0.81% for the reference condition and -0.40% ± 1.49%, -2.92% ± -0.80%, and-0.80% ± 0.93% for the non-reference condition at 6 cm × 6 cm, 10 cm × 10 cm, and 15 cm × 20 cm FS, respectively.

Table 3*:* Preliminary audit results of electron beams for reference and non-reference conditions for first-round irradiation.

Linac	Nominaal beam energy (MeV)	Deviation of measured dose relative to delivered dose (%)			
		Reference condition	Non-Reference condition		
			6 cm × 6 cm	10 cm × 10 cm	15 cm × 20 cm
1	6	-1.79	-4.36	-4.18	-2.91
	9	-2.40	-0.52	-4.15	3.13
2	6	0.21	-44.32	-1.35	-0.46
	8	1.22	11.22	-0.15	-0.79
3	6	-3.60	-4.37	-4.10	-0.54
4	6	-3.59	-0.72	-3.59	-3.21

2.11 Measurement uncertainty

The combined standard uncertainty for determining the measured dose from the nanoDot is summarised in Table 4. The main source of uncertainty in this study arises from the ionisation chamber calibration (0.62%) and the stability of the OSL reader (0.47%). The combined standard uncertainty was 1.41% for a coverage factor, *k* of 1, which aligns with the findings of Wesolowska et al. (2017), who suggested a 1.46% combined standard uncertainty for photon beam audits. Conversely, Kumar et al. (2020) reported a much higher combined standard uncertainty of 3.3%.

Table 4:Combined standard uncertainties of measured absorbed doses from nanoDots.

Uncertainty component	Relative standard uncertainty (%)	
	Type A	Type B
Calibration of the nanodot OSLD dosimetry system		
Determination of absorbed dose from PPC 40 ionization chamber	-	0.62
Water phantom positioning during irradiation	-	0.04
Dosimeter positioning during irradiation	-	0.04
Dosimeter readout	0.26	-
Stability of OSL reader	0.47	-
Combined standard uncertainty (*k*=1)	**0.54**	**0.62**
Determination of the absorbed dose from nanodot OSLD		
Calibration coefficient of the nanodot OSLD dosimetry system	0.54	0.62
Dosimeter readout	0.26	-
Sensitivity correction factor	-	1.00
Stability of OSL reader	0.47	-
Dose-response linearity correction factor	0.07	-
Beam energy correction factor	0.03	-
Signal fading correction factor	0.05	-
Holder correction factor	0.08	-

Combined standard uncertainty (*k*=1)	**1.41**	-

4.0 CONCLUSIONS

A preliminary study was conducted to develop and evaluate a method for remote dosimetry auditing of electron beams under reference and non-reference conditions using a nanoDot OSLD dosimetry system. The dosimetry system performed admirably in terms of dosimeter sensitivity, readout reproducibility, and stability of the OSL reader. Additionally, correction factors were implemented for dose-response linearity, beam energy, signal fading, and a PMMA-fabricated OSLD holder to improve dose accuracy. With a coverage factor of k=1, the combined standard uncertainty of the dose measurement was 1.41%. The preliminary audit of electron beams from two radiotherapy centres showed percentage dose deviations within the ICRU Report No. 24 tolerance of ± 5%, except for three beams. There was a marked improvement in the dose deviation after subsequent irradiation. This pilot study laid the groundwork for the subsequent development and successful implementation of a method for conducting remote dosimetry audits of electron beams using nanoDots. Thus, it is now possible to conduct a national electron beam dosimetry audit on a regular basis.

ACKNOWLEDGMENT

This work was supported by the Prototype Research Grant Scheme PRGS/1/2021/SKK07/UPM/02/1 from the Ministry of Higher Education Malaysia, with the Jabatan Perkhidmatan Awam Malaysia (Hadiah Latihan Persekutuan 2021) partially funded tuition fees.

CONFLICT OF INTEREST STATEMENT

This work was supported by the Prototype Research Grant Scheme PRGS/1/2021/SKK07/UPM/02/1 from the Ministry of Higher Education Malaysia, with the Jabatan Perkhidmatan Awam Malaysia (Hadiah Latihan Persekutuan 2021) partially funded tuition fees.

6.0 REFERENCES

[1] ICRU, *Determination of absorbed dose in a patient irradiated by beams of X or gamma rays in radiotherapy procedures*. International Commission on Radiation Units and Measurements, 1976.

[2] IAEA, *Accuracy Requirements and Uncertainties in Radiotherapy*. Vienna, Austria: International Atomic Energy Agency, 2016.

[3] J. Izewska, T. Bokulic, P. Kazantsev, P. Wesolowska, and D. van der Merwe, '50 Years of the IAEA/WHO postal dose audit programme for radiotherapy: what can we learn from 13756 results?', *Acta Oncol (Madr)*, vol. 59, no. 5, pp. 495–502, May 2020, doi: 10.1080/0284186X.2020.1723162.

[4] C. H. Clark *et al.*, 'Radiotherapy dosimetry audit: Three decades of improving standards and accuracy in UK clinical practice and trials', *British Journal of Radiology*, vol. 88, no. 1055, p. 20150251, 2015, doi: 10.1259/BJR.20150251.

[5] J. Izewska, W. Lechner, and P. Wesolowska, 'Global availability of dosimetry audits in radiotherapy: The IAEA dosimetry audit networks database', *Phys Imaging Radiat Oncol*, vol. 5, pp. 1–4, Jan. 2018, doi: 10.1016/j.phro.2017.12.002.

[6] D. Van Der Merwe *et al.*, 'Accuracy requirements and uncertainties in radiotherapy: a report of the International Atomic Energy Agency', *Acta Oncol (Madr)*, vol. 56, no. 1, pp. 1–6, 2016, doi: 10.1080/0284186X.2016.1246801.

[7] C. H. Clark, N. Jornet, and L. P. Muren, 'The role of dosimetry audit in achieving high quality radiotherapy', *Phys Imaging Radiat Oncol*, vol. 5, pp. 85–87, Jan. 2018.

[8] N. Abdullah, N., Kadni, T., & Dolah, 'Malaysian participation in the IAEA/WHO TLD postal dose quality audit service: data analysis from 2011-2015.', *Jurnal Sains Nuklear Malaysia*, vol. 30, no. 1, pp. 36–45, 2018.

[9] Bahagian Kawalselia Radiasi Perubatan, 'Senarai Radas Penyinaran Linac dan Cyberknife di Bawah Akta 304', Portal Data Terbuka Malaysia. Accessed: Jan. 21, 2024. [Online]. Available: https://archive.data.gov.my/data/ms_MY/dataset/senarai-radas-linac-dan-cyberknife-di-bawah-akta-304

[10] Bahagian Kawalselia Radiasi Perubatan, 'Statistik Bilangan Radas Penyinaran Dan Bahan Radioaktif Dalam Perkhidmatan Radioterapi', Portal Data Terbuka Malaysia. Accessed: Jan. 21, 2024. [Online]. Available: https://www.data.gov.my

[11] N. Abdullah, N. Mohd Noor, J. K. Sangau, and M. T. Dolah, 'The roles of Nuklear Malaysia's SSDL in the national radiotherapy dosimetry audit', Alor Setar, Kedah, Malaysia, 2022.

[12] S. F. Kry *et al.*, 'Remote beam output audits: A global assessment of results out of tolerance', *Phys Imaging Radiat Oncol*, vol. 7, pp. 39–44, Jul. 2018, doi: 10.1016/j.phro.2018.08.005.

[13] C. W. Hurkmans, M. Christiaens, S. Collette, and D. C. Weber, 'Beam Output Audit results within the EORTC Radiation Oncology Group network', *Radiation Oncology*, 2016, doi: 10.1186/s13014-016-0733-4.

[14] IAEA, 'New Dosimetry Audit Service for Linacs Used in Radiotherapy', International Atomic Energy Agency. Accessed: Apr. 25, 2022. [Online]. Available: https://www.iaea.org/newscenter/news/new-dosimetry-audit-service-for-linacs-used-in-radiotherapy?msclkid=16fef9f9c45711eca5f413e342ec33ed

[15] M. McEwen, P. Sharpe, and S. Vörös, 'Evaluation of alanine as a reference dosimeter for therapy level dose comparisons in megavoltage electron beams', *Metrologia*, vol. 52, no. 2, pp. 272–279, Apr. 2015, doi: 10.1088/0026-1394/52/2/272.

[16] A. Dimitriadis *et al.*, 'IAEA/WHO postal dosimetry audit methodology for electron beams using radio photoluminescent dosimeters', *Med Phys*, no. June, pp. 1–8, 2023, doi: 10.1002/mp.16776.

[17] L. de Prez *et al.*, 'An on-site dosimetry audit for high-energy electron beams', *Phys Imaging Radiat Oncol*, vol. 5, pp. 44–51, Jan. 2018, doi: 10.1016/j.phro.2018.02.001.

[18] J. M. Park, S. Y. Park, M. Chun, and S. T. Kim, 'On-site audits to investigate the quality of radiation physics of radiation therapy institutions in the Republic of Korea', *Physica Medica*, vol. 40, pp. 110–114, Aug. 2017, doi: 10.1016/j.ejmp.2017.07.021.

[19] A.-C. Shiau *et al.*, 'Dosimetry audits in Taiwan radiotherapy departments', *BJR|Open*, vol. 3, no. 1, 2021, doi: 10.1259/bjro.20210002.

[20] P. Alvarez, A. Molineu, J. Lowenstein, P. Taylor, S. Kry, and D. Followill, 'IROC Houston QA center S independent peer review quality assurance program for the veteran affairs VA radiotherapy facilities', *Med Phys*, vol. 44, no. 6, p. 2881, 2017.

[21] T. Kron, A. Haworth, and I. Williams, 'Dosimetry for audit and clinical trials: Challenges and requirements', in *Journal of Physics: Conference Series*, Institute of Physics Publishing, 2013. doi: 10.1088/1742-6596/444/1/012014.

[22] P. E. Wesolowska, A. Cole, T. Santos, T. Bokulic, P. Kazantsev, and J. Izewska, 'Characterization of three solid state dosimetry systems for use in high energy photon dosimetry audits in radiotherapy', *Radiat Meas*, vol. 106, pp. 556–562, Nov. 2017, doi: 10.1016/j.radmeas.2017.04.017.

[23] R. Ponmalar, R. Manickam, K. Ganesh, S. Saminathan, A. Raman, and H. Godson, 'Dosimetric characterization of optically stimulated luminescence dosimeter with therapeutic photon beams for use in clinical radiotherapy

measurements', *J Cancer Res Ther*, vol. 13, no. 2, p. 304, Apr. 2017, doi: 10.4103/0973-1482.199432.

[24] K. Hoshida and F. Araki, 'Physica Medica Response of a nanoDot OSLD system in megavoltage photon beams', *Physica Medica*, vol. 64, no. June, pp. 74–80, 2019, doi: 10.1016/j.ejmp.2019.06.014.

[25] A. Ruiz, J. Irazoqui, S. Bianchini, and D. Tolabin, 'PO-1714 Commissioning of an OSLD dosimetric system for level I postal audits for radiotherapy in Argentina', *Radiotherapy and Oncology*, vol. 161, 2021, doi: 10.1016/s0167-8140(21)08165-2.

[26] S. F. Kry *et al.*, 'AAPM TG 191: Clinical use of luminescent dosimeters: TLDs and OSLDs', *Med Phys*, vol. 47, no. 2, pp. e19–e51, Feb. 2020, doi: 10.1002/MP.13839.

[27] P. A. Jursinic, 'Characterization of optically stimulated luminescent dosimeters, OSLDs, for clinical dosimetric measurements', *Med Phys*, vol. 34, no. 12, pp. 4594–4604, 2007, doi: 10.1118/1.2804555.

[28] E. G. Yukihara, G. Mardirossian, M. Mirzasadeghi, S. Guduru, and S. Ahmad, 'Evaluation of Al2O3:C optically stimulated luminescence (OSL) dosimeters for passive dosimetry of high-energy photon and electron beams in radiotherapy', *Med Phys*, vol. 35, no. 1, p. 260, 2008, doi: 10.1118/1.2816106.

[29] IAEA, *Absorbed Dose Determination in External Beam Radiotherapy: An International Code of Practice for Dosimetry Based on Standards of Absorbed Dose to Water*. Vienna, Austria: International Atomic

Energy Agency, 2000. doi: 10.1097/00004032-200111000-00017.

[30] N. Abdullah, N. M. Noor, M. T. Dolah, and J. K. Sangau, 'Precision and reliability: Calibration coefficients and long-term stability analysis of radiotherapy dosimeters calibrated by SSDL, Nuklear Malaysia', *Asian Journal Of Medical Technology*, vol. 3, no. 2, pp. 15–32, 2023.

[31] E. G. Yukihara and S. W. McKeever, 'Optically stimulated luminescence (OSL) dosimetry in medicine', *Phys Med Biol*, vol. 53, no. 20, 2008, doi: 10.1088/0031-9155/53/20/R01.

[32] D. Marre *et al.*, 'Energy correction factors of LiF powder TLDs irradiated in high-energy electron beams and applied to mailed dosimetry for quality assurance networks', *Phys Med Biol*, vol. 45, no. 12, pp. 3657–3674, 2000, doi: 10.1088/0031-9155/45/12/311.

[33] JCGM-100, *Evaluation of measurement data — Guide to the expression of uncertainty in measurement*, First edit., vol. 50, no. September. 2008. [Online]. Available: http://www.bipm.org/en/publications/guides/gum.html

[34] Y. Retna Ponmalar, R. Manickam, S. Sathiyan, K. M. Ganesh, R. Arun, and H. F. Godson, 'Response of nanodot optically stimulated luminescence dosimeters to therapeutic electron beams', *J Med Phys*, vol. 42, no. 1, pp. 42–47, Jan. 2017, doi: 10.4103/0971-6203.202424.

[35] G. K. Jain, A. Chougule, A. Kaliyamoorthy, and S. K. Akula, 'Study of dosimetric characteristics of a commercial optically stimulated luminescence system', *J Radiother Pract*, vol. 16, no. 4, pp. 461–475, Dec. 2017, doi: 10.1017/S1460396917000346.

[36] L. Dunn, J. Lye, J. Kenny, J. Lehmann, I. Williams, and T. Kron, 'Commissioning of optically stimulated luminescence dosimeters for use in radiotherapy', *Radiat Meas*, vol. 51–52, pp. 31–39, Apr. 2013, doi: 10.1016/j.radmeas.2013.01.012.

[37] L. J. S. Raj, B. Pearlin, B. S. T. Peace, R. Isiah, and I. R. R. Singh, 'Characterisation and use of OSLD for in vivo dosimetry in head and neck intensity-modulated radiation therapy', *J Radiother Pract*, vol. 20, no. 4, pp. 448–454, Dec. 2021, doi: 10.1017/S146039692000062X.

[38] P. Kumar *et al.*, 'Relative energy response of indigenously developed optically stimulated luminescence dosimeters Al2O3:C, LiMgPO4:B and LiCaAlF6:Eu,Y in therapeutic photon and electron beams', *Luminescence*, vol. 35, no. 8, pp. 1217–1222, Dec. 2020, doi: 10.1002/BIO.3832.

[39] F. Attix, *Introduction to radiological physics and radiation dosimetry.* USA,: John Wüey & Sons., 1986.

[40] P. N. Mobit and T. Kron, 'Applications of Thermoluminescent Dosimeters in Medicine', in *Microdosimetric Response of Physical and Biological Systems to Low- and High-LET Radiations Theory and Applications to Dosimetry*, Elsevier, 2006, pp. 411–465. doi: 10.1016/B978-044451643-5/50019-8.

[41] T. Kirby, W. Hanson, and D. Johnston, 'Uncertainty analysis of absorbed dose calculations from thermoluminescence dosimeters', *Med Phys*, vol. 19, no. 6, pp. 1427–1433, 1992, doi: 10.1118/1.596797.

[42] P. A. Jursinic, 'Changes in optically stimulated luminescent dosimeter (OSLD) dosimetric characteristics with accumulated dose', *Med Phys*, vol. 37, no. 1, 2010, doi: 10.1118/1.3267489.